

*Surface/Groundwater Interactions and Sediment Characteristics of Headwater Streams in the  
Piedmont of North Carolina.*

by

Cameron David Moore

Approved by:

---

Dr. Anne J. Jefferson

---

Dr. Martha C. Eppes

---

Dr. Craig J. Allan

## Table of Contents

<b>ACKNOWLEDGEMENTS</b> .....	<b>7</b>
<b>ABSTRACT</b> .....	<b>8</b>
<b>1.0 - INTRODUCTION AND PURPOSE</b> .....	<b>11</b>
<b>2.0 - LITERATURE REVIEW</b> .....	<b>12</b>
2.1 - HEADWATER STREAMS: HETEROGENEITY OF GROUNDWATER/SURFACE WATER INTERACTIONS .....	12
2.2 - IMPORTANCE OF THE HYPORHEIC ZONE.....	15
2.3 - DETERMINING GROUNDWATER-STREAM WATER INTERACTIONS .....	15
2.4 - FRACTURED ROCK FLOW AND HYDROGEOLOGY OF THE NC PIEDMONT .....	17
2.5 CONTROLS ON SEDIMENT DEPTH AND SIZE DISTRIBUTION.....	19
<b>3.0 - HYPOTHESES</b> .....	<b>19</b>
3.1 RATIONALE FOR HYPOTHESES.....	20
<b>4.0 - SETTING</b> .....	<b>23</b>
<b>5.0 - METHODS</b> .....	<b>25</b>
5.1 SELECTION OF STUDY CREEKS .....	25
5.2 REACH SCALE GEOMORPHIC CHARACTERIZATION .....	26
5.3 DISCHARGE MEASUREMENTS .....	27
5.4 REPEAT TEMPERATURE AND SPECIFIC CONDUCTANCE MEASUREMENTS .....	29
5.5 SEDIMENT DEPTH MEASUREMENTS.....	29
5.6 PIEZOMETER MEASUREMENTS .....	30
5.7 WATER CHEMISTRY AND ISOTOPES.....	32
5.8 BEDROCK MAPPING .....	33
5.9 LONGITUDINAL PROFILE MEASUREMENT .....	33
<b>6.0 - RESULTS</b> .....	<b>34</b>
6.1 GEOMORPHIC DESCRIPTIONS .....	34
6.1.1 Deep Creek .....	34
6.1.2 Cabin Creek.....	35
6.1.3 Creek 90.....	36
6.2 STREAM LONGITUDINAL PROFILES AND BEDROCK MAPPING .....	37
6.3 SEDIMENT SIZE.....	38
6.4 SEDIMENT DEPTH .....	41
6.5 HYDROLOGY.....	43
6.6. TEMPERATURE AND SPECIFIC CONDUCTANCE.....	44
6.7 VERTICAL HEAD GRADIENTS, HYDRAULIC CONDUCTIVITY, AND DARCY FLUX VALUES.....	47
6.8 LONGITUDINAL DISCHARGE MEASUREMENTS .....	52
6.9.1 Stream Chemistry.....	55
<b>7.0 DISCUSSION</b> .....	<b>58</b>
7.1 HYPOTHESIS 1: .....	58
7.2 HYPOTHESIS 2: .....	60
7.3 HYPOTHESIS 3: .....	60
7.4 GENERAL DISCUSSION.....	62

**8.0 CONCLUSIONS.....63**  
**9.0 REFERENCED FIGURES .....66**

## List of Referenced Figures

Figure 1. Sub-surface hydrologic interactions between streams.....	66
Figure 2. Schematic showing sub-surface flow paths for a stream.....	66
Figure 3. Figure showing the study area in Gaston county North Carolina.....	67
Figure 4: Schematic showing how sediment depth was measured.....	68
Figure 5. Map showing Deep Creek watershed with the repeat 25 m measurement sites.....	69
Figure 6. Figure showing alluvial vs. bedrock coverage and pool vs. riffle distribution for Deep Creek.....	70
Figure 7. Map showing Cabin Creek with downstream measurement points labeled.....	71
Figure 8. Data for Cabin Creek showing alluvial vs. bedrock and pool vs. riffle distribution.....	72
Figure 9. Map showing Creek 90 with downstream measurement points indicated with dots.....	73
Figure 10. Distribution of pool vs. riffle and alluvial vs. bedrock sequences for Creek 90.....	74
Figure 11. Longitudinal profile of Deep Creek.....	74
Figure 12. Longitudinal profile of Cabin Creek.....	75
Figure 13. Longitudinal profile of Creek 90.....	75
Figure 14. Joint density per square meter plotted against stream slope.....	76
Figure 15. $D_{50}$ -watershed area relationship for the 27 pebble counts from summer 2009.....	76
Figure 16. Slope vs $D_{50}$ values.....	77
Figure 17. Downstream coarsening trends.....	77
Figure 18. Downstream coarsening trends.....	78
Figure 19. $D_{50}$ -distance downstream plot for Deep Creek, Cabin Creek, and Creek 90.....	78
Figure 20. Sediment size distribution graph for Deep Creek.....	79
Figure 21. Sediment size distribution graph for Cabin Creek.....	79
Figure 22. Sediment size distribution graph for Creek 90.....	80
Figure 23. Sediment depth versus downstream distance plot for Deep Creek.....	80
Figure 24. Sediment depth versus downstream distance plot for Cabin Creek.....	81
Figure 25. Sediment depth versus downstream distance plotted for Creek 90.....	81
Figure 26. Trends between sediment depth and $D_{50}$ values.....	82
Figure 27. Hydrograph of Deep Creek.....	82
Figure 28. Hydrograph of Cabin Creek.....	83
Figure 29. Hydrograph of Creek 90.....	83
Figure 30. Relationship between specific conductance and distance downstream for Deep Creek.....	84
Figure 31. Relationship between specific conductance and distance downstream for Deep Creek during summer.....	84
Figure 32. Plot of temperature vs. distance downstream for Deep Creek during summer months.....	85
Figure 33. Specific conductance vs. distance downstream for Deep Creek during the winter months only.....	85
Figure 34. Temperature vs. downstream distance for Deep Creek during winter months shows.....	86
Figure 35. Specific conductance vs. distance downstream for Deep Creek during the fall months only.....	86
Figure 36. Temperature vs. downstream distance for Deep Creek during the fall.....	87
Figure 37. Specific conductance vs. distance downstream for Deep Creek for spring months.....	87
Figure 38. Temperature vs. distance downstream for Deep Creek during the spring.....	88
Figure 39. Figure shows a cumulative plot of all specific conductance measurements for Cabin Creek.....	88
Figure 40. Relationship between specific conductance and downstream distance for Cabin Creek during summer.....	89
Figure 41. Summer relationships of temperature vs. downstream distance for Cabin Creek.....	89
Figure 42. Specific conductance vs. downstream distance for Cabin Creek during winter.....	90
Figure 43. Fall trends in specific conductance vs. downstream distance in Cabin Creek.....	90
Figure 44. Specific conductance vs. downstream distance for Cabin Creek in the spring.....	91
Figure 45. Plotting temperature vs. distance downstream in Cabin Creek during winter months.....	91
Figure 46. Temperature vs. downstream distance on Cabin Creek for fall measurements.....	92
Figure 47. Temperature vs. downstream distance along Cabin Creek in the spring.....	92

Figure 48. Plot of all specific conductance measurements in relation to downstream distance for Creek 90. ....	93
Figure 49. Specific conductance vs. downstream distance for Creek 90 in the summer .....	93
Figure 50. Specific conductance measurements during the fall at Creek 90 .....	94
Figure 51. The general trend for winter specific conductance values at Creek 90. ....	94
Figure 52. Trends that dominate fall and winter conductance values at Creek90.....	95
Figure 53. Summer temperature patterns at Creek 90 .....	95
Figure 54. Winter stream temperatures at Creek 90 .....	96
Figure 55. Fall stream temperatures at Creek 90 .....	96
Figure 56. Spring stream temperatures at Creek 90.....	97
Figure 57. Vertical hydraulic gradient vs. downstream distance for Deep Creek.....	97
Figure 58. Vertical hydraulic gradient vs. downstream distance for Cabin Creek .....	98
Figure 59. Vertical hydraulic gradient vs. downstream distance for Creek 90. ....	98
Figure 60. Stage height values for the South Fork of the Catawaba River .....	99
Figure 61. Relationship between streambed slope and vertical hydraulic gradient. ....	99
Figure 62. The relationship between sediment depth and vertical hydraulic gradient .....	100
Figure 63. Relationship between hydraulic conductivity and $D_{50}$ for Deep Creek, Cabin Creek, and Creek 90. ....	100
Figure 64. Hydraulic conductivity versus sediment depth for Deep Creek, Cabin Creek, and Creek 90. ....	101
Figure 65. Sediment depth versus average Darcy flux for Deep Creek, Cabin Creek, and Creek 90. ....	101
Figure 66. Relationship between $D_{50}$ and average Darcy flux for Deep Creek, Cabin Creek, and Creek 90. ....	102
Figure 67. Longitudinal discharge measurements for Deep Creek .....	102
Figure 68. Longitudinal discharge measurements at Cabin Creek .....	103
Figure 69. Longitudinal discharge measurements for Creek 90 .....	103
Figure 70. Stable isotope data for Deep Creek .....	104
Figure 71. Stable isotope data for Cabin Creek .....	104
Figure 72. Stable isotope data for Creek 90.....	105
Figure 73. Nitrate concentration in the study creeks .....	105
Figure 74. Nitrate versus ammonium concentrations at Deep Creek.....	106
Figure 75. Nitrate versus ammonium concentrations for Cabin Creek.....	106
Figure 76. Nitrate versus ammonium concentrations at Creek 90. ....	107
Figure 77. Calcium versus magnesium concentrations at Deep Creek s. ....	107
Figure 78. Calcium versus magnesium concentrations at Cabin Creek .....	108
Figure 79. Sulfate concentrations .....	108

## List of Referenced Tables

Table 1. Temperature and specific conductance record days and precipitation characteristics for the days leading up to them.

Table 2. Cumulative sediment depth data for every 25 m measurement point showing distance downstream, average sediment depth at each 25 m measurement point, as well as standard deviation.

Table 3. Table showing all point discharge measurements for each of the three study creeks.

Table 4: Unit discharge for summer baseflow in the three study creeks.

Table 5: Unit peak flow data for a selected high discharge event. Table also shows time taken to attain peak flow from the beginning of the precipitation event.

Table 6: Average unit discharge for water year 2010 and 2011 shows Cabin Creek having the largest values from available data sets in 2010 and 2011.

## *Acknowledgements*

Completion of this research would not have been possible without the support, advice, and encouragement of a great many people. First, I would like to extend a special thank you to my advisor, Dr. Anne Jefferson, whose stellar advice guided me through this project to completion. Her incredible knowledge of the field of hydrology proved invaluable for answering my numerous questions and editing drafts of this document. Thanks also goes out to the other two members of my committee Dr. Craig Allan and Dr. Missy Eppes, who helped direct this project to completion by helping me focus and execute a plan of action. Also, I'd like to thank my parents, who have encouraged me through this whole process and are responsible for sparking my love and interest of the natural world and learning in general. Thank you to Haywood and Sabine Rankin for not only allowing me to conduct research on their beautiful property, but also for ensuring that this incredible piece of land is preserved for generations to come. Many thanks also go out to everyone who assisted me along the way in field and/or lab work. I'd like to thank Ralph McGee for help in the field and for his unwavering determination and sense of humor, which helped me stay motivated and on schedule with my work. I'd also like to thank Jennifer Aldred, who helped me through several sessions of field data collection and gave me moral support and encouragement. Also thank you to Rebecca Deal and Claire Chadwick, who both assisted me in completing water chemistry lab work. Finally, I'd like to thank my undergraduate advisor Dr. Wes Dripps, whose enthusiasm for the subject of hydrology rubbed off on me, prompting me to pursue my master's degree.

## ***Abstract***

Despite their size, the health of headwater streams has enormous implications in terms of water quality and general downstream health for larger river systems. The ecological micro-niches provided by headwater systems foster biodiversity and help process pollutants and excess nutrient loads. More research is needed to understand the dynamics of surface and subsurface hydrologic interactions and how they vary based on extremely localized geomorphic influences. There is still much to learn regarding how groundwater and surface water interact because the processes that control these interactions change greatly over space and time. This study quantifies the degree of surface and groundwater interaction in three streams in the Piedmont region of the Carolinas. The streams in this study may serve as reference reaches for stream restoration projects in the southeast, as very few anthropogenic factors are thought to be influencing the three study streams.

Field work conducted in 2009 in 13 watersheds on 307 ha of relatively undisturbed land in the Piedmont region of North Carolina showed indications of downstream sediment coarsening in 10 of 13 streams. Large woody debris jams were found to contribute to accumulations of poorly sorted sediment that had low  $D_{50}$  values relative to overall mean  $D_{50}$  values for the stream as a whole. Additional work in 2010 – 2011 focused heavily on three specific 1<sup>st</sup> order streams that, after thorough geomorphic characterization, were determined to be representative of typical environments found on the property.

In order to quantify specific surface/groundwater interaction points and to standardize data collection, repeat measurement areas were established at 25 meter intervals in each of the three intensively studied streams. Eighteen rounds of temperature and specific conductance measurements were collected along these 25 m intervals at each creek from July of 2009 – April



of 2011. Temperature and specific conductance measurements repeatedly showed evidence for groundwater upwelling in specific areas of two creeks. The third creek, located in a different lithology, showed no evidence for distinct groundwater upwelling zones, instead showing a pattern of more gradual and diffuse contributions of groundwater to baseflow. Where bed substrate allowed, piezometers were installed at 25 m increments on each of the three creeks and five separate rounds of head gradient measurements were collected from autumn 2010 to spring 2011. Vertical head gradients showed repeated upwelling trends that corresponded with where specific conductance and temperature perturbations were observed in two of the creeks.

Sediment depth measurements were performed at 25 m increments prior to the installation of piezometers, and  $D_{50}$  values were calculated for sediments at each piezometer. Negative correlations were found for sediment depth versus vertical hydraulic gradient ( $p = 0.05$ ) and for sediment depth versus  $D_{50}$  ( $p = 0.001$ ). Longitudinal profile surveying of each creek allowed for a comparison of  $D_{50}$  versus streambed slope, for which a positive correlation was found ( $p = 0.028$ ). Water chemistry samples taken at repeat 25 m sampling points were found to have elevated  $\text{Ca}^{2+}$  concentrations at probable areas of groundwater upwelling. Stream water had elevated nitrate concentrations upstream of debris jams. In several instances nitrate diminished by as much as 50% immediately below large woody debris jams and  $\text{NH}_4^+$  concentrations tended to be highest where nitrate was low.

Overall, the results of this research provide information on the factors that influence surface and groundwater interaction and the degree to which they vary based on surface changes in geomorphology. Large woody debris jams were found to be most influential in creating surface/sub-surface exchange processes. The results highlight the need for stream restoration projects to include debris jams and coarse woody material in restored headwater systems.

Increased interaction between surface and groundwater systems will result in natural filtration and bioremediation processes, which will be beneficial for downstream water quality and the millions of people and animals that depend on clean drinking water.

## ***1.0 - Introduction and Purpose***

In terms of total combined linear distance, headwater streams (1<sup>st</sup>, 2<sup>nd</sup>, and 3<sup>rd</sup> order) are the most common type of stream encountered in any landscape (Peterson et al., 2001). As such, headwater streams strongly influence landscape geomorphology and often determine the overall characteristics of a watershed. This study will focus on 13 first to third-order streams located within second growth forest in Gaston County, North Carolina. All the streams are located on a relatively pristine tract of land, a rarity for the quickly expanding Charlotte area. Initial field observations have revealed the presence of hyporheic flow in a subset of the streams as well as varying degrees of surface water and groundwater interaction. The purpose of this study is twofold: (1) to examine how much of baseflow is contributed by either concentrated or diffuse source areas, and (2) to analyze the role stream bed sediments play in determining groundwater-stream exchange. These data may be used to help restore watersheds that are in need of restoration and may serve a role in helping to better manage dwindling and over-allocated water resources.

Headwater streams are widely cited as being integral to proper ecological functioning of downstream environments (Karr and Dudley, 1981; MacDonald and Coe, 2007). The fact that small streams can provide micro-ecologic niches suited to specific organisms in a manner that larger (>4<sup>th</sup> order) streams can't means that destruction of headwater environments can have enormous impacts in terms of water quantity and quality (Alexander et al., 2007; Meyer et al., 2007). Disruption of hydrologic flowpaths through urbanization and forest clearing can severely limit that watershed's ability to process pollutants and will negatively influence biodiversity (Meyer et al., 2007). As the population of North Carolina continues to grow and more land is converted from forest and agriculture to urban development, more headwater stream watersheds

will be cleared (Elmore and Kaushal, 2008), impacting the hydrology, geomorphology, water quality, and ecology of the headwater streams themselves and larger rivers downstream. Few studies have been conducted in the Piedmont region of North Carolina that quantify hydrologic interactions in relatively unaltered environments. In the future, hopefully information from this study will be used in headwater stream restoration projects, perhaps with streams in this study serving as reference reaches.

## ***2.0 - Literature Review***

### ***2.1 - Headwater Streams: Heterogeneity of Groundwater/Surface water Interactions***

Groundwater and surface water represent one connected resource, though, historically, they have been considered separate systems (Kalbus et al., 2006). Processes between the two are interrelated to such a degree that it is now seen as more logical to treat it as one system. Over the past ten to fifteen years, studies concerning the mixing of groundwater and surface water within the stream bed have grown more prevalent within the hydrologic literature, partly because groundwater-surface water interaction is now seen as important for water resource management, contaminant tracking, and chemical exchange processes (Kennedy et al., 2008; Oxtobee and Novakowski, 2002; Sophocleous, 2002).

Many complex processes that occur within streams are influenced by hydraulic conductivity and the groundwater gradient compared to the current stream stage height. Figure 1 shows how water table gradient relative to stream stage height influences local flowpaths. Water either comes from the streambed into the stream (gaining stream) or flows through the sediment and into the groundwater (losing stream). Streams may said to either be gaining or losing based on variations in streambed topography (Figure 2) (Kalbus et al., 2006). One component of groundwater-stream interaction is the hyporheic zone, which is defined as the mixing area

between the surface streambed and reserves of deep groundwater. The hyporheic zone functions as a dynamic environment critical to nutrient cycling and as an important habitat for aquatic organisms (Biksey and Gross, 2001; Boulton et al., 1998; White, 1993).

According to Darcy's Law, discharge ( $Q$ ) is proportional to the difference in water elevation (i.e. hydraulic head,  $(dh)$ ), and is inversely proportional to the length of the flow path ( $dl$ ). In other words, as hydraulic head differences increase, discharge will increase and when the flow path is lengthened (i.e. a decrease in gradient) discharge will decrease (Darcy, 1854). Darcy's Law is described by the equation below, where  $A$  is equal to cross sectional area (proportional to discharge) and is combined with hydraulic conductivity ( $K$ ) of the porous media. The negative sign shows that flow is toward the direction of decreasing hydraulic head (Fetter, 1994).

$$Q = -KA(dh/dl)$$

Over their entire linear length, streams are rarely homogenous in terms of bed slope. A deviation in slope in the form of either convex or concave areas has been shown to have measureable effects on groundwater interactions with stream water (Harvey and Bencala, 1993). Stream water recharges the subsurface in zones where there is a decrease in slope (i.e. concave) and discharges to the stream in areas where slope increases (i.e. convex).

Wondzell and Swanson (1999) found that major floods can cause vast changes to the groundwater and surface water exchange dynamics. The floods serve to rearrange large woody debris jams and can often change channel bed topography such that areas that were once zones of upwelling change to downwelling zones and vice versa. Changes were found to be heavily scale dependent. At the sub-reach scale, changes in subsurface flowpath length, as well as changes to

the lateral continuity of the hyporheic zone were found to be extensive, with massive reworking following very large (recurrence interval of 50 or more years) floods (Wondzell and Swanson, 1999). Conversely, at the reach scale, variations were often found to cancel one another out, resulting in little net change to surface and subsurface water interaction. In other words, a shortened flow path at one end of the reach may be balanced out by a lengthened one at the opposite end.

Hydraulic conductivity of streambed sediment has also been found to be heavily scale dependent. Schulze-Makuch et al., (1999) found that hydraulic conductivity ( $K$ ) increased in heterogeneous porous media by half an order of magnitude for every full order of magnitude increase in scale. No scale variations in  $K$  were found in homogenous materials (Schulze Makuch et al., 1999). This relationship is believed to exist because as scale increases the likelihood of having large, preferential flowpaths present in the area increases as well. Sperry and Peirce (1995) examined three characteristics of porous media (particle size, particle shape, and porosity) and found that particle size was the most influential on hydraulic conductivity. Thus in general, the smaller the grain size the lower the hydraulic conductivity. Particle shape was found to be next most important (although only for grains larger than 295 – 351  $\mu\text{m}$ ) and porosity was determined to be least influential (Sperry and Peirce, 1995).

In addition to variability in space, groundwater and surface water interaction zones vary a great deal over time. Changes in either river stage or groundwater flow alter the subsurface flow regime. Consequently, different hyporheic zones within a single reach may contrast starkly in terms of their respective proportions of groundwater vs. surface water (Biksey and Gross, 2001). This extreme complexity underscores the difficulty associated with attempting to directly measure flux rates within the hyporheic zone.

## ***2.2 - Importance of the Hyporheic Zone***

The hyporheic zone is of interest to more than hydrologists, as the implications of groundwater-stream mixing are far reaching and also encompass the fields of ecology, biology, and chemistry. An important factor to remember when attempting to gain perspective on the importance of groundwater and surface water interactions is the concept of dynamic gradients, which are present at all scales within an ecosystem. As Boulton et al. (1998) noted, gradients that exist at the microscopic scale, such as variations in redox potential, are vital in controlling processes that influence nutrient cycling and the basic functioning of an ecosystem. At the megascale, the mixing of groundwater and surface water within a hyporheic corridor has dire implications for both aquifers and surface water bodies if either of the water sources contains pollutants. Effects can propagate for many kilometers beyond the site of initial contamination. Thus, there is a practical interest in actively studying the hyporheic zone and recognizing its role as an active ecotone with the ultimate goal being to protect valuable sources of surface water and groundwater. Although not the primary focus of this study, it is important to note that surface-subsurface exchange is highly complex and vital for ecologic health, as nutrient flux from one zone to the other has been shown to create suitable habitat for aquatic organisms and control chemical cycling in streams (Brunke and Gonser, 1997; Findlay, 1995).

## ***2.3 - Determining Groundwater-Stream Water Interactions***

There are several methods for identifying locations where groundwater and stream water are interacting, and for quantifying the magnitude of these interactions. Some of these methods include well and piezometer installation and monitoring, longitudinal stream discharge measurements, and temperature and specific conductance measurements. These methods are briefly described below.

Determining the magnitude and flow direction between groundwater and surface water can be accomplished through measuring water levels in wells and piezometers that have been installed along the banks of the stream as well as within the stream bed itself. A number of studies have illustrated the effectiveness of this technique (Baxter et al., 2003; Lee and Cherry, 1979; Wondzell, 2006; Wroblicky et al., 1998). Measuring the degree of surface vs. groundwater interaction is easily and accurately accomplished using piezometers, which measure hydraulic conditions at a single depth in the aquifer (Freeze and Cherry, 1979; Kalbus et al., 2006). Multiple piezometers are always used, and the difference in head elevation over a lateral distance is noted in order to determine horizontal hydraulic gradient. In a vertical piezometer nest, groundwater upwelling is occurring if heads are lower in the shallower piezometers and downwelling is occurring if heads are higher in the shallower piezometers. The same idea can be applied to groundwater-surface water interactions, by comparing the head in a streambed piezometer to the elevation of the stream surface.

Measuring stream discharge can be a valuable method when assessing the degree of surface/groundwater interaction (Kalbus et al., 2006). Taking cross sectional discharge measurements along the length of a stream allows for quantification of large scale water gain or loss in a stream (Kalbus et al., 2006). In reaches with no tributaries, the difference between successive discharge measurements quantifies water gain or loss. Velocity gauging measurements can be taken using a flow meter or with a simple tracer experiment. Provided that the instrument is calibrated correctly, flow meter error has been estimated to be as low as 2 percent (Carter and Anderson, 1963). While not quite as accurate, salt dilution gauging is said to have median error values that typically fall in the range of 4.7 – 7.3 percent (Day, 1976). Salt



dilution gauging is useful in streams that are either stagnant or too shallow to support use of a flow meter and this range of error is still acceptable for many applications.

Compared to surface water temperature, groundwater temperature shows little temporal variation (Kalbus et al., 2006; Scanlon et al., 2002; White et al., 1987). Groundwater maintains a relatively constant temperature with no diurnal temperature cycles and only subdued seasonal changes in temperature. During the summer, groundwater discharge zones will show up as distinct cold spots when compared to the warmer surface water that has had more time to be heated by solar radiation and sensible heat transfer. Conversely, during the winter when atmospheric temperatures drop, groundwater discharge zones will be warmer than baseflow (Poole and Berman, 2001). When identifying zones of groundwater discharge, temperature signals are commonly used in conjunction with elevated salinity readings (Oxtobee and Novakowski, 2002). Conductivity higher than overall background levels in surface water is another indication of groundwater discharge. Groundwater moves through the subsurface very slowly and the longer it stays in contact with underground geologic material, the more dissolved mineral constituents are likely to be present. Higher concentrations of dissolved solutes relative to the streams background salinity are indicative of groundwater discharge zones (Fernald et al., 2006).

#### ***2.4 - Fractured Rock Flow and Hydrogeology of the NC Piedmont***

When compared to flow in porous media, flow through fractured rock is often a great deal more complex because of the difficulty in modeling the variability in rock fractures. This increased complexity is especially true with non-interconnected fracture systems, the geometry of which is difficult to accurately define (Cook, 2003; Oxtobee and Novakowski, 2003). The properties of flow through such fractures are heavily scale dependent and the hydrologic

literature separates fractured rock flow into two categories: the continuum approach and the discrete fracture approach (Eaton, 2006; Hsieh, 1998). In the continuum model approach, water flow through each individual fracture is not taken into account. Rather, the dynamics of the fracture network are equated more toward those attributed to flow through a porous media. Conversely, in the discrete fracture approach flow volume is quantified through data collected from individual fractures (i.e., size, transmissivity, etc.) (Hsieh, 1998).

Few studies have attempted to quantify the amount of groundwater contributed by diffuse versus discrete source areas in fractured bedrock. Although variations in local lithology may apply to certain situations, fractured bedrock streams from one study performed in Ontario were found to have more water contributed through discrete fracture zones than by diffuse seepage areas (Oxtobee and Novakowski, 2002). The authors also state that it is believed to be uncommon to lose surface water in the stream to fractures in the bedrock

The hydrogeology of the North Carolina Piedmont is extremely complex owing to the fact that much of it is underlain by metamorphic and igneous fractured crystalline bedrock. These rocks have all been uplifted, weathered, or eroded to some degree, which has caused widening of preexisting fractures as well as the creation of entirely new ones. Within the Piedmont region it is common for bedrock outcrops to be exposed along ridgelines as well as within stream valleys. Areas where surface bedrock is not visible is often overlain by regolith comprised of saprolite, alluvium, and soil that has been described as being less than 100 ft thick in most instances (Daniel, 1989; Daniel and Dahlen, 2002).

## ***2.5 Controls on Sediment Depth and Size Distribution***

Large woody debris jams have been shown to have a great impact on sediment size distribution as well as sediment depth (Manga and Kirchner, 2000). Large woody debris jams increase flow resistance within a stream channel, resulting in increases in sediment storage, the influence of which can be seen in sediment size distribution in reaches downstream of these debris jams. Much research has demonstrated that wood is less mobile in headwater streams than it is in other, higher order streams (Wohl and Jaeger, 2009). In general watersheds with less forest cover may be expected to have fewer large woody debris jams. Less overall wood load in a stream equates to less congestion meaning the channel is kept open, thus preventing wood from accumulating. Once out of headwater streams, wood generally decreases in the downstream direction as total stream power increases (Wohl and Jaeger, 2009).

## ***3.0 - Hypotheses***

The goal of this study is to identify, quantify, and explain spatial variability in groundwater-stream interactions in Piedmont headwater streams, as they are related to stream sediments and geomorphic features. To assist in that goal, study methods were designed around testing the three hypotheses, as listed below.

1. Null Hypothesis: Median streambed grain size ( $D_{50}$ ) at the reach scale has no correlation with stream slope.

Alternate Hypothesis: Median streambed grain size ( $D_{50}$ ) is positively correlated with stream slope.

2. Null Hypothesis : Baseflow flowing into the streams is being contributed via diffuse source areas in an even longitudinal pattern along the streambed.

Alternate Hypothesis: Concentrated source areas at places along the streambed are responsible for the majority of baseflow contributions.

3. Null Hypothesis: Streambed sediment thickness and surface size distribution do not correlate with zones of groundwater upwelling or downwelling or predict hydraulic conductivity.

Alternate Hypothesis: Streambed sediment thickness positively correlates with upwelling zones and coarser and better sorted sediments have greater hydraulic conductivities than finer or more poorly sorted sediments.

### *3.1 Rationale for Hypotheses*

Hypothesis 1:

**Median streambed grain size ( $D_{50}$ ) is positively correlated with stream slope.**

Several studies in headwater streams have found a downstream coarsening trend in watersheds up to 10 km<sup>2</sup> in area, above which point a more typical downstream fining trend is usually observed (Brummer and Montgomery, 2003). Wolman pebble counts performed in this study suggest downstream coarsening is present in 10 of 13 streams on the Redlair Forest property. The reasons for this are likely explained by two mechanisms. First, woody debris and debris jams spaced throughout the streams may be constraining and trapping large amounts of fine grained sediment, thus preventing larger accumulations downstream of these debris jams that result in higher median grain sizes. Changes in streambed slope are also likely a factor, as stream slope in a given area is a determinant of unit stream power and the size of the individual grain that can be mobilized. To determine whether slope or the presence of debris jams has the greatest influence on downstream sediment size more research is needed in these small 1<sup>st</sup> order headwater streams, which have received little study compared to larger streams and rivers.

Understanding the extent that changes in slope alter the normal downstream fining sequence is important for landscape stability analyses and determining where incision versus accretion zones may be occurring.

Hypothesis 2:

**Concentrated source areas at places along the streambed are responsible for the majority of baseflow contributions.**

In addition to stream slope, discharge is also a factor in determining stream power. Being able to determine whether headwater streams in the Piedmont of North Carolina derive the majority of their baseflow diffusely and gradually or in a more concentrated fashion is also important in terms of landscape stability and in the maintenance of general stream health. Given that headwater streams are the most common type of stream encountered on any landscape, some degree of urban development within many watershed boundaries is unavoidable as population continues to increase. Knowing if a concentrated discharge pattern is associated with streams in an area proposed for development is important for deciding where to build a new structure in terms of both water quantity and quality. If construction begins in a watershed that contains flowpaths contributing to stream baseflow in a relatively diffuse pattern, the influence of several small buildings in the watershed will likely be minimal in terms of effects on stream baseflow. Conversely, if a building is constructed over a high permeability fracture network that contributes disproportionately to baseflow, it may have a large effect on the total water volume in the stream. Similarly, in terms of water quality and pollutant transfer to a stream, a zone of high permeability like a fracture network will likely discharge concentrated pollution-laden water more quickly to a stream than will a system that is dominated by diffuse baseflow contributions. In the diffuse system, although the same toxin may be present, more unpolluted

water will also be available to dilute the pollutant, thus mitigating some of the negative ecological consequences.

Additionally, discrete fracture zones in streams may also act as biological hotspots as they serve to moderate stream temperature in localized areas during extreme temperatures of summer and winter (Boulton, 2000). During summer, large volumes of discharging groundwater could serve as a refuge from the much warmer surrounding surface water heated through solar insolation. In the winter the reverse would be true, where this zone of cooler upwelling would transition to one of warmer discharge as the lack of solar insolation would leave the stream much colder.

Hypothesis 3:

**Streambed sediment thickness positively correlates with upwelling zones and coarser and better sorted sediments have greater hydraulic conductivities than finer or more poorly sorted sediments.**

Being able to definitively correlate sediment thickness with upwelling and downwelling zones is important for fostering greater interaction between surface and subsurface water.

Through this research, structures can be better engineered to encourage downwelling in desired areas. The more interaction surface water has with the hyporheic zone, the greater the potential microbial bioremediation benefit and the more natural filtration will take place. Understanding how upwelling and downwelling zones vary based on sediment size and sorting and how these changes influence hydraulic conductivity is important in determining the rate of potential flux from surface to subsurface.

Stream structures such as debris jams and general debris spaced along the length of the channel introduces heterogeneity that promotes groundwater/surface water interaction. Without

their presence, fewer pronounced changes in head gradient would be seen and less pronounced upwelling and downwelling would result (Wondzell and Swanson, 1999). The downwelling and upwelling induced by these debris jams would likely result in preferential movement of water through subsurface flowpaths with better sorted, coarser sediments. Thus the location of upwelling zones would likely be controlled in part by the size and extent of surface debris jams, as well as the subsurface locations of high hydraulic conductivity zones. Wolman pebble counts, used to assess the streambed sediment size distribution, are easily performed in the field and any strongly positive correlations found between median streambed grain size and hydraulic conductivity or upwelling would be a powerful tool to quickly assess potential subsurface flow patterns.

#### ***4.0 - Setting***

The study area comprises the Redlair Forest, 307 ha encompassing 13 watersheds, in Gaston County, North Carolina. Redlair Forest spans 5.1 km along the east bank of the South Fork of the Catawba River, a 5<sup>th</sup> order stream in the Santee River basin. The study area lies at 35.301276° latitude and -81.084429° longitude, in the Piedmont physiographic province. The Redlair study site represents a relatively undisturbed study location for the Piedmont of North Carolina, the vast majority of which has been subject to agricultural processes or other anthropogenic changes at some point during its history. Many of the valleys surrounding the streams at Redlair were never plowed because of the steepness of the terrain. Nowhere on the property, however, is old growth forest present (Rankin, The Redlair Preserve, 2007).

Bedrock in the study area is quartz-sericite schist or felsic meta-volcanic rock (Links, 2008). Bedrock exposures in stream channels generally increase when moving north to south in the study area. Many areas of exposed bedrock within the creeks are highly weathered, having

degraded to saprolite in some cases. Soils in the study area are dominantly Tatum Gravelly Loam in the northern half of the property with Cecil Sandy Clay Loam, Pacolet Sandy Clay Loam, and Pacolet Sandy Loam dominating the southern part of the property (Soil Survey Staff, USDA). Slopes range from 0 – 8% in areas closer to the river and from 8 – 20% in steeper areas around the headwaters of streams.

The climate of the North Carolina Piedmont is humid subtropical with hot, humid summers, and cool winters. Mean annual temperature for Gastonia, NC, the closest city to the study site, is approximately 15°C with average annual precipitation of 114 cm. Mean daily temperature during summer usually ranges between 25 - 28°C with maximum daytime temperatures reaching as high as 38°C several times per summer. Mean daily temperature during winter is typically between 2 - 5°C with lows reaching -12°C during a few nights each winter. Precipitation is evenly distributed throughout the year with no prominent wet or dry season. March and September tie for highest monthly average precipitation (10.82 cm) while lowest monthly average precipitation is seen in April (7.34 cm) (State Climate Office of North Carolina).

Vegetation is composed of plants typically found in a temperate mixed-hardwood deciduous forest and appears to gradually become denser when moving north to south on the property. Oak, tulip poplar, sweetgum, hickory, ash, and maple trees make up some of the most commonly found trees (Rankin, 2007). Low lying shrubs, such as mountain laurel, and smaller trees fill the understory in many areas, making several distinct and well-developed canopies at varying heights. Some upland parts of the study area are used as pasture or have residential development, and parts of the lowlands near the South Fork of the Catawba River are planted with row crops or used for hay.



## ***5.0 - Methods***

Many methods exist for determining zones of groundwater discharge to streams. Methods employed to determine locations of groundwater discharge/interaction to streams as well as properties of the stream bed porous media itself include: 1) reach scale geomorphic characterization; 2) repeat temperature and specific conductance surveys; 3) discharge measurements; 4) sediment depth measurements; 5) piezometer measurements; 6) stable isotope composition of surface water; 7) major cation and anion chemistry of surface water; 8) channel bedrock mapping; and 9) long profile surveying.

### ***5.1 Selection of Study Creeks***

Deep Creek, Cabin Creek, and Creek 90 were chosen because they are thought to be representative of a number of characteristics found in the streams at Redlair Forest. The lithology of Creek 90 is dominated by quartz-sericite schist and the soil at this northern extreme on the property has been described as being a Tatum Gravelly Loam (Soil Survey Staff, USDA). Moving further south on the property slope steepness and bedrock exposure were generally observed to increase, thus Cabin Creek was selected to represent a near end member stream on the property with Creek 90 representing the opposite extreme. The lithology of Cabin Creek is dominated by felsic meta-volcanic rocks with Cecil Sandy Clay Loam and Pacolet Sandy Clay Loam being the dominant soils. Lithology and soil type at Deep Creek were the same as at Cabin Creek. Deep Creek was included so as to better observe how changes in slope may influence stream characteristics if both streams have the same lithology and soil properties. These differences also gave the ability to potentially identify whether changes in slope or soil properties between watersheds are responsible for certain stream characteristics.

## ***5.2 Reach Scale Geomorphic Characterization***

For thirteen first to third order streams in the study area, geomorphology was described for multiple stream reaches. Reaches were defined as stream lengths with consistent bedrock coverage, dominant riparian vegetation type, channel slope, and valley geometry. The first reach was always described at the first appearance of water in the headwater portion of the stream. Reaches never exceeded 50 m in length. Each described reach was separated from upstream and downstream reach descriptions by a distance of anywhere between 10 – 50 m. This separation was designed to facilitate the description of geomorphically homogeneous reaches away from transitions in bedrock exposure, riparian vegetation, and valley geometry.

Within select reaches, Wolman pebble counts were performed to characterize surface sediment size distributions (Wolman and Union, 1954). Pebble counts involved pacing along diagonal transects of a reach while randomly and individually selecting 200 clasts. Typically, pebble counts involve collecting a minimum of 100 clasts. In this case, a sample size of 200 was selected because it has been estimated this reduces margin of error of grain size percentiles to less than 10% (Rice and Church, 1996). Error calculation was performed using the bootstrap statistical technique (Efron and Tibshirani, 1991); as cited by Rice and Church, 1996). Standardization was achieved by selecting the grain under the toe of the leading foot after each step. After selecting the pebble, the length of the intermediate axis was measured and recorded.

In most streams, three pebble count locations were selected per stream: one in the headwaters, one in the mid-stream area, and a final one close to where the stream flowed into the South Fork of the Catawba River. A total of 27 Wolman pebble counts were performed and basic statistics were calculated for each reach, including the size distribution, median grain size, and

degree of sorting. For each of those reaches, watershed area and stream gradient were delineated using a 3 m DEM in ArcGIS 9.3.

Upon completion of these general field descriptions and pebble count measurements, three first-order streams were selected for more focused study. These streams are referred to as Deep Creek, Cabin Creek, and Creek 90 (Figure 3). Throughout this study, streams will be referred to in this order, moving from Deep Creek in the central portion of the property to Cabin Creek in the south and finally Creek 90 in the north. Streams will be discussed in this order because Deep Creek represents the intermediate size between the two other streams, so presenting in this order will facilitate comparison. The streams were selected on the basis of being representative of streams in the field area and having watersheds that drain only one rock type, are dominantly forested, entirely contained in the study area, and lack dams.

### ***5.3 Discharge Measurements***

Odyssey water level loggers were installed in July 2009, 50-75 m upstream of the outlets of Cabin Creek, Deep Creek, and Creek 90. The stage recorder at Deep Creek is in an alluvial bedded pool just below a small knickpoint (~25cm). Stage recorders at Cabin Creek and Creek 90 are also in small pools, but have riffle sequences immediately upstream. The cross-sections at the stage recorders on Cabin Creek and Creek 90 are alluvial, but have more overall bedrock coverage in the general vicinity than is present at Deep Creek. Stage data was recorded at 15 minute intervals at each creek. A stage-discharge rating curve was developed for each stream, and used to attain a continuous estimate of discharge. Since the focus of this project was on groundwater contributions to baseflow, incorrect estimations of peakflows are not a significant problem.

Discharge measurements for the rating curves were taken during low, moderate, and high flow events using a Swoffer Model 3000 current meter in deep, narrow cross-sections, as these were the only areas that provided sufficient flow depth, even during rainstorms. Low flow gauging was completed with the Swoffer current meter, but required slight channel modification in order to concentrate the flow into a measureable volume. Concrete bricks were used to create a temporary v-shaped weir that funneled water to a depth and velocity adequate for measurement with the Swoffer current meter. Clay was spread along the upstream side of the bricks to ensure the bricks were as impermeable as possible. On three occasions, salt dilution and Swoffer gauging were performed together at each creek's stage gauge in order to better quantify discharge with multiple methods for error analysis purposes.

Salt dilution gauging is a widely accepted and proven method of discharge gauging within the literature and is one of the best methods to use in cases of very low discharge (Moore, 2004; Moore, 1990). Due to the fact that flow volume was very small ( $< 1$  L/sec), a constant rate injection method via Mariotte's bottle was used. Suitable measurement reaches for this technique were approximately 10-15 meters in length, had few if any obstructions (organic debris), and had enough turbulent flow to ensure adequate mixing throughout the entire lateral extent of the stream. Complete lateral mixing was verified using the YSI meter and checking that a consistent specific conductance value was obtained. It was difficult to find reaches that met all requirements, in particular finding ones with little organic debris and at least some turbulent flow. Measurement site heterogeneity is believed to be the largest sources of error when using this method. Channel modification was not necessary for measuring high and moderate flow events.

Error in low flow measurements was estimated by completely removing the brick weir from the stream and then rebuilding it in the same spot. After the weir was rebuilt discharge was measured. At most, discharge varied by 20% from one measurement to the next, and was usually only about 10% different.

Swoffer measurements and salt dilution measurements performed at the same time were generally not in agreement. Salt dilution measurements during low flow on Deep Creek yielded values that were 65% less than what was measured with the Swoffer method (0.65 L/sec vs. 1.83 L/sec). Results were in slightly better agreement on Cabin Creek, differing by 45%, but salt dilution still reported the lower value of the two methods (5.03 L/sec vs. 9.20 L/sec). Creek 90 showed the best agreement between the two methods (31% difference) and differed from Cabin Creek and Deep Creek in that salt dilution returned the higher of the two measurements.

#### ***5.4 Repeat Temperature and Specific Conductance Measurements***

In order to identify possible concentrated groundwater upwelling zones, temperature and specific conductance data were collected at 25 meter increments over the length of Deep Creek, Cabin Creek, and Creek 90. Surveys were made using a calibrated YSI 556 MPS meter over the course of a single morning or afternoon. Data were collected every four weeks beginning in July 2009. Measurements were taken only on days with no precipitation in the forecast and measurements were delayed a minimum of 24 hours following a rain event (Table 1). The YSI 556 MPS has temperature accuracy of  $\pm 0.15^{\circ}\text{C}$  and specific conductance accuracy of  $\pm 1\%$  of the actual reading.

#### ***5.5 Sediment Depth Measurements***

Sediment depth was measured by using a post pounder to drive a masonry spike into the streambed. The spike was marked in 5 cm increments. The bottom of the sediment was defined

as the depth at which five drops of the post pounder did not produce further measureable penetration of the rebar. After measurement depths had been recorded, at select sites the masonry spike was driven further into the streambed to qualitatively get a sense for what was impeding the spike's penetration. If an additional five to ten pounds produced consistent penetration, it was assumed that the substrate was sand to coarse gravel. If further pounds produced very little additional penetration large cobbles or saprolite were probably the cause of stoppage. Finally, if pounding the spike a further five to ten times produced zero additional penetration bedrock was assumed to be the reason for refusal.

Sediment depth measurements were taken in the study creeks at 25 m increments. At each point, five individual measurements were taken, centered around the temperature and conductance measurement site. One measurement was taken directly under the temperature and conductance measurement site, while the second measurement was taken one meter upstream in the thalweg, and the third measurement was taken one meter downstream in the thalweg. The fourth and fifth measurements were taken at the right and left water's edge in a cross-section that included the temperature/conductance measurement site and was perpendicular to channel orientation. Figure 4 illustrates how the measurements were configured. Sediment depth was recorded and averaged for all five measurement points.

### ***5.6 Piezometer Measurements***

Hydraulic head differences between the streambed and surface flow were measured using piezometers installed at each 25 meter measurement point where feasible, which was dependent on the streambed substrate. Piezometers are affordable and easy to construct and are capable of producing accurate and precise hydraulic gradient measurements (Baxter et al., 2003).

Piezometers were constructed of  $\frac{3}{4}$  inch inside diameter PVC pipe and were screened over the

bottom 8 cm of piping. All piezometers were 91 cm in length. In thin sediments, the piezometer was vertically driven as far down as is possible while in thicker sediments the depth of insertion did not exceed 36 cm. An insertion range of 31 – 36 cm below the top of the stream bed has been found to be adequate (Kennedy et al., 2008). A washer was fitted over a hex bolt and inserted into the base of each piezometer before the instrument was driven into the streambed to ensure the base did not become clogged with sediment. Upwelling was indicated by water in the piezometer being higher than the surface of the stream while downwelling was said to be present when water in the piezometer was lower than that of the surface stream water. Hydraulic gradient was calculated by dividing the difference in head values versus stream surface elevation by the depth of penetration of the screened interval as measured from the top of the screened interval to the streambed.

Falling-head slug tests were performed in each of the piezometers. Using the Hvorslev method, hydraulic conductivity was measured by rapidly adding a known volume of water to the piezometer and monitoring how quickly the system returned to equilibrium (Fetter, 1994). If a pebble count had not already been conducted at each location, one was completed at the time of hydraulic conductivity measurement using the methods described above.

Darcy flux values were calculated for the sediment at each piezometer by multiplying hydraulic conductivity by the measured vertical head gradients ( $K \cdot (dh/dl)$ ). Darcy flux values give an idealized flow velocity for a given area of sediment in units of distance/time. The flow velocity is said to be idealized because it does not take into account sediment porosity, and thus the tortuous path water must take around individual grains (true velocity) is not taken into account. Darcy flux values do incorporate hydraulic gradients, however, so they are a useful

means through which to compare relative flow velocity at each piezometer in terms of upwelling and downwelling.

Repeat falling head tests were conducted on two piezometers in Cabin Creek (275 m and 300 m) for purposes of error analysis. Repeat measurements found hydraulic conductivity values were in very good agreement, differing by about 2% from one measurement to the next.

### ***5.7 Water Chemistry and Isotopes***

Water samples were collected at 25 meter increments along the study streams, with the goal of characterizing spatial heterogeneity in chemical and isotopic composition of baseflow. Isotopic samples were collected during the summer of 2009 as well as a second collection round on 8/31/10. Water chemistry samples were collected on 8/31/10. On each collection date samples were taken approximately one week after the most recent rainfall to absolutely ensure the creeks were at baseflow conditions. Post-collection, samples for isotopic analysis were stored in a dark area at room temperature. Water chemistry samples were filtered and frozen until they were processed for major cation and anion composition.

Samples for isotopic analysis were processed using the Liquid Water Isotope Analyzer (DTL-100) manufactured by Los Gatos Research. Accuracy is estimated at  $\pm 1\%$  for hydrogen and  $\pm 0.3\%$  for oxygen (Jefferson, pers. comm.). Between three and four lab replicate samples were processed for each analysis run in order to assess measurement precision and repeatability.

Samples for water chemistry were processed using a Dionex DX 500 Ion Chromatograph at UNC Charlotte. Percent variation from true value is estimated as follows:  $\text{NO}_3^- = 0.49\%$ ,  $\text{NH}_4^+ = 7.75\%$ ,  $\text{SO}_4^{2-} = 1.91\%$ ,  $\text{Na}^+ = 0.67\%$ ,  $\text{Mg}_2^+ = 3.15\%$ ,  $\text{Ca}_2^+ = 0.28\%$  (Chadwicke, pers. comm). Ammonium and nitrate were reported from the Dionex DX 500 Ion Chromatograph in terms of the formula weight of the ions, not in terms of total nitrogen present.



To correct for this, concentration values reported from the ion chromatograph in parts per million were converted to values in millimoles of nitrogen per liter of stream water.

### ***5.8 Bedrock Mapping***

Bedrock joint sets in the study streams were mapped using a Brunton compass. Mapping began at the beginning of perennial flow in each of the three streams and continued downstream to the confluence with the South Fork of the Catawba River. Joint sets were measured wherever possible, but in some instances large accumulations of sediment or organic debris covered measurement sites. In some cases, joint sets were weathered to such an extent that measurements were not possible. Strike and dip measurements were plotted using GEORient© version 9.5.0 (Holcombe, 2003). Statistical analysis on strike and dip measurements was performed in Oriana© v. 3.21.

### ***5.9 Longitudinal Profile Measurement***

Longitudinal profiles for the study streams were obtained using a Topcon® GTS-226 Electronic Total Station. A location with a view of as much of the channel as possible was chosen for the initial set up site. Points were then shot down the thalweg of each stream to its confluence with the South Fork of the Catawba River, or in the case of Cabin Creek, the confluence with South Rhyne Creek. When vegetation or topography obstructed line of sight for further measurements, the station was moved. A shot from the old site to the new site was performed before the instrument was moved, and a backsight shot was taken once the station was set up at the new site. Measurements were then continued down the creek thalweg. In general, points were spaced 2 – 5 m apart, with more points taken along areas of great slope change. Point density was also increased at the repeat temperature and specific conductance sites. For each

repeat measurement point, slope was calculated over a distance of 10 m, 5 m upstream and downstream of each measurement site.

Because of the long distance of the study streams from the nearest National Geodetic Survey benchmark, GPS points were recorded wherever the total station was set up. The GPS point where the instrument was first set up was imported into ArcGIS 9.3 and displayed on a digital elevation model (DEM) for the study area. The DEM elevation of the first total station set-up site was used as the starting elevation from which readouts from the relative elevations reported by the instrument could be either added or subtracted to calculate the actual elevation. For example, the real elevation where the total station was set up at Creek 90 was 208 m. From this first set up point, shots were taken down the thalweg of the stream until vegetation became too thick or topography obstructed the line of sight at which point a shot to a new site was taken. The total station was then moved to the new site and a backsight shot to the previous point was taken to account for the different orientation at the new site. The total station tracked elevation difference from one shot to the next based on the set up site location and changes in elevation values were then subtracted from the original value of 208 m.

## ***6.0 - Results***

### ***6.1 Geomorphic Descriptions***

#### ***6.1.1 Deep Creek***

During dry conditions, the first appearance of water in Deep Creek occurred where a very small spring emerged at the base of a 5 m knickpoint, located at N 35.2999° W 81.0902° (Figure 5). Of sixteen equally-spaced measurement points in the stream bed, 12 were fully covered by alluvial substrate, two were dominated by exposed bedrock, and two had roughly equal distributions of alluvium and bedrock (Figure 6). Exposed bedrock is most prominent in the

middle third of the creek, with a small amount in the first third and virtually none exposed in the final third. Flow patterns in Deep Creek more closely resemble pool riffle sequences seen in typical Piedmont streams than those seen in Cabin Creek, described in section 6.1.2.

Steep, v-shaped valley banks typify the first 200 m of perennial flow in Deep Creek. Beyond 200 m, the valley ceases being predominantly v-shaped and quickly develops a prominent floodplain that is between 2 – 5 m on both side of the stream from 200 m to 225 m. From 225 m down to the confluence with the South Fork Catawba River the valley is approximately 5 – 10 m wide on both sides of the stream. There is a large woody debris jam in Deep Creek at 99 m downstream that measures about 50 cm high and is located where valley confinement of the stream is at its greatest. Deep sediment has accumulated behind this jam for a distance of 5 – 7 m.

Deep Creek has three ephemeral tributaries, one of which joins the main stem 210 m downstream from perennial flow initiation. The two other ephemeral tributaries are upstream from the first appearance of perennial flow.

### ***6.1.2 Cabin Creek***

The first appearance of perennial water (hereafter designated as 0 m with subsequent downstream distances based off of this point) in Cabin Creek occurred at N 35.2941° W 81.0919°, 5 m below the confluence of two ephemeral channels (Figure 7). Cabin Creek has more exposed bedrock in its channel than the other two study streams and of the 14 measurement points along Cabin Creek, five were bedrock dominated, seven were dominantly alluvial, and two were roughly equal combinations of bedrock and alluvium (Figure 8). In some locations, bedrock was covered only with a thin veneer of sediment 2-4 cm thick.

Pools are more prevalent than riffle sequences along Cabin Creek. For the most part, this creek lacks the repeated pool riffle morphology, like that seen in Deep Creek. Instead of riffles, Cabin Creek loses elevation through a number of knickpoints that range in size from 20 cm – 2.5 m. This type of morphology is typical of steeply sloping streams, and Cabin Creek is the steepest of the three with an average slope of 5.4%. Valley confinement of the creek is most pronounced through the middle reaches (175 - 250 m) before the valley opens more again at 275 m and the stream flows into South Rhyne Creek. A very large (75 - 100 cm high) debris jam has constrained flow at 200 m where the valley is at its narrowest. Thick sediment accumulations are visible for 10 – 15 m behind the debris jam.

Vegetation along Cabin Creek is very similar to that found along Deep Creek. Vegetation along the banks appeared thickest along this stream, particularly in the middle reaches (100 m – 250 m). Two substantial tributaries feed the main stem of Cabin Creek: one ephemeral tributary above the point of perennial flow initiation and one that flows into the creek 160 meters downstream from perennial initiation. This second tributary is ephemeral along most of its length, with the perennial flow initiation point occurring only 20 meters before joining Cabin Creek.

### ***6.1.3 Creek 90***

Perennial flow initiation at Creek 90 occurs just below a 50 cm high bedrock knickpoint at N 35.3119° W 81.0967° (Figure 9). The knickpoint near the perennial flow initiation site is one of the only places where bedrock is exposed in the headwater reaches. Very little exposed bedrock is present within the channel, and what little bedrock there is appears almost exclusively 225 m – 300 m downstream of the perennial initiation point. Out of 15 measurement points along Creek 90, 13 were dominantly alluvial and two were mixed bedrock and alluvium (Figure 10).

One very small 25 cm high debris jam is located at 150 m. Similar to Deep Creek, Creek 90 had evenly spaced riffle pool sequences with few bedrock knickpoints in between.

Creek 90 contained a 27 meter dewatered section where flow has only been observed for very brief periods during or immediately following large precipitation events. A sediment wedge filling the channel in this dewatered section is likely an artifact of past land use, such as an old road bed. Below this segment, water reappears at the base of a 3 m knickpoint.

Once past 275 m the valley widens considerably and slope lessens, creating a swampy area with relatively few trees compared to other areas of the valley. Creek 90 empties into a backwater section of the South Fork of the Catawba River about 360 m downstream of its perennial initiation point. The valley that holds Creek 90 is the widest and appears most open in terms of vegetation density of any of the study creeks.

## ***6.2 Stream Longitudinal Profiles and Bedrock Mapping***

Longitudinal profiles of each stream showed differences in the average slope and number and height of knickpoints. However, in terms of bed substrate composition, all streams were dominated by bedrock where riffles were present and were dominantly composed of alluvium in pools. Of the three streams, Deep Creek (Figure 11) had the lowest average slope at 3.9%, with five prominent (25 – 100 cm) knickpoints and a large debris jam from 96 m to 99m. Cabin Creek (Figure 12) had the highest slope at 5.4%, and had four prominent knickpoints that were larger in size (50 – 250 cm) than the ones found in Deep Creek. Cabin Creek also had a much taller (~75 cm) debris jam causing an accumulation of sediment that extended from 194 m to 208 m. Creek 90 (Figure 13) had an average slope of 4.5%, intermediate between Cabin and Deep Creeks, and had two prominent knickpoints (~50 cm and 100 cm). Although Creek 90 lacked debris jams comparable in size to those seen on Deep Creek and Cabin Creek, one small

(25 – 50 cm tall) jam caused sediment backup for 2 m upstream. The slope of the dewatered reach was 2.7%, making it the third lowest slope of any of the repeat measurement reaches. The knickpoint below the dewatered section is about 3 m in height.

Both Deep Creek and Cabin Creek are dominated by felsic meta-volcanic rocks whereas quartz-sericite schist is the dominant rock at Creek 90. Strike and dip of bedrock joints and their downstream location in each creek channel were recorded and joint density per square meter was compared against stream slope (Figure 14). Of the 127 joints measured, 80% were found between 100 and 270 m, the middle portion of the stream comprising 45% of the stream's total length. When joint density per square meter was plotted against stream slope, a significant positive relationship was found ( $p = 0.000348$ ). As stream gradient increases joint density also increases because the more exposed joints there are, the higher the weathering potential will be. Another possible interpretation is that highly jointed bedrock in low slope areas is hidden by sediment. No relationship between joint density and upwelling at any of the probable upwelling zones was observed (described later).

Rose diagrams of bedrock orientation for Deep Creek, Cabin Creek, and Creek 90 were plotted in GeoOrient with statistics calculated in Oriana v. 3.21. Mean vector angles were  $111^\circ$  for Deep Creek,  $180^\circ$  for Cabin Creek, and  $55^\circ$  for Creek 90. All three creeks show a general NW – SE orientation of bedrock, with Cabin Creek having the most scatter.

### ***6.3 Sediment Size***

Sediment size data from the summer of 2009 showed a downstream coarsening trend in 10 of 13 streams where pebble counts were performed in 2 to 3 locations per stream. Data from the 13 streams suggested that woody debris jams lead to accumulations of poorly sorted sediment with small  $D_{50}$  relative to the mean  $D_{50}$  for the stream. Local influences may exert a stronger

influence on grain size than drainage area or slope in Piedmont headwater streams (Figure 15 - Figure 16). Typically grain size will be larger in areas where stream slope is higher, partly because stream slope is a factor in determining stream power. Higher stream power means that smaller sediments are transportable and winnowed out.

Of the three study streams, two showed a downstream coarsening trend in the 2009 data set (Figure 17 - Figure 18), but in winter 2010/2011, a larger number of pebble counts (3-10 per stream) were performed in them, and no downstream trend in median grain size ( $D_{50}$ ) was found (Figure 19). The finer scale at which the 2010/2011 pebble counts were performed shows more clearly what influence geomorphic variations such as debris jams or rock outcrops may have. Downstream fining is not seen at Redlair probably because the streams simply aren't long enough for appreciable changes in stream slope and width to lessen stream power and bring about noticeable downstream fining. Also, there is a continuous sediment source along the streams that produces coarse sediment throughout the study area.

Seven of the nine pebble counts performed in Deep Creek have similar  $D_{50}$  values of 12 to 17 mm (Figure 20). The smallest and largest  $D_{50}$  values are located within 50 meters of each other. It is possible that the  $D_{50}$  for 125 m would not be quite as large (23mm) if there were not a debris jam 25 m upstream at 100 m that traps finer grains resulting in a  $D_{50}$  of 5 mm.

The grain size distribution curve for Cabin Creek (Figure 21) shows no downstream trend, but the number of sites where pebble counts were conducted was limited by the extensive bedrock exposure. Median grain size values for the 200 m site in Cabin Creek were very low because of a large woody debris jam blocking sediment transport in the channel. Over 90% of the randomly selected grains were classified as medium to coarse grained sand. Within the very narrow thalweg of the channel at that site, flow velocity is sufficiently high to prevent finer

grains from settling and  $D_{50}$  is much higher ( $D_{50} = 17\text{mm}$ ). Once outside the thalweg (in areas next to and around the piezometer), flow velocity decreases markedly and surface accumulations of fine grain sediment thickens thus resulting in a large decrease in median diameters.  $D_{50}$  was assigned a value of 1 mm for this reach.

In most locations in Creek 90,  $D_{50}$  was between 16 and 22mm (Figure 22). The 150 m site had the largest median grain size (30 mm) due to a small debris jam that trapped finer sediment immediately upstream. The debris jam can be seen in the longitudinal profile of Creek 90 as a break in slope at 150 m. Similar to the Cabin Creek 200 m site, obtaining  $D_{50}$  values in Creek 90 at 325 and 350 m was complicated by a debris jam. Near the mouth of Creek 90, slackwater deposits from high flows on the South Fork of the Catawba River may also influence sediment sizes. At the two most downstream sites (325 m and 350 m), the  $D_{50}$  values were estimated to be in the sand and clay size classes, respectively. For these sites,  $D_{50}$  was assigned a value of 1 mm. Texture was determined by the “feel” method, whereby the sand felt gritty when rubbed between the thumb and forefinger and the clay particles were sticky, forming a strong ribbon when moist.

Consistent with the spatial variability in median grain size, the sediments in the three study creeks show no downstream trend in sorting. Uniformity coefficients ( $D_{60}/D_{10}$ ) ranged from 1.8 (very uniform) to 7.6 (poorly sorted/non-uniform), but 90% fell within a range of 2.5 – 4.5. Streambed sediment usually becomes increasingly well sorted in the downstream direction as slope decreases and stream channel width increases (Hoey and Bluck, 1999). Consequently, stream power decreases in the downstream direction and streambed sediments become better sorted as the range in particle size that can be transported decreases (Brierley and Hickin, 1985).



The mean  $D_{50}$  for 2010/2011 was 15 mm for the three creeks in this study whereas the mean from summer of 2009 for these three was 27 mm. Differences between mean sediment sizes measured in 2009 and 2010/2011 may be explained by a site selection bias in 2010/2011. While most reaches of Cabin Creek, Deep Creek, and Creek 90 had gravel alluvial cover, there were also bedrock and mixed bedrock-alluvial reaches in these streams. Where bedrock was present, it was not possible to install piezometers, and sometimes large cobbles inhibited piezometer installation. Pebble counts performed in 2010/2011 were performed at sites with installed piezometers, and are likely systematically biased to  $D_{50} \leq 30$  mm. The largest difference in grain size between the 2009 and 2010/2011 measurement sets was in Cabin Creek.

#### ***6.4 Sediment Depth***

In Deep Creek, 10 of 80 locations where sediment depth was measured had exposed bedrock, while 70 had alluvial cover (Figure 23). Average sediment depth at Deep Creek was 20.4 cm and standard deviation was 6.8 cm (Table 2). At 250 m, all five measurement points had exposed bedrock, and this site represents the minimum in terms of sediment depth on Deep Creek. Similarly thin alluvium ( $\leq 5$  cm) was also found in comparable riffle sequence locations on other streams. Deep Creek 250 m has a slope of 5.4%, creating a riffle sequence that likely prevents the accumulation of sediment. Measurement points in steeply sloping sections of the channel at 0 m and 25 m likely have sediment as their substrate because the very low discharge there limits stream power and the steep channel walls input much more colluvium here than at 250 m, particularly at 0 m. The deepest sediment occurred near the mouth of stream where the valley is widest and the stream is at its lowest slope. The lower stream gradients may result in a more frequently depositional environment. Of 70 sediment depth measurements along Cabin Creek, 39 points had exposed bedrock, the most of any stream (Figure 24). Overall, sediment

depth in Cabin Creek averaged 16.8 cm. The deepest sediment measured in any of the study streams occurred at 200 m on Cabin Creek, where sediment depth was ~80 cm. Deep sediment accumulated here because of a large woody debris jam 206 meters downstream that obstructed the channel.

Creek 90 was dominantly alluvial, with only 13 of 70 measurement points having exposed bedrock (Figure 25). The deepest sediment (71 cm) occurred at 325 m where slope is lowest and the valley reaches its widest point.

Overall, Creek 90 had the greatest average sediment depth (25 cm), while Deep Creek was intermediate (20 cm), and Cabin Creek was the least (17 cm). Creek 90 also had the greatest variability in sediment depth, with an average standard deviation for each group of five measurement points of  $\pm 10$  cm, while Cabin Creek and Deep Creek were approximately equal (6.5 cm and 6.8 cm, respectively).

At the time of sediment depth measurement, each point was also characterized as located within a pool or riffle. Riffles were assigned a score of 1, and pools were assigned a score of 0. Similarly, alluvial cover was assigned a score of 1, and exposed bedrock was assigned a score of 0. Five points were measured at each site, and average pool/riffle and alluvium/bedrock indices were calculated. Alluvium vs. bedrock and pool vs. riffle data for Deep Creek (Figure 6), Cabin Creek (Figure 8), and Creek 90 (Figure 10) all show similar patterns with the association for Cabin Creek being the most pronounced. Bedrock tends to be the dominant substrate in riffle sequences, while alluvial cover occurs dominantly in pools. The increased slope that characterizes riffle sections leads to a localized increase in stream power thus inhibiting the accumulation of large alluvial deposits. Pools are characterized by a decrease in slope and

therefore have lower stream power and deeper sediment accumulations. A statistically significant relationship was seen between  $D_{50}$  and sediment depth (Figure 26).

## 6.5 Hydrology

Stream gauging stations were set up near the mouth of each creek and discharge was calculated by constructing a rating curve for each stream (Table 3). When comparing the hydrographs of Deep Creek (Figure 28), Cabin Creek (Figure 27), and Creek 90 (Figure 29) there are differences in the manner each stream responds to precipitation. The largest peak discharge value (94 l/sec) occurred in Cabin Creek during a storm on March 28, 2010. A localized intense storm caused a 70 l/sec rise in discharge over the course of 30 min. This storm is the second largest over the period of record in Creek 90, although this creek only saw a peak discharge of just over 8 L/sec. The largest discharge event in Creek 90 occurred on the morning of August 19, 2010, when 10.9 cm of rain fell over the course of a few hours. The period of record for the gauge at Deep Creek is from October of 2010 to April of 2011, and the peak flow during this time was 20 L/sec on February, 5<sup>th</sup> 2011. The record is shorter here due to a malfunction of the data logger from possible tampering by hikers. Watershed area calculated upstream of each gauging site was 83,058 m<sup>2</sup> at Creek 90, 130,843 m<sup>2</sup> at Deep Creek, and 168,653 m<sup>2</sup> at Cabin Creek.

Unit discharge (L/sec/km<sup>2</sup>) comparisons of the three study streams show baseflow averaging about 30 L/sec/km<sup>2</sup> for Cabin Creek for summer of 2009 and 2010 (Table 4). Average unit discharge baseflow for Creek 90 was 13.3 L/sec/km<sup>2</sup>. Due to malfunctions of the gauge at Deep Creek, data for summer is not available, but based on a comparison of baseflow to the two other creeks during seasons when data overlaps, unit discharge baseflow is estimated at about 15

L/sec/km<sup>2</sup> for Deep Creek. Overall the data indicate slightly higher baseflow discharge at Deep Creek than Creek 90, which is logical given that drainage area for Deep Creek is 35% larger than at Creek 90. Drainage area for Cabin Creek is 24% larger than Deep Creek and 51% larger than Creek 90. However, unit discharge for Cabin Creek still seems large given the drainage area of 168,000 m<sup>2</sup>. There is a cow pasture above the headwaters of Cabin Creek that may possibly be contributing to the higher discharge during moderate and large peak flow measurements during storm events that were used in construction of the rating curve.

Peak flow data for a selected high discharge event show Cabin Creek's unit peak flow discharge as being 36% larger than for Deep Creek and 45% larger than Creek 90 (Table 5). Cabin Creek had the fastest time to peak flow, showing the influence larger watershed slope has in determining water transit characteristics.

Average water year unit discharge for data available in water year 2011 also shows Cabin Creek being the largest (Table 6). Average unit discharge for water year 2011 at Cabin Creek is 53% larger than at Creek 90 and 67% larger than Deep Creek. Here Deep Creek has the lowest unit discharge of the three, and is particularly different from Creek 90, which usually has the lowest values. However, it is worth remembering that Deep Creek has the shortest period of record due to logger malfunctions and the data set may display some level of bias.

## ***6.6. Temperature and Specific Conductance***

In Deep Creek, temperature and specific conductance measurements have a consistent groundwater upwelling signature at 125 meters characterized by increased specific conductance and a temperature perturbation (Figure 30). Every set of temperature and specific conductance data has shown perturbation at 125 m. In summer, temperature drops between 2 - 3 °C and specific conductance increases by 30 – 40 µS/cm (Figure 31). Overall summer temperature

trends show a gradual and consistent increase in temperature in the downstream direction (Figure 32). In winter, 125 m has a localized temperature increase of 2 - 3 °C (Figure 33). The increase in specific conductance during winter is not as marked as summer, with increases ranging from 5 – 15  $\mu\text{S}/\text{cm}$ . During fall (Figure 35) and spring (Figure 37) conductance increased by 10 – 15  $\mu\text{S}/\text{cm}$ . Other less consistently observed groundwater upwelling zones appear at 0 m and 275 m and appear in the temperature perturbation graphs most clearly during summer and winter. During the transition months of fall and spring the signatures at 0 m, 125 m, and 275 m are less pronounced (0.5 – 1 °C), but still visible (Figure 36 - Figure 38). Downstream trends in temperature during fall and spring fluctuate between a slight overall warming trend and a slight overall cooling trend.

Repeat temperature and specific conductance measurements in Cabin Creek show two zones of possible groundwater discharge, at 50 m and 200 m (Figure 39). Seasonal plots of specific conductance show elevated values at these two points most consistently during summer (Figure 40). A drop in temperature at both points supports the inference that groundwater is discharging there (Figure 41). During the summer, a temperature decrease ranging from 1.5 – 3 °C was observed at the 50 m point and a smaller cooling signature (0.25 – 1 °C) was seen at 200 m. Specific conductance measurements for winter, fall, and spring show the continued reappearance of elevated conductance at 50 m, while only a very small rise in conductance (1 – 5  $\mu\text{S}/\text{cm}$ ) is seen at 200 m (Figure 42) (Figure 43) (Figure 44). In some cases no rise in conductance was observed at 200 m. In general, specific conductance in Cabin Creek gradually decreases in the downstream direction. During the summer stream temperature was lowest at the 50 m point and gradually increased in the downstream direction. Winter shows a reversal of this trend with water temperature often being warmest at the 50 m point and gradually decreasing for

much of the remaining 275 m (Figure 45). Studies have shown that in the absence of significant upwelling stream temperature is influenced heavily by ambient air temperature, with stream temperature slowly rising in the downstream direction in the summer when mean air temperature is substantially above stream temperature and slowly cooling in the winter when mean air temperature is lowest (Mohseni and Stefan, 1999; Storey et al., 2004). Excluding 25 m where water was present only once during fall measurements, water was warmest at the 50 m point for every round of measurements (Figure 46 - Figure 47). It is likely that 25 m represents a strong downwelling zone at Cabin Creek since it totally dewatered during dry months in late summer/early fall. There was little variation in downstream water temperature during the spring (Figure 47).

Discrete zones of groundwater discharge were not identified through repeat temperature and specific conductance surveys along Creek 90. Specific conductance values for all measurement dates showed a gradual increase of 15 -20  $\mu\text{S}/\text{cm}$  from 0 m up to a peak that occurred between 150 m – 275 m (Figure 48). Conductance values then decreased slightly (5 – 10  $\mu\text{S}/\text{cm}$ ) before the Creek discharged into the South Fork River. In terms of seasonal variations, this trend changed very little. From the 0 m point to the middle reaches of the creek conductance always increased by an average of 30 – 40  $\mu\text{S}/\text{cm}$ . The final third of the creek generally displayed a mean decrease of 5 – 15  $\mu\text{S}/\text{cm}$ . Summer months were the outliers in this pattern as the final measurement point (350 m) for each respective sampling date always had the highest conductance of any point along the stream (Figure 49). Fall and winter conductance measurements displayed the usual 5 – 15  $\mu\text{S}/\text{cm}$  decrease over the final third of the creek (Figure 50 - Figure 51). A seasonal component to specific conductance values at Creek 90 is suggested in the spring (Figure 52), where conductance actually displayed an increase over the final few

reaches in late May. May is believed to be the transition month to a higher summer pattern of specific conductance measurements. Summer temperature patterns along Creek 90 are typified by a 3 °C rise in temperature from 0 m – 75 m, after which temperature plateaus, staying essentially the same until the creek disappears under the sediment wedge at 200 m (Figure 53). Stream temperature is more variable on the downstream side of the sediment wedge but still follows the same general pattern of increasing temperature over downstream distance that is typical during summer. During winter the 0 m point is consistently the warmest point in the creek. Temperature declines by 1 – 3 °C over the first 75 m at which point a more gradual decline is seen for the remaining length of creek (Figure 54). Similar changes in temperature are seen at the 75 m point for both fall (Figure 55) and spring (Figure 56), although the signatures are not as pronounced as winter and summer.

### ***6.7 Vertical Head Gradients, Hydraulic Conductivity, and Darcy Flux Values***

Repeat head gradient measurements at piezometers along Deep Creek show trends that confirm the presence of major upwelling and downwelling zones (Figure 57). Although head gradients indicate the first upwelling zone is located at 50 m, temperature and specific conductance measurements fail to show perturbations here that might indicate groundwater as the source. The piezometer installed at the 50 m point is in a pool 1 m downstream of a knickpoint, so this zone of upwelling probably represents the influence of a very short, shallow hyporheic flowpath beginning at the top of the knickpoint and ending in the pool just downstream. Subsurface water transit time is likely not long enough or deep enough to alter the temperature and conductance profile. This upwelling zone quickly transitions to a sharp downwelling area at 75 m, thought to be present because of a large woody debris jam, the effects of which can be seen for 20 m, from 80 – 100 m downstream. The sharp downwelling is likely a

product of this obstructed flow area, which serves to reduce flow velocity. The hydraulic gradient is steep in the subsurface because of this jam produced knickpoint. Immediately below the jam, at approximately 100 m, water is either slightly upwelling or slightly downwelling depending on the season. On 11/19/2010 there was no measureable vertical gradient. Despite the head gradients indicating a large degree of upwelling at 175 m, it is likely that the majority of upwelling is occurring from 100 – 125 m, based on the temperature and conductance measurements. The 175 m point is located at the base of an alluvial riffle sequence where upwelling may be occurring as a consequence of a much shorter, shallower hyporheic flowpath, similar to 50 m. Temperature and conductance perturbations are perhaps not seen here because the flowpath does not penetrate deep enough to intersect groundwater. After 175 m trends were more difficult to see because piezometer installation was possible only at 225 m, 350 m, and 375 m. Nonetheless, a moderate degree of upwelling was observed at each piezometer on every measurement date. This suggests that the final third of Deep Creek shows a generally consistent upwelling trend. Additionally, it seems unlikely that downwelling would be present to the degree noted at 75 m because the final third of the creek lacks the number of large debris jams and knickpoints that characterize the first two-thirds of the creek.

Due to the large amount of bedrock in Cabin Creek it was only possible to install three piezometers, at 200 m, 275 m, and 300 m. Nevertheless, vertical head gradient measurements help reinforce conclusions reached at Deep Creek. Temperature and specific conductance profiles at Cabin Creek 200 m suggest upwelling groundwater is present, although the piezometer at 200 m shows a consistent downwelling trend (Figure 58). Probably some combination of the two is taking place. From the initiation point down to 180 m slope in Cabin Creek is relatively consistent, averaging about 7%. From 180 m – 210 m slope abruptly levels



out at 0.7%. It is very likely that upwelling water in the first part of the reach is flowing down to where temperature and specific conductance measurements are made at the piezometer. The piezometer itself is much closer to the enormous debris jam that is responsible for the very low slope of this reach. As was the case in Deep Creek, this debris jam is causing prominent downwelling. Hydraulic gradient measurements at the piezometer at 275 m show it is a zone of consistent upwelling. The piezometer at 275 m is located in a pool beneath the largest bedrock knickpoint of all (~2 m). Temperature and specific conductance measurements, however, do not indicate this point as a groundwater upwelling zone. The pool this piezometer is located in is quite large (4.5 m wide x 3 m long x 0.5 m deep) and it could be that an upwelling signature is not seen here because the pool is diluting the temperature and specific conductance signatures. The final piezometer at 300 m shows downwelling occurring at the beginning of fall before the transition is made to it being an upwelling zone from November through winter and early spring.

Piezometers in Creek 90 show very few instances of negative vertical head gradient, with positive gradients seen most prominently in the middle reaches (150 – 225 m) of the creek (Figure 59). The piezometer at 350 m by far displays the most variability out of all piezometers with very sharp negative gradients seen in early fall. This gradient lessens through the middle of November becoming zero by mid January. In late January to early February the gradient reaches its maximum positive value. Positive gradient values in April are slightly lower than those in January suggesting a beginning of the return to a summer pattern where negative head gradients dominate. Since Creek 90 350 m is less than 10 m from the South Fork River, this vertical gradient pattern is almost certainly from interactions between the Creek 90 and the river. Looking at the South Fork River stage height values for the past year confirms this assumption,

with mean river stage reaching its lowest point in October before gradually increasing to higher values in January (Figure 60).

Measurements of vertical head gradients support the finding that one of the largest drivers on groundwater/surface water interaction is large woody debris jams. Deep Creek and Cabin Creek both have very prominent debris jams that block the entire channel, and are associated with clear downwelling and upwelling signals, whereas Creek 90 lacks jams of this size and has fewer indicators of groundwater/surface water interactions. Although Creek 90 does show an upwelling signature at 350 m, a corresponding temperature and specific conductance perturbation is not seen. These data seem to suggest that the size of the debris jam governs the degree of groundwater/surface water interaction, which is visible through the temperature and specific conductance signatures. In places like 150 and 175 m in Creek 90, where piezometers were driven into a pool at the end of a riffle sequence, upwelling would be expected and was indeed observed, but temperature and specific conductance perturbations were not seen. The presence of high vertical head gradients and associated temperature and conductance perturbations around debris jams, but not in riffle-pool sequences suggests that large woody debris jams are driving much of the groundwater surface water interactions in these three small creeks.

To examine the strength geomorphic factors as a control on vertical hydraulic gradients, correlations were tested between slope, sediment depth, and hydraulic gradient. A statistically significant relationship between streambed slope and vertical hydraulic gradient was not seen ( $p$ -value = 0.10) (Figure 61). However, a significant relationship between sediment depth and vertical hydraulic gradient was seen ( $p$ -value = 0.05) (Figure 62).

Hydraulic conductivity measurements at Deep Creek spanned three orders of magnitude. Conductivity measurements at the first four sites (25 – 100 m) were nearly constant, ranging from  $1.04 \times 10^{-4}$  to  $1.10 \times 10^{-4}$  cm/sec. At 125 m, conductivity increases nearly a full order of magnitude to  $9.14 \times 10^{-4}$  cm/sec. Hydraulic conductivity at the three measurement points in Cabin Creek spanned two orders of magnitude, from  $1.16 \times 10^{-4}$  cm/sec to  $9.89 \times 10^{-5}$  cm/sec. Like Cabin Creek, Creek 90 had hydraulic conductivity values that spanned two orders of magnitude, ranging from as fast as  $3.09 \times 10^{-4}$  cm/sec to as slow as  $5.20 \times 10^{-5}$  cm/sec.

The highest hydraulic conductivity values were found to be related to the presence of large woody debris jams. Median grain size for any point on Deep Creek was largest at 125 m ( $D_{50} = 23$  mm). At Deep Creek, this high  $D_{50}$  value, in conjunction with the fact that the large woody debris jam 25 – 35 m upstream has blocked channel flow and drastically reduced fine sediment accumulation immediately downstream, is responsible for the conductivity increase. Hydraulic conductivity is highest ( $3.77 \times 10^{-3}$  cm/sec) at Deep Creek 350 m, probably due to past flooding events that have resulted in an accumulation of very well sorted sediment. The highest hydraulic conductivity at Cabin Creek was measured at 275 m, in a large plunge pool ( $1.16 \times 10^{-4}$  cm/s) where  $D_{50}$  reaches a maximum of 19 mm. Hydraulic conductivity at Creek 90 150 m was where the fastest measurement was recorded and where the highest  $D_{50}$  was measured (30 mm). In all three creeks the greatest hydraulic conductivity was recorded a minimum of 25 m and no more than 75 m downstream of large woody debris jams. (Figure 63 - Figure 64).

Low hydraulic conductivity areas on all three creeks were influenced by a number of factors including slope and the presence of large woody debris jams. At Deep Creek 175 m, streambed sediment has a lower hydraulic conductivity value ( $8.04 \times 10^{-5}$  cm/sec), which is surprising considering that 175 m is the zone of largest and most frequent upwelling at Deep

Creek. However, the section of stream immediately above this piezometer has the third highest slope of any measurement location on the creek (4.8%). Since groundwater discharge is a function of both slope and area, it is likely that the higher gradient is overcoming the low conductivity to give a higher discharge. The lowest hydraulic conductivity on Cabin Creek was measured at 200 m ( $7.99 \times 10^{-5}$  cm/sec) just behind the large debris jam, which supports the belief that debris jams on first order streams not only influence hydraulic gradients, but also affect hydraulic conductivity, sediment depth (Figure 23 - Figure 25), and median grain size (Figure 19). This zone was consistently measured losing water to the subsurface, with downwelling seen on four out of five measurement rounds. The single time downwelling was not observed was during a measurement run a few days after a large storm in the spring when water table levels are typically highest.

Darcy flux values were calculated at each piezometer so as to try and better understand flux velocity in the subsurface as it relates to the upwelling and downwelling zones. The Darcy flux value is calculated by multiplying hydraulic conductivity by vertical hydraulic gradient. No statistically significant relationships between Darcy flux and geomorphic factors were identified. (Figure 65) (Figure 66). The net Darcy flux for all three streams averaged  $1.86 \times 10^{-5}$  cm/s based on measurements at 22 piezometers. The net positive Darcy flux shows that the study streams are primarily gaining streams, and longitudinal discharge measurements were used to identify the locations where baseflow gains occurred.

### ***6.8 Longitudinal Discharge Measurements***

Longitudinal discharge measurements were taken at all three creeks on 6/15/2010, 7/10/2010, and 4/3/2011. Data from 6/15/2010 best approximates the typical longitudinal discharge profile at all three creeks and is used as an example in the following discussion.

At Deep Creek discharge was measured at 25 m, 85 m, 105 m, 127 m, 149 m, 225 m, 318 m, and 365 m. Measurements from 6/15/2010 show that from 25 m - 85 m, discharge increased from 0.028 L/sec to 0.14 L/sec, a factor of 5 increase in 60 m (Figure 67). From 85 m – 105 m, discharge decreased slightly from 0.14 L/sec to 0.11 L/sec. After 105 m, discharge rapidly increased to 0.85 L/sec at 225 m, a factor of 8 increase in 100 m. Downstream from 225 m, moderate gains were seen in discharge, with a discharge at the mouth of 1.13 L/sec. The large increase in discharge could possibly be the result of preferential flow through a large fracture in the bedrock. Although bedrock presence was quantified along Deep Creek, it is possible that large contributions to discharge via fracture flow are taking place beneath the sediment where bedrock could not be observed.

Discharge measurements on 6/15/2010 at Cabin Creek were measured at 27 m, 85 m, 126 m, 194 m, and 297 m (Figure 68). Discharge rapidly increased from 27 m (0.11 L/sec) to 194 m (1.63 L/sec), a factor ~15 increase in 167 m. Downstream of 194 m, no gain in discharge was measured, with discharge at the mouth of the creek being nearly the same and well within the margin for error at 1.58 L/sec. Slope of Cabin Creek is greatest from 0 m – 180 m, at which point the large woody debris jam causes a large reduction in slope. Slope is greater over the first half of Cabin Creek (7.3%) than it is over the second (4.3%). It is possible that this reduction in slope beginning around 200 m is responsible for less upwelling resulting in less discharge from 200 m onward.

Discharge at Creek 90 was measured at 27 m, 115 m, 183 m, 223 m, 297 m, and 348 m. Measurements on 6/15/2010 revealed that discharge actually appears to peak at 183 m (1.27 L/sec) before declining gradually from that point onward, for a discharge at the mouth of 0.64 L/sec (Figure 69). Measurements on other dates confirm this general trend. It is possible that

water is being lost to the groundwater system where it disappears underneath the sediment wedge at 183 m. Longitudinal discharge on other measurement dates shows a recovery of discharge to pre-sediment wedge values by the time Creek 90 discharges into the South Fork of the Catawba River. Perhaps a longer flowpath created by the large knickpoint downstream of the sediment wedge allows some fraction of this water to bypass measurement sites immediately downstream of the sediment wedge.

### ***6.9 Stable Isotopes***

Stable isotope ratios can be used to trace the history of water through both the hydrosphere and biosphere (West et al., 2006). By determining the ratio of deuterium to hydrogen (D/H) and oxygen 16 to oxygen 18 ( $^{16}\text{O}/^{18}\text{O}$ ) molecules in surface water samples, it is possible to determine the relative contributions of water from different locations. As water moves through the water cycle lighter isotopes are preferentially transported during a process known as fractionation, the principle driver of which is temperature. Other factors influencing the degree of fractionation include the latitude, altitude, elevation, and the distance from the coast a given water sample is collected (Dansgaard, 1964). Heavier isotopes will condense more easily so as distance from the equator increases, precipitation becomes gradually enriched with increasingly lighter isotopes closer to the poles.

Variations in D/H and  $^{16}\text{O}/^{18}\text{O}$  ratios in stream water on 8/31/10 at Redlair show no evidence of water being derived from multiple source areas. Plots of D/H and  $^{16}\text{O}/^{18}\text{O}$  ratios for Deep Creek (Figure 70), Cabin Creek (Figure 71), and Creek 90 (Figure 72) versus downstream distance show isotopic values that vary relatively little as a function of downstream distance. The one possible exception is at 350 m in Creek 90, where stream water appears to be slightly

enriched in heavier isotopes, suggesting interaction with the South Fork River or a regional groundwater system.

### ***6.9.1 Stream Chemistry***

Many studies have found elevated nutrient contents in streams draining agricultural land and urban land, with forested catchments having the lowest nutrient loads (Gburek and Folmar, 1999; Langland et al., 1995). Redlair Forest fits with this trend when comparing stream nutrient content with typical urban and agricultural surface water chemistry (Liu et al., 2000). Chemical variations in stream water at Redlair are assumed to have a very small anthropogenic component, with stream chemistry being determined largely by processes relating to the interaction of water with geologic material.

Watershed land area used for agricultural purposes has been shown as being one of the greatest determining factor for stream nitrate concentrations (Hamilton and Helsel, 1995; Weller et al., 2003). Although Redlair has seen some degree of agriculture use in the past (80 – 100 years ago), this was before the advent of commercial fertilizer production. Nitrate concentrations for all three streams at Redlair are very low (< 0.6 mg/L) and are probably derived mainly from atmospheric deposition and N<sub>2</sub>-fixation by plants along the riparian corridor (Figure 73). Of the 45 sites sampled, nitrate does not exceed 0.23 mg/L at 43 sites and ranges between 0.07 mg/L and 0.18 mg/L at most other sites. Nitrate levels in Deep Creek vary between 0.08 – 0.18 mg/L, while in Cabin Creek nitrate varies between 0.14 mg/L and 0.18 mg/L, and in Creek 90 ranges from 0.06 – 0.60 mg/L.

Nitrate has been shown to be present in larger quantities in surface water and downwelling zones while ammonium is often present in upwelling zones (Storey et al., 2004). In hyporheic exchange zones, microbes reduce nitrate concentrations through a combination of

denitrification and dissimilatory nitrate reduction to ammonium. Appearance of ammonium may also be partly due to ammonification processes (Storey et al., 2004).

In the streams at Redlair, fluctuations in nitrate and ammonium concentrations were associated with debris jams and upwelling zones identified using temperature and specific conductance measurements. Deep Creek clearly shows drops in nitrate levels and increases in ammonium concentrations occurring at 25 m, 100 m, and 225 – 250 m. (Figure 74). Biofilm accumulation and periphyton mass were visually observed immediately below the debris jam at 100 m, further suggesting the water upwelling here is enriched in ammonium. Peaks in nitrate concentration in Cabin Creek occur in areas where downwelling is occurring and peaks in ammonium are thought to coincide with upwelling zones (Figure 75). Ammonium is only present at three sites at Cabin Creek and is probably readily taken up by vegetation soon after it is produced. No distinct patterns were seen in nitrate and ammonium concentrations in Creek 90, perhaps suggesting that downwelling and upwelling are taking place much more diffusely along the longitudinal length of the stream (Figure 76). This is in agreement with temperature and specific conductance measurements which suggest gradually increasing contributions from small, diffuse sources along the stream. The only site where ammonium is above the detectable limit in Creek 90 is at 0 m. Upwelling water is a certainty here as this is the first place where perennial flow is observed in Creek 90.

At 350 m in Creek 90 higher nitrate concentrations (0.60 mg/L) are possibly due to greater contributions from nitrogen fixing plants along the riparian corridor, as a very high positive head gradient was recorded here during early fall/late summer. It is unlikely that 350 m represents groundwater upwelling given the six-fold increase in nitrate which would have been reduced during transit in the hyporheic zone by denitrifying bacteria.



When precipitation encounters CO<sub>2</sub> in the atmosphere, a weak carbonic acid is formed. This coupled with the fact that water is a good solvent because of its polarity, means that water will dissolve nearly anything it comes in contact with over time. Weathering of parent rock is said to be the most influential factor in determining stream water and groundwater chemistry (Markewitz et al., 2001). Research shows that in general, the longer groundwater remains in contact with geologic material the more dissolved constituents are likely to be present (Gburek and Folmar, 1999). In terms of dissolved concentrations in all three streams, calcium was the dominant cation, followed by sodium, and magnesium. The concentrations of these elements in stream water can be said to vary based on mineral weathering (Likens et al., 1967). When concentrations of both magnesium and calcium are graphed against downstream distance, calcium concentrations most clearly show the probable upwelling zones in Deep Creek (Figure 77) and Cabin Creek. Trends in magnesium in Deep Creek fail to highlight any upwelling areas, but magnesium peaks at the 50 m point in Cabin Creek (Figure 78), one of the zones of probable discharge. No trends were observed in sodium concentrations at any creek and no pattern in sulfate concentration was seen at Deep Creek or Cabin Creek. However, Creek 90 has higher sulfate concentrations relative to Deep Creek and Cabin Creek and a clear consistently increasing trend in sulfate dissolved in the downstream direction (Figure 79). The high sulfate concentrations in Creek 90 are likely the result of weathering of sulfate containing accessory minerals such as hematite and pyrite that are present in the underlying quartz-sericite schist (Links, 2008).

Moderate variation was observed in major cation and anion concentrations between streams. Of the cations present in greatest concentrations (calcium, magnesium, and sodium) average values between streams differed by no more than 2 mg/L. This was most significant in terms of

magnesium as this ion was present in the lowest concentrations. Individual values for magnesium ranged from 2 – 4 mg/L, values for sodium varied between 3 – 6 mg/L, and calcium ranged from 5 – 16 mg/L. Ammonium was above the detectable limit in only one site at Creek 90, Deep Creek had four measurement points where ammonium was found, and Cabin Creek had three. Average ammonium concentrations at Deep Creek (0.13 mg/L) are thought to be higher than that seen at Cabin Creek (0.06 mg/L) because of higher amounts of biological nitrogen fixation. Average nitrate concentrations present in all three streams varied by no more than 0.03 mg/L, with averages calculated at 0.14, 0.16, and 0.13 mg/L for Deep Creek, Cabin Creek, and Creek 90, respectively.

Sulfate had the greatest difference between streams. Average sulfate concentrations were measured at 1.18 and 1.39 mg/L for Deep Creek and Cabin Creek, respectively. Sulfate concentrations at Creek 90 averaged 5.12 mg/L. The difference in sulfate is attributed to the different lithology at Creek 90 where sulfur bearing minerals such as pyrite and hematite have been shown to be present in greater quantities in the quartz-sericite schist that dominates the watershed (Horton, 2008).

## **7.0 Discussion**

### *7.1 Hypothesis 1:*

**Median streambed grain size ( $D_{50}$ ) is positively correlated with stream slope.**

Median grain size and stream slope were, in fact, found to be positively correlated. As  $D_{50}$  increased slope was found to increase based on the pebble count data sets collected in 2009

and 2010 – 2011 ( $p = 0.0001$ ). The mechanism for this can be attributed to variations in stream power, discussed in section 6.3.

In addition to slope, contributing area (or distance downstream) is another classic predictor of stream sediment size (Leopold et al., 1995). In a typical stream, grain size becomes finer in the downstream direction, because of abrasion and selective transport (Frings, 2008; Gomez et al., 2001; Rice, 1999; Seal and Paola, 1995). However, downstream fining is not always the rule, particularly in headwater streams (Brummer and Montgomery, 2003; Marren et al., 2006). At Redlair, results from pebble counts performed in 2009 suggested downstream coarsening of sediments in a majority of creeks (10 of 13) where multiple counts were performed. In 2010, no trend in sediment size distribution was observed in the downstream direction. The more randomized pebble counts performed in 2009 suggest results that are similar to those of Brummer and Montgomery (2003), who were investigating headwater streams in mountainous drainage basins in western Washington. They observed downstream coarsening in drainage basins  $<10 \text{ km}^2$ . Once drainage area exceeded  $10 \text{ km}^2$  downstream fining was observed. None of the creeks at Redlair exceed  $10 \text{ km}^2$ , a size which potentially represents a threshold over which the creek sediment is dominantly controlled by fluvial processes. For watersheds smaller than the  $10 \text{ km}^2$  threshold, differences in slope, debris slides and debris jams may control  $D_{50}$  values to a greater extent than contributing area, potentially leading to downstream coarsening or a lack of downstream size trends.

Sediment size distributions were influenced greatly by large woody debris jams, which tended to foster accumulations of sediment that had low  $D_{50}$  values relative to the mean  $D_{50}$  value for the entire stream. The influence of these woody debris jams on sediment accumulation must

be taken into account if data from this study are to be used by stream restoration managers to help restore urban streams.

### *7.2 Hypothesis 2:*

**Concentrated source areas at places along the streambed are responsible for the majority of baseflow contributions.**

A primary goal of this study was to determine whether groundwater was being contributed diffusely along the streambed or if concentrated source areas were the primary contributor to baseflow in Piedmont headwater streams. The data suggest that for first order headwater streams there really is no definite answer, as the presence or absence of certain geomorphic features along the channel controls most surface/groundwater interaction. For example, compared to the other two creeks, Deep Creek can be characterized as having a more concentrated discharge pattern. By the time Deep Creek reaches the South Fork of River it is discharging 1.13 L/sec. A full 41% of this discharge is contributed over just 40 m of channel length. In other words, 41% of the total discharge is upwelling over 11% of the total stream length. Conversely, most data sets for Creek 90 suggest a much more diffuse baseflow contribution pattern that is perhaps more typical of creeks that lack large scale obstructions as is the case at Creek 90.

### *7.3 Hypothesis 3:*

**Streambed sediment thickness positively correlates with upwelling zones and coarser and better sorted sediments have greater hydraulic conductivities than finer or more poorly sorted sediments.**

A statistically significant negative correlation was seen between streambed sediment thickness and vertical hydraulic gradient. In general, as vertical hydraulic gradient increased

(meaning upwelling was present) sediment depth decreased, a contradiction to what was first hypothesized might happen. It was initially thought that as vertical gradient increased sediment depth would increase as well. Evidently, stream slope has a much larger influence on sediment depth than was originally considered, and both factors influence the hydraulic gradient in a particular area. Such a finding is in line with past research that has determined streambed topography to be one of the determining factors for hyporheic exchange (Harvey and Bencala, 1993). The relationship between stream slope and sediment depth was found to be highly significant ( $p = 0.000261$ ) with sediment depth decreasing with increasing slope (Figure 16).

Although a statistically significant relationship was not observed between hydraulic conductivity and  $D_{50}$ , many geomorphologic factors could potentially confound these relationships on the stream wide scale. When similar sites are compared, for example the first site beneath the large debris jams in both Cabin Creek and Deep Creek and the smaller jam in Creek 90, relationships begin to emerge. The highest  $D_{50}$  value anywhere in the stream was always found downstream of debris jams. Some of the largest values in hydraulic conductivity were also observed at these three sites. Again, this suggests that the relationship between hydraulic conductivity and sediment size distribution is perhaps most heavily influenced by geomorphic variations such as stream slope and channel obstructions.

Future research should focus on further quantification of differences in vertical hydraulic gradients. A total of 22 piezometers were installed out of a possible 42 sites, with Cabin Creek having the fewest piezometers with only three installed over its entire length. The fact that bedrock coverage and large cobble coverage prevented installation of piezometers at many of these sites perhaps means there is some degree of bias in the results. Based on this knowledge,

future studies that focus on vertical hydraulic gradient and sediment relationships should attempt piezometer installation at 10 – 15 m increments instead of the 25 m used in this study.

Although a piezometer installation density of one per 25 m point, or wherever bed substrate allowed, proved more than adequate, there are several repeat measurement points where more piezometers could help give a more complete picture of subsurface flow. Creek 90 350 m is one of these points. Vertical head gradients here were found to be strongly negative during late summer/early fall. The gradient became increasingly neutral as winter approached, eventually becoming strongly positive during the late winter. Creek 90 350 m is located very close to the South Fork of the Catawba River and the negative head gradients in the early fall are well aligned with the river hitting its annual lowest stage reading at this time. However, elevated levels of most nutrients at this point during late summer go against the idea that water is infiltrating from the river. Future collection of more detailed vertical head gradients as well as additional chemistry data would be needed to ascertain what is truly happening here.

#### ***7.4 General Discussion***

The placement/construction of debris jams can be used as a way to slow water in artificially straightened channels as well as a method for pollution reduction. The strong downwelling signatures produced by large woody debris jams create longer deeper flowpaths through the hyporheic zone that would help reduce common pollutants, such as nitrate. Nitrate pollution is a common problem in many urban and agricultural areas where stream restoration is most needed. Attacking the problem of excess nitrate in headwater streams is the most logical course of action, as headwater streams have been found to contribute 55% of mean annual water volume and 45% of total nitrogen flux to downstream 4<sup>th</sup> order and higher rivers (Grimm and Fisher, 1984). Promoting hyporheic flow in restored reaches through the placement of debris

jams would also help moderate surface water temperatures thus increasing habitat suitability possibly resulting in the return of organisms that were previously unable to tolerate extreme water temperatures (Grimm and Fisher, 1984).

## **8.0 Conclusions**

Results from this study show that the factors determining headwater stream groundwater/surface water interactions are very complex, often varying extensively over both space and time. In terms of spatial differences, woody debris jams and areas where stream slope changed abruptly were found to most prominently feature upwelling. At these places, evidence of both hyporheic exchange and true groundwater upwelling (increasing discharge) was seen. Some streams showed concentrated areas of upwelling while others showed more diffuse contribution patterns. Changes in contributions over time were observed through seasonal differences in upwelling/downwelling signatures as seen in the vertical head gradient data and temperature and specific conductance signals.

Large woody debris jams were found to have the greatest influence on many hydrologic and geomorphic parameters. Prominent variations in sediment depth, water chemistry, grain size, slope, and vertical head gradient were all recorded as a consequence of large woody debris jams on Deep Creek and Cabin Creek. The broader 2009 survey of streambed sediments supports conclusions drawn from Deep and Cabin Creeks on the influence large woody debris jams have on sediment size distribution. Debris jams in low discharge 1<sup>st</sup> order streams appear to exert a greater influence over grain size than stream slope. Debris jams were observed to limit the amount of fine sediment available for up to 75 m downstream of the jam. Beyond this distance, and given the lack of a subsequent debris jam in the channel, slope likely returns to being the dominant influence over grain size distribution. Upwelling was most often observed in areas of

the stream that had low sediment depth, likely a product of the fact that upwelling zones occur along riffle segments that have higher slope and thus higher stream power.

Groundwater/surface water interaction was, in general, most pronounced in areas where there were abrupt changes in streambed slope. These drastic changes in hydraulic gradient cause longer and deeper hyporheic flowpaths to intersect groundwater, which eventually returned to the surface. Once mixed with surface water, altered temperature signatures, higher specific conductance values, and higher levels of dissolved minerals were found relative to normal background surface water levels for areas downstream of abrupt changes in slope.

The Redlair Forest is located on a pocket of relatively undisturbed land that is thought to be fairly representative of 1<sup>st</sup> order headwater stream environments in the Piedmont of North Carolina. As the Charlotte metropolitan area continues to expand and develop land, studies such as this one will become increasingly important for the stream restoration sector. In this study I have intensively characterized the hydrology and geomorphology of three streams, which can be used as reference streams for future restoration or protection efforts.

Because headwater streams are so prevalent over most landscapes they have a large impact on downstream water quality and quantity. The abundance of headwater streams and their natural variability provides a diverse range of micro-niches that allow valuable ecosystem services to take place. Thus, the restoration of headwater ecosystems is critical to improving water quality in larger downstream rivers on which millions of people depend. Restoration managers would be advised to take particular note of the importance woody debris jams appear to play in promoting groundwater-stream interaction and establishing spatial variability of sediments and habitats. . Improving connections between the surface and subsurface ecosystems in heavily degraded streams is paramount in restoring water quality and habitat, and large woody debris jams



encourage this to happen. Debris jam structures in restored headwater stream reaches should be designed to trap small debris among the larger woody pieces that form the framework for the jam, essentially creating a small dam-like structure. Field evidence for these low discharge headwater streams shows this type of structure allows for maximal hyporheic zone interaction, which would potentially allow the greatest bioremediation benefit in heavily polluted systems.

### 9.0 Referenced Figures

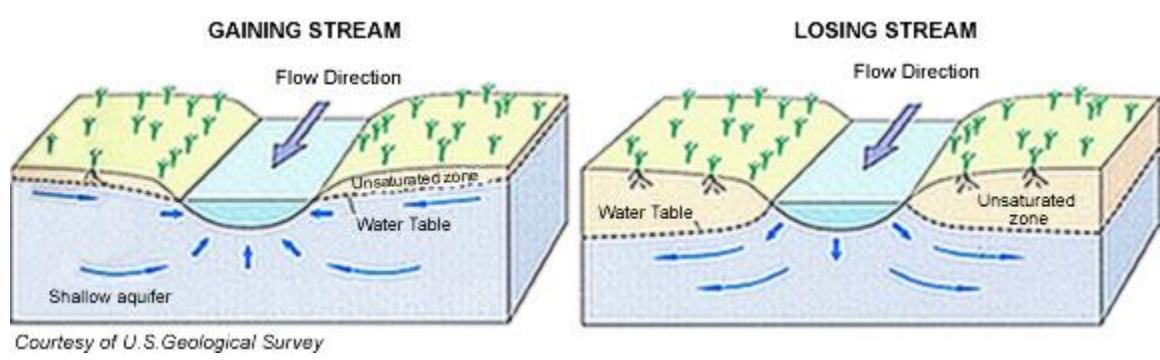


Figure 1. Sub-surface hydrologic interactions between streams that are replenished by the water table (gaining) versus those streams that lose water to the water table (losing). Source: USGS.gov URL: [http://pubs.usgs.gov/circ/circ1139/htdocs/natural\\_processes\\_of\\_ground.htm](http://pubs.usgs.gov/circ/circ1139/htdocs/natural_processes_of_ground.htm)

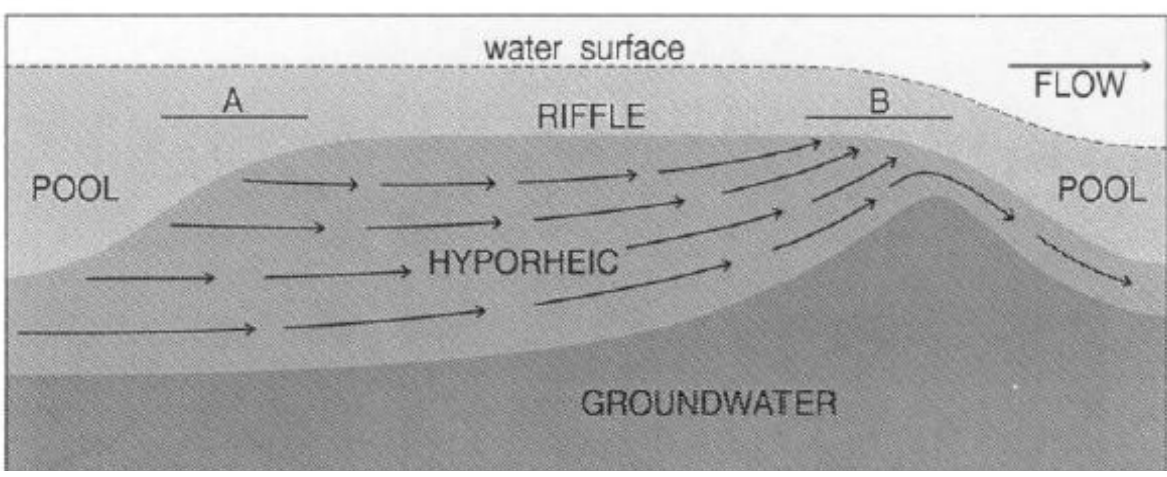


Figure 2. Schematic showing sub-surface flow paths for a stream. In this case, groundwater and surface water exchange would occur mainly at the topographically high portion of the bed in the downstream segment of the reach (White, 1993).

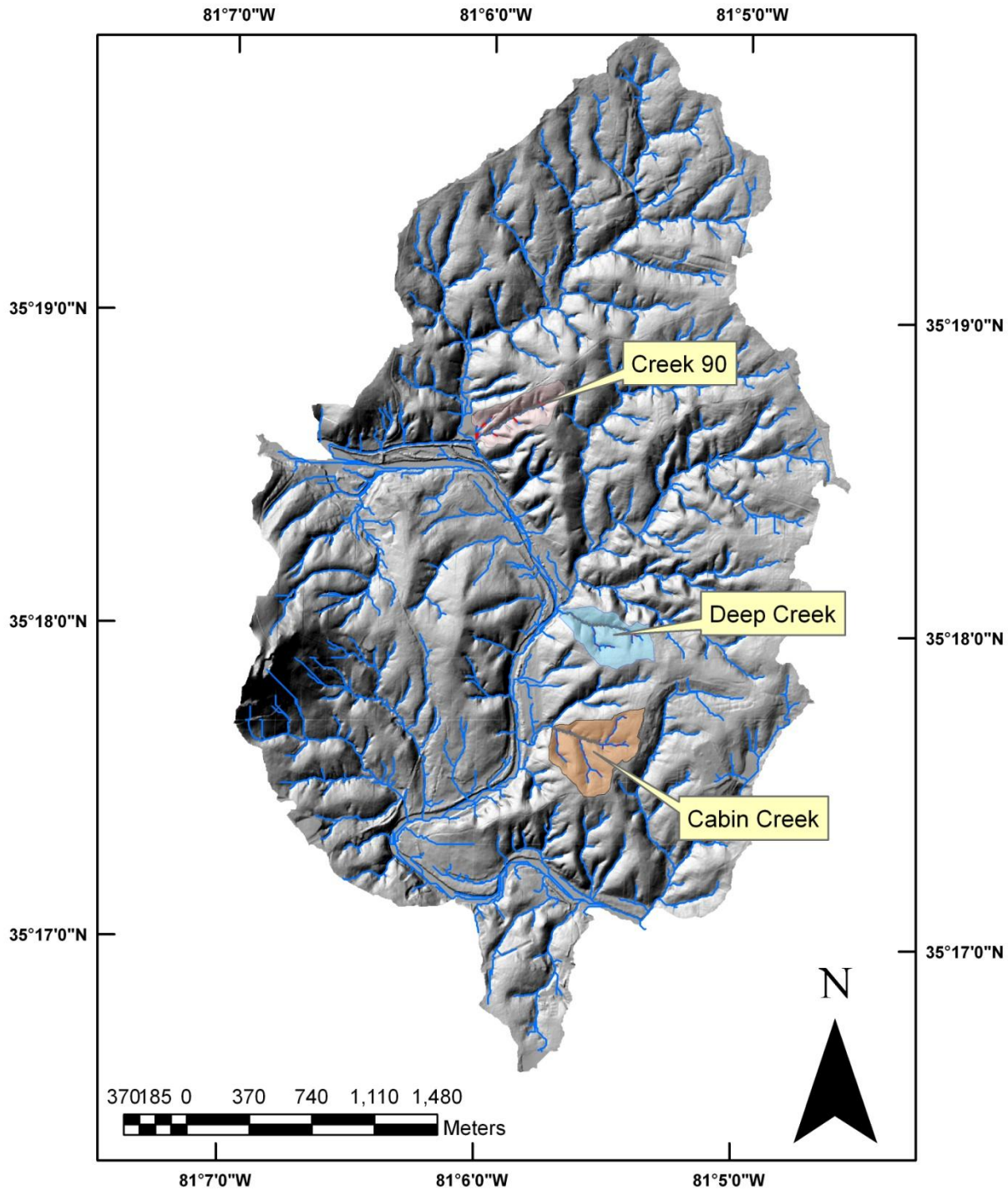


Figure 3. Study area in Gaston county North Carolina with the watersheds of Creek 90, Deep Creek, and Cabin Creek highlighted.

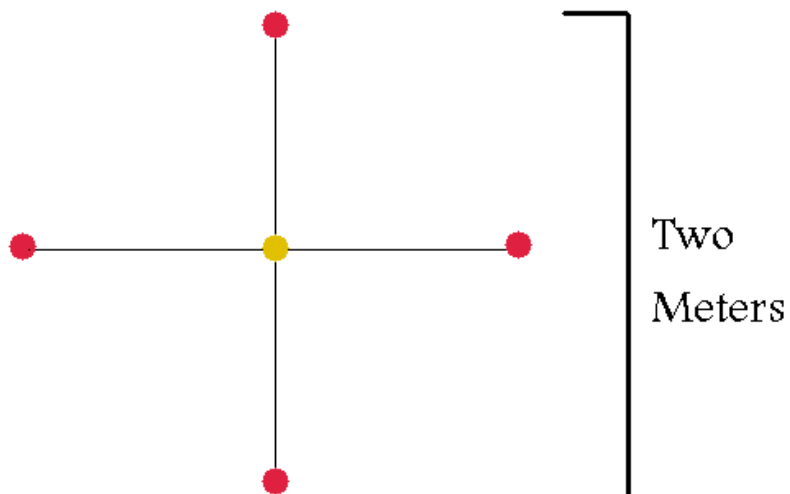


Figure 4: Schematic showing how sediment depth was measured. Red dots indicate unique measurement points while the yellow dot in the center is a shared measurement point. The yellow dot is also the approximate area where temperature and specific conductance readings were recorded.

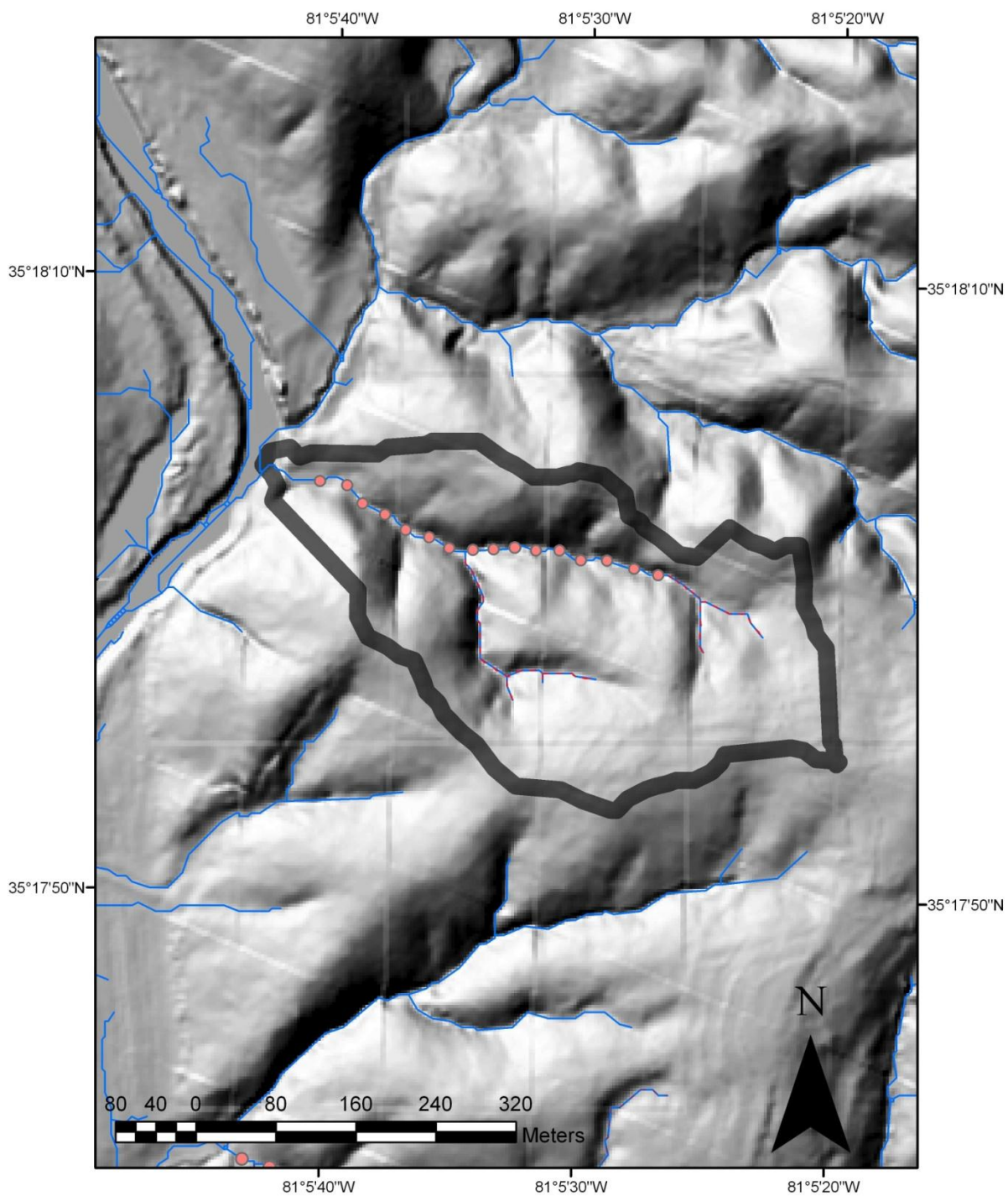


Figure 5. Map of Deep Creek watershed with the repeat 25 m measurement sites indicated with light red dots. Perennial flow on Deep Creek is indicated with a solid line whereas ephemeral flow is indicated with red dashes.

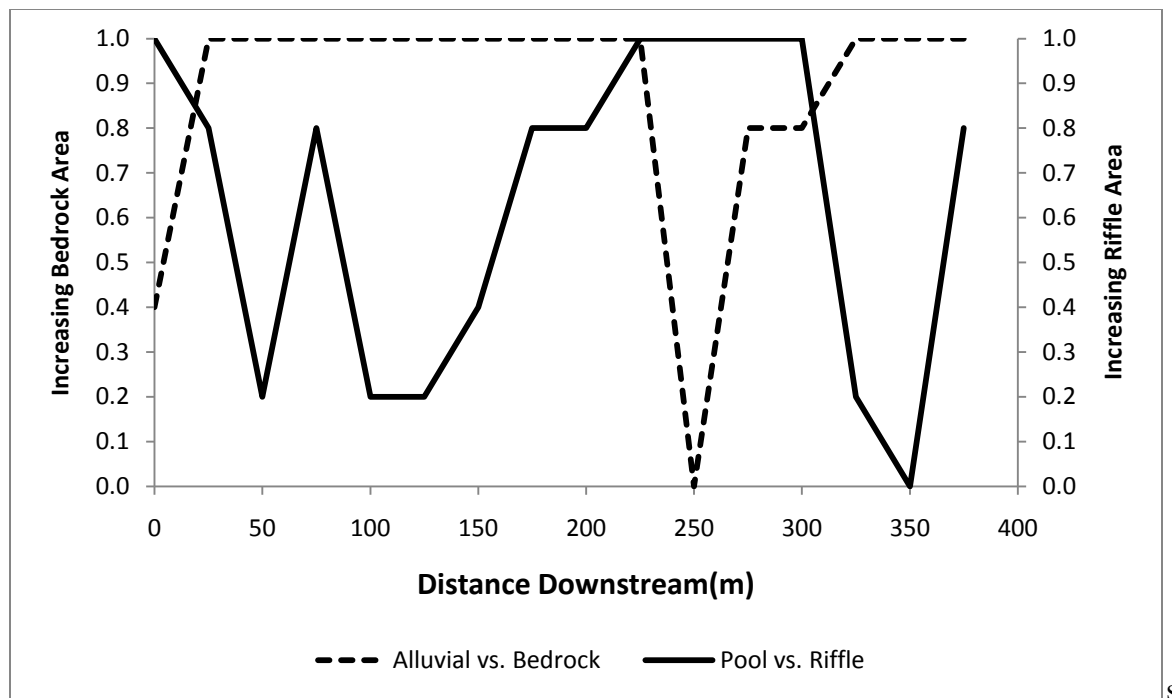


Figure 6. Alluvial vs. bedrock coverage and pool vs. riffle distribution for Deep Creek. The data indicate that alluvium is the dominant substrate in pools and bedrock tends to be found more at sites dominated by riffles.

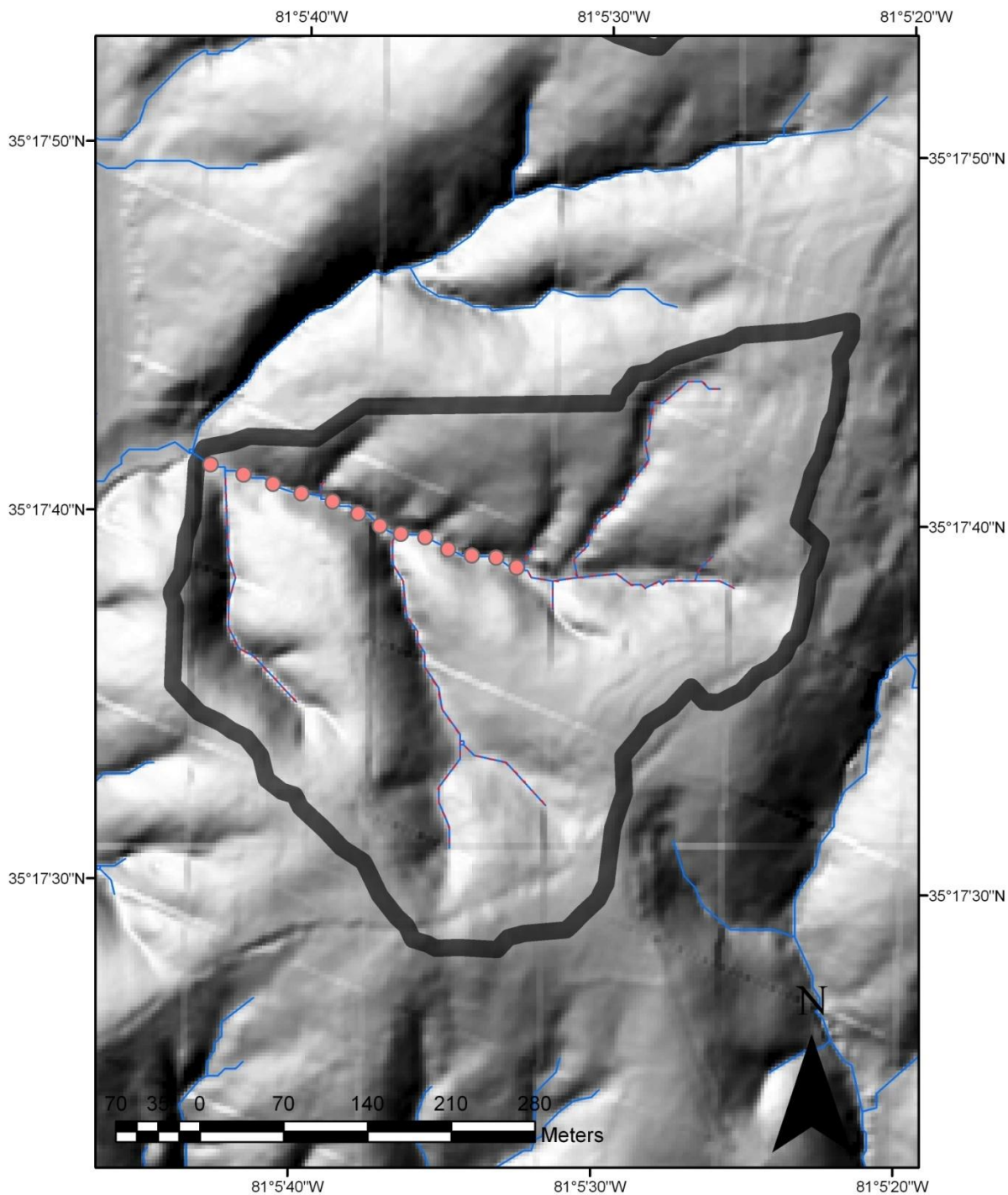


Figure 7. Map of Cabin Creek with downstream measurement points indicated with dots and appearing sequentially from 0 m in the upstream most portion down to 325 m in the final reach. Ephemeral tributaries are indicated by dotted lines while perennial is solid.

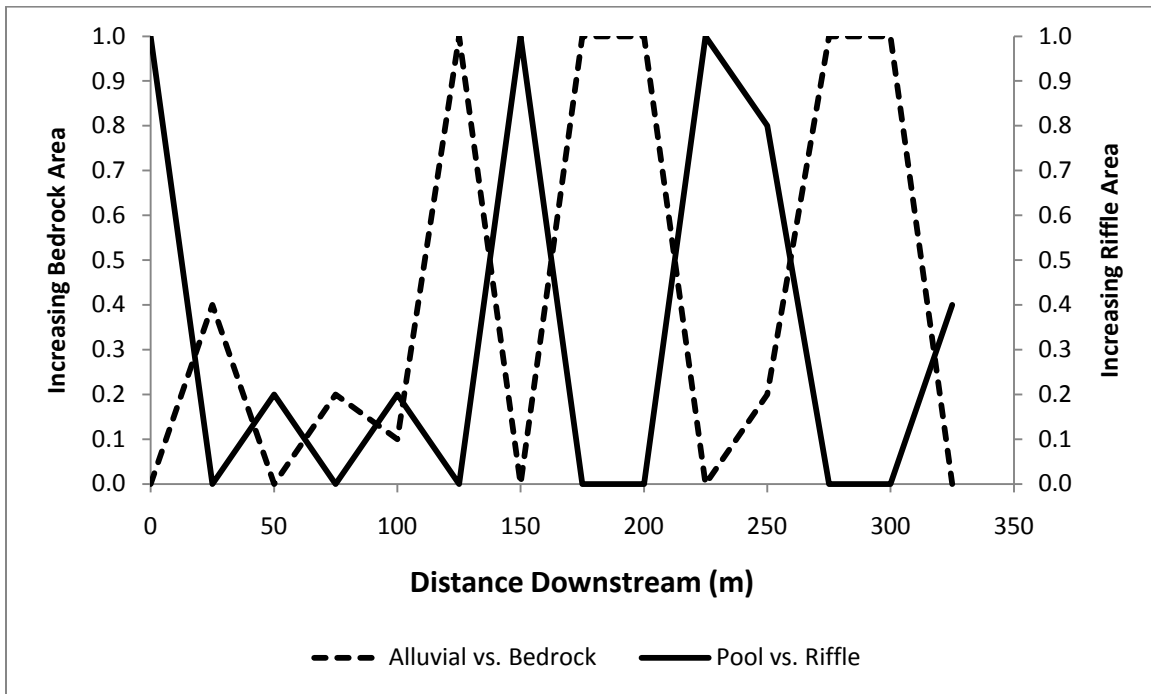


Figure 8. Data for Cabin Creek of alluvial vs. bedrock and pool vs. riffle distribution show a clear pattern with bedrock dominating riffle sequences while alluvium tends to appear only in pools.



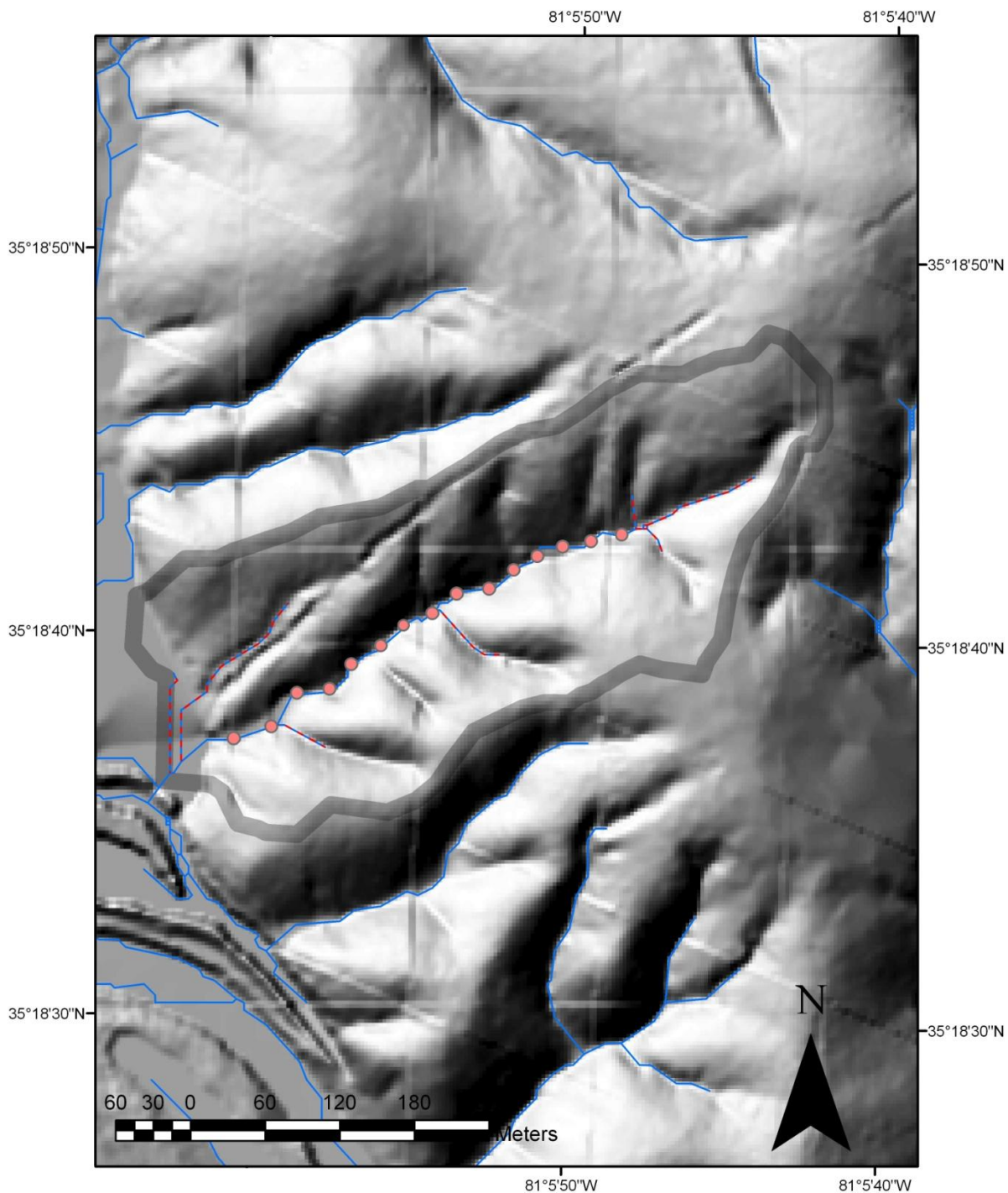


Figure 9. Map showing Creek 90 with downstream measurement points indicated with dots and appearing sequentially from 0 m in the upstream most portion down to 325 m in the final reach. Ephemeral tributaries are indicated by dotted lines while perennial is solid.

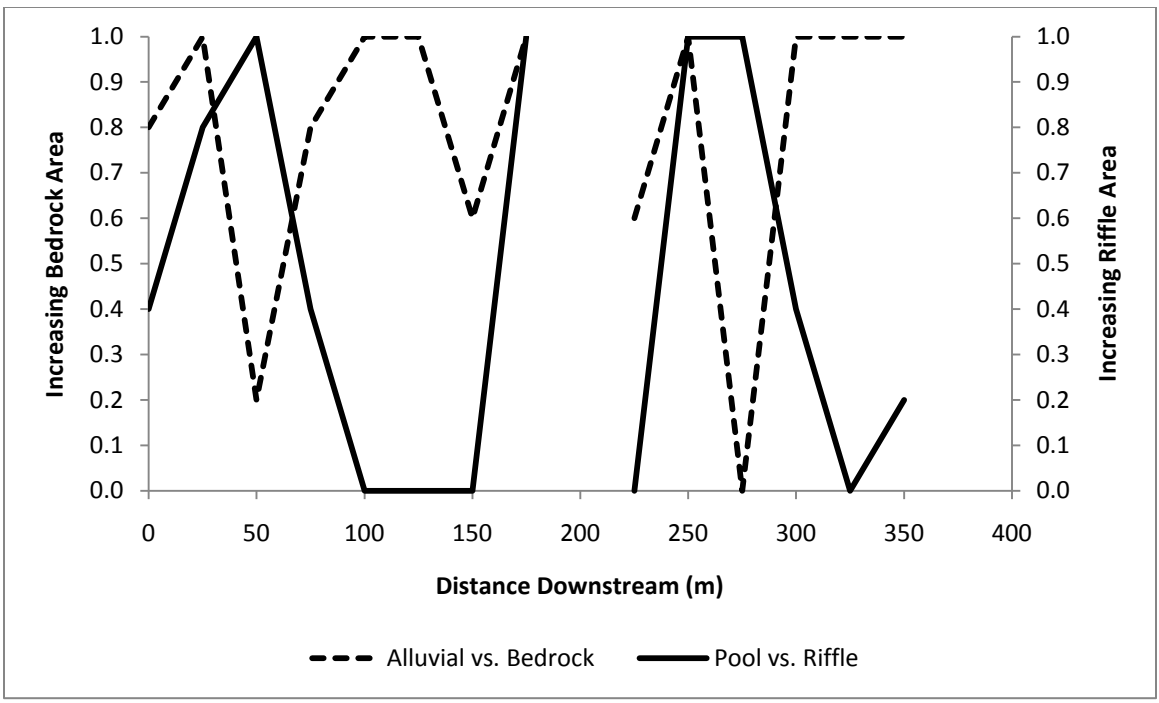


Figure 10. Distribution of pool vs. riffle and alluvial vs. bedrock sequences for Creek 90 show trends similar to those of both Cabin Creek and Deep Creek. Riffles tend to dominate bedrock covered areas while pools tend to have a much greater degree of alluvial composition.

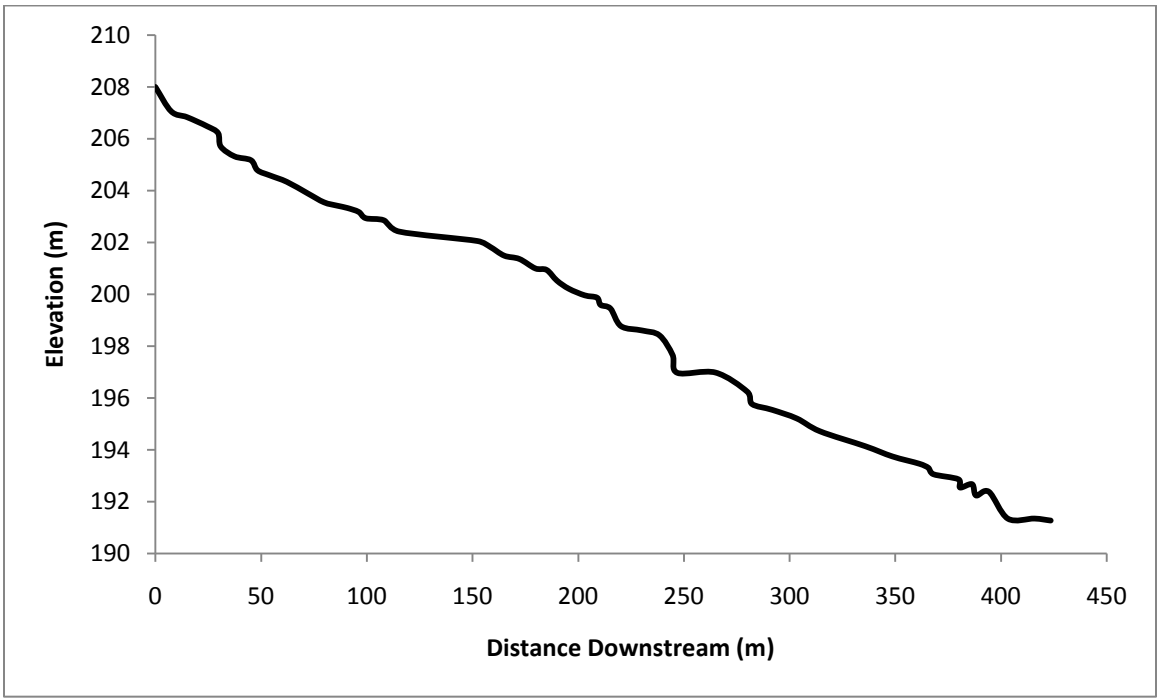


Figure 11. Longitudinal profile of Deep Creek showing distance downstream vs. elevation above mean sea level. Data collected 2/11/2011.

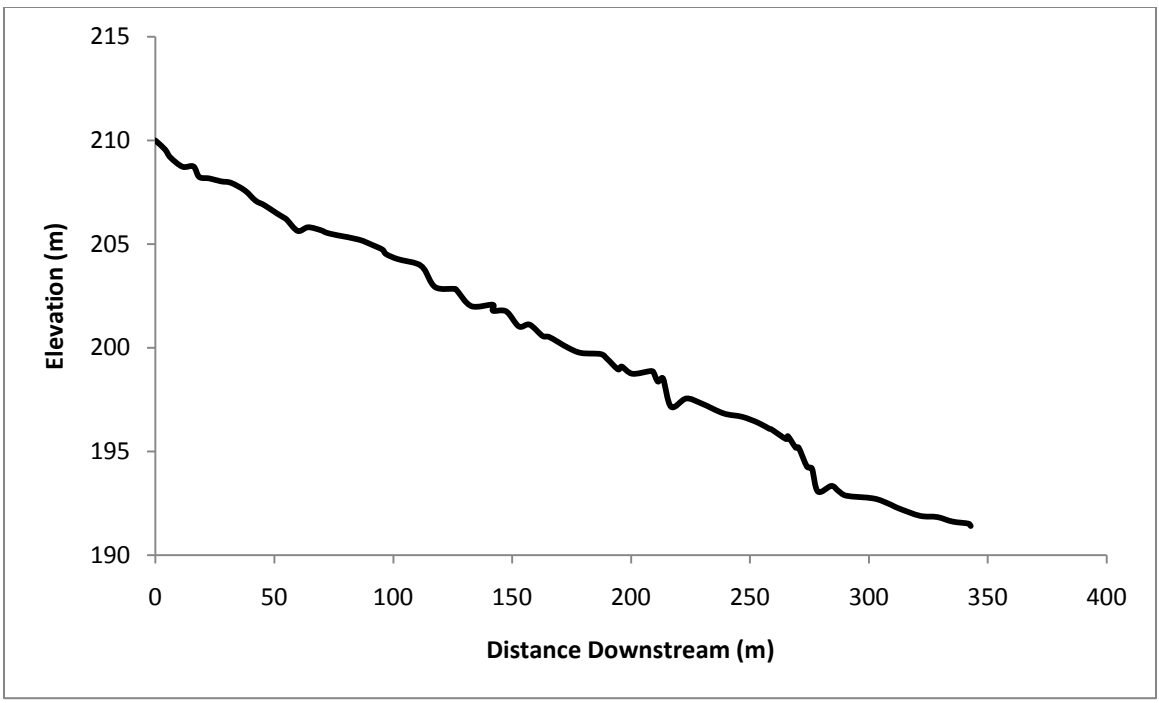


Figure 12. Longitudinal profile of Cabin Creek showing distance downstream vs. elevation above mean sea level. Bedrock knickpoints with downstream plunge pools are visible in the profile wherever there is an abrupt change in elevation. Data collected 03/12/2011.

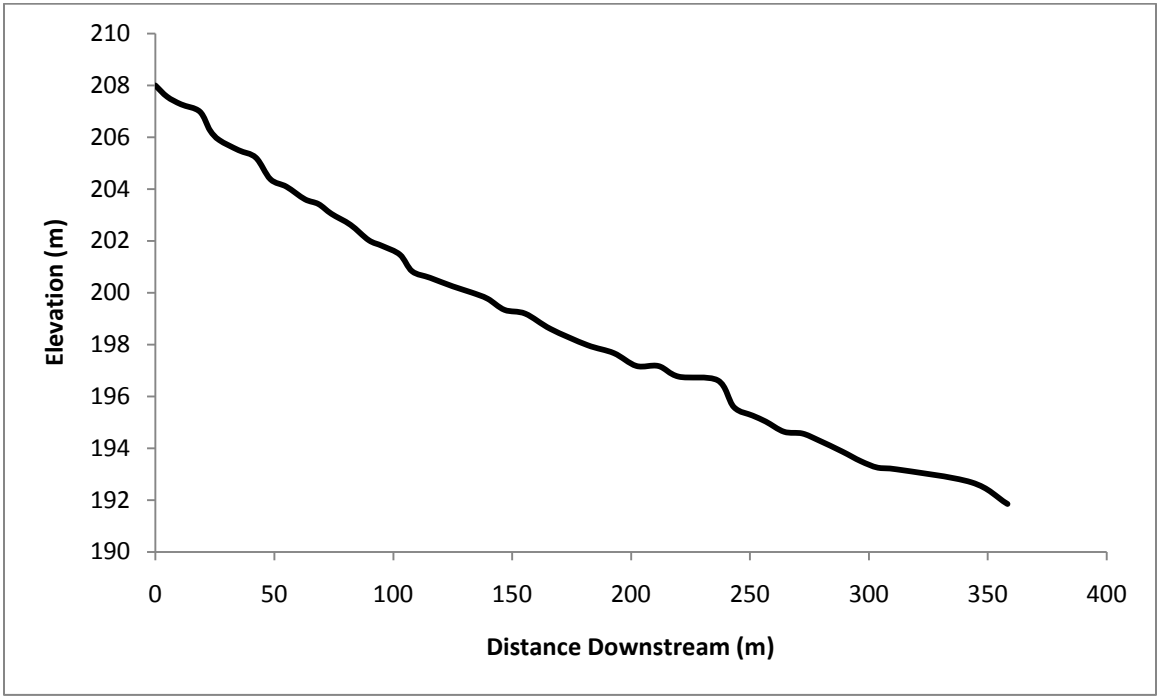


Figure 13. Longitudinal profile of Creek 90 showing distance downstream vs. elevation above mean sea level. The dewatered section is located from 183 m – 210 m. Data collected 8/27/2010.

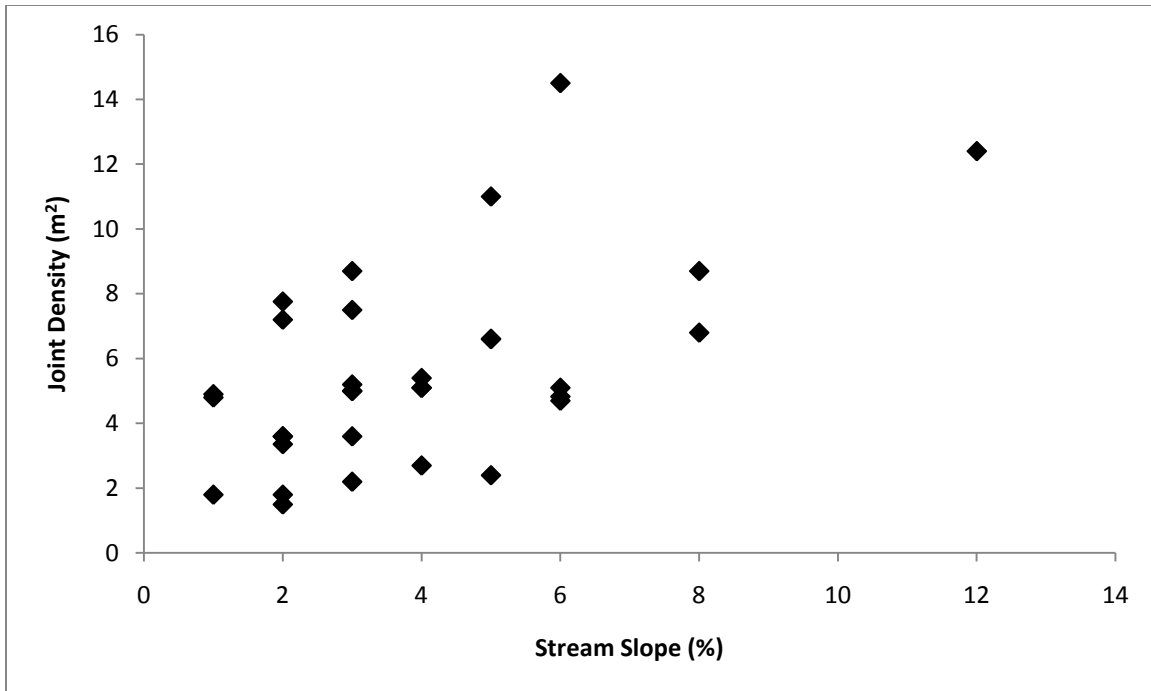


Figure 14. When joint density per square meter is plotted against stream slope a statistically significant correlation is found. ( $p = 0.000348$ ).

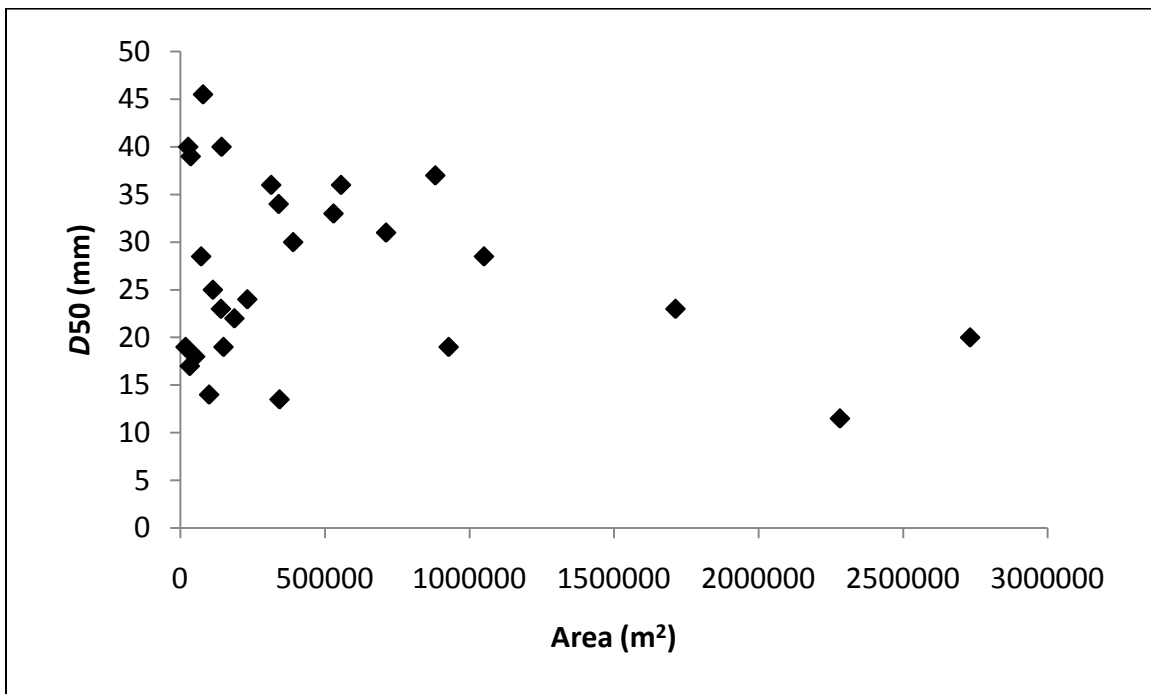


Figure 15.  $D_{50}$ -watershed area relationship for the 27 pebble counts from summer 2009 show no statistically significant distribution trends ( $p = 0.17$  for a linear fit).

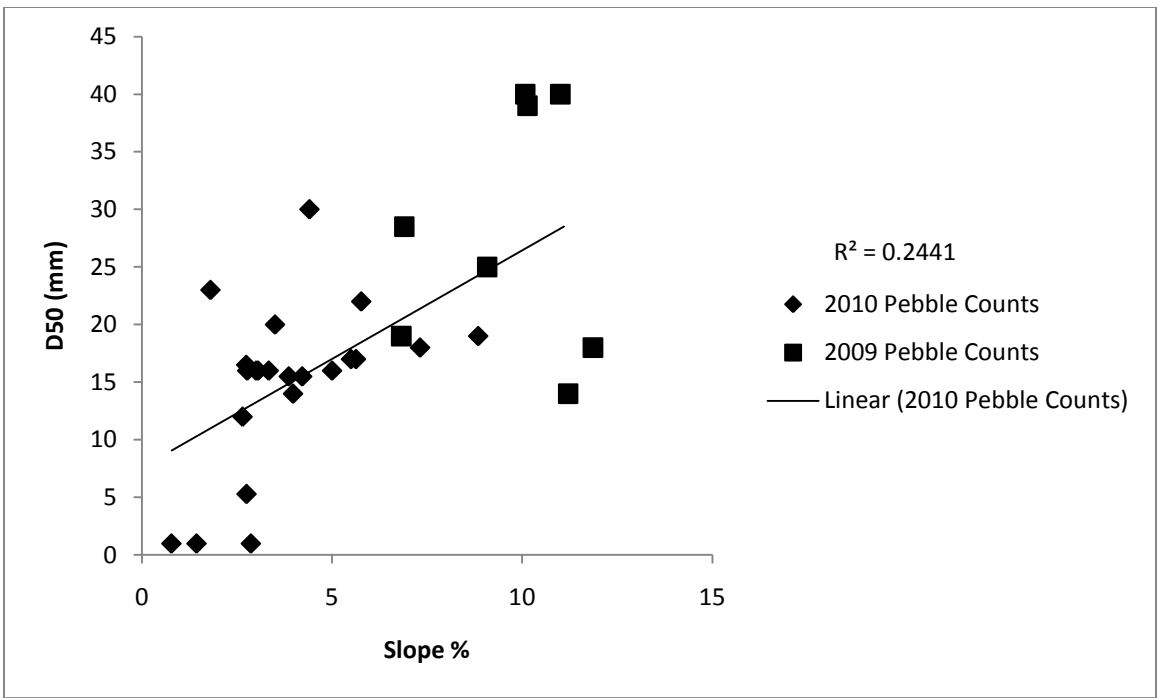


Figure 16. Slope was found to increase as  $D_{50}$  values increased. Slope values are for the pebble counts measured in the three study creeks. This relationship was statistically significant for the combined multi-year data set ( $p = 0.0001$ ).

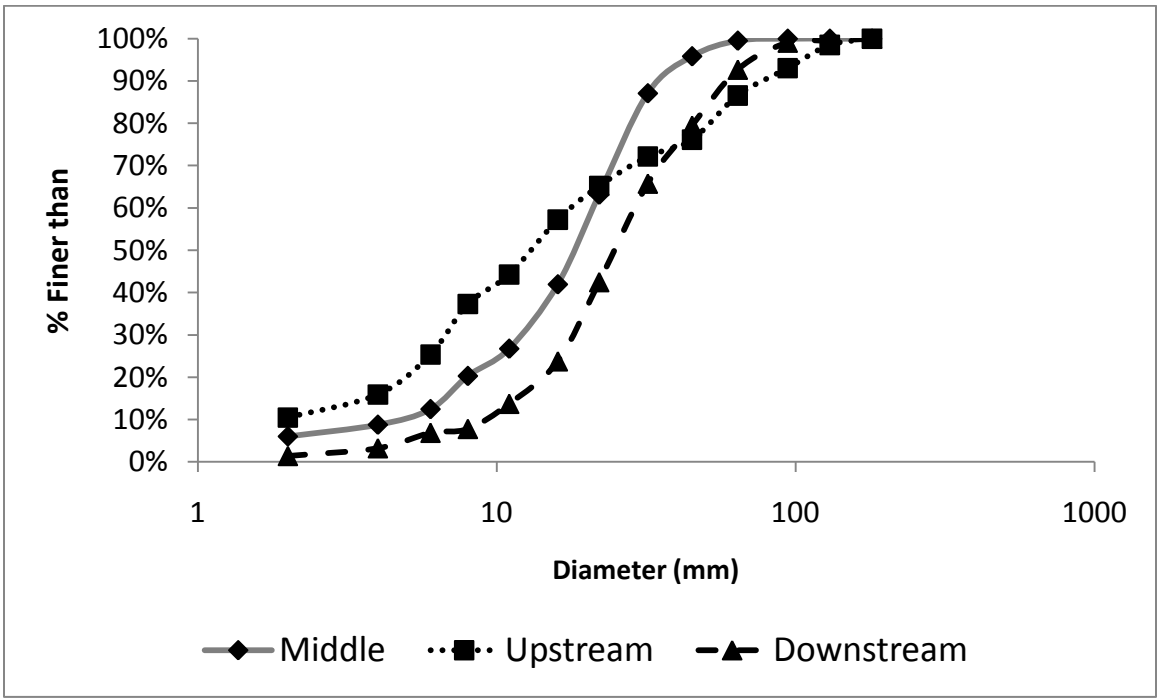


Figure 17. A downstream coarsening trend was noted for three pebble counts performed at varying downstream distances in Deep Creek during the summer of 2009.

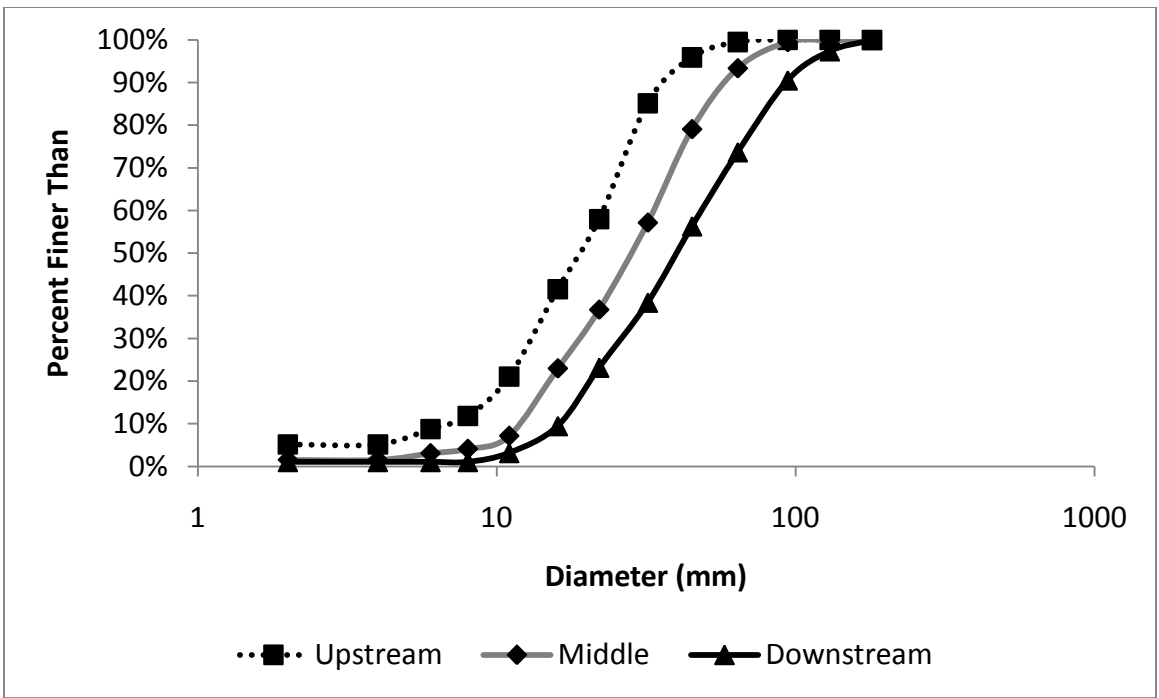


Figure 18. A downstream coarsening trend was noted for three pebble counts performed at varying downstream distances in Cabin Creek during the summer of 2009.

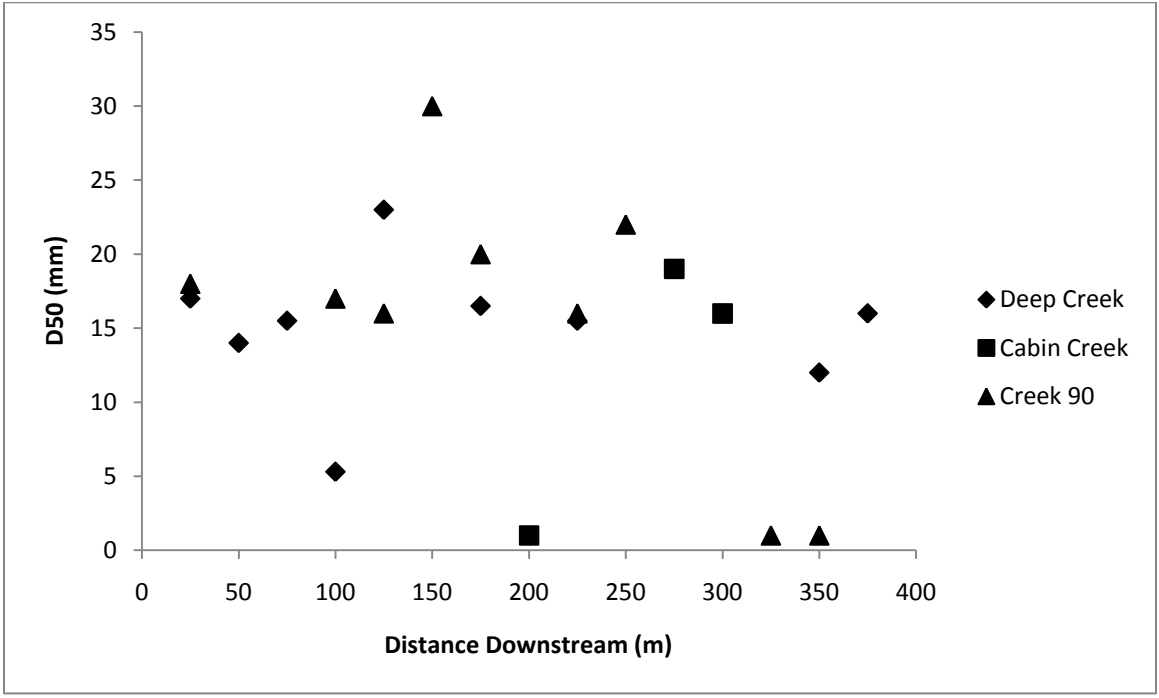


Figure 19.  $D_{50}$ -distance downstream plot for Deep Creek, Cabin Creek, and Creek 90. Pebble counts were performed only at piezometers, so only three were performed in Cabin Creek.  $D_{50}$  was estimated at Deep Creek 200 m and in Cabin Creek at 325 and 350 m, as described in the text.

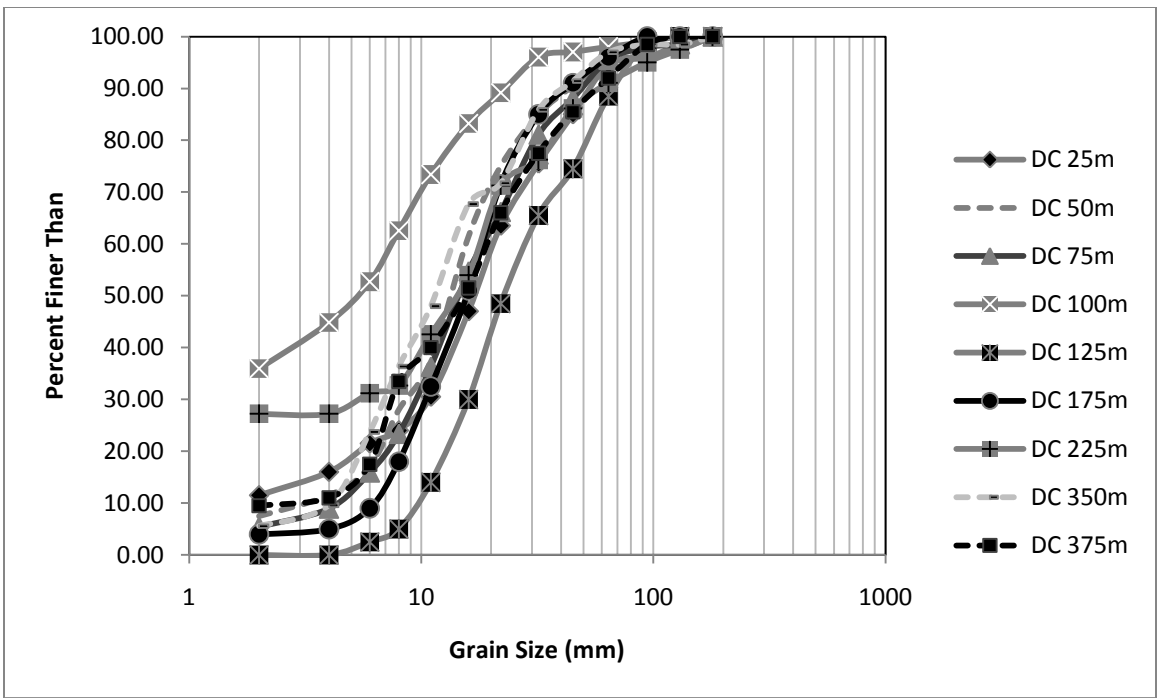


Figure 20. Sediment size distribution graph for Deep Creek. Most  $D_{50}$  values fall within a narrow range (12 – 17 mm). Two of the outliers along Deep Creek are at 100 m ( $D_{50} = 5$  mm) and 125 m ( $D_{50} = 23$  mm)). These sites are affected by a debris jam, with the 100 m site just upstream of the jam, and the 125 m site downstream of it. Data collected January 2011.

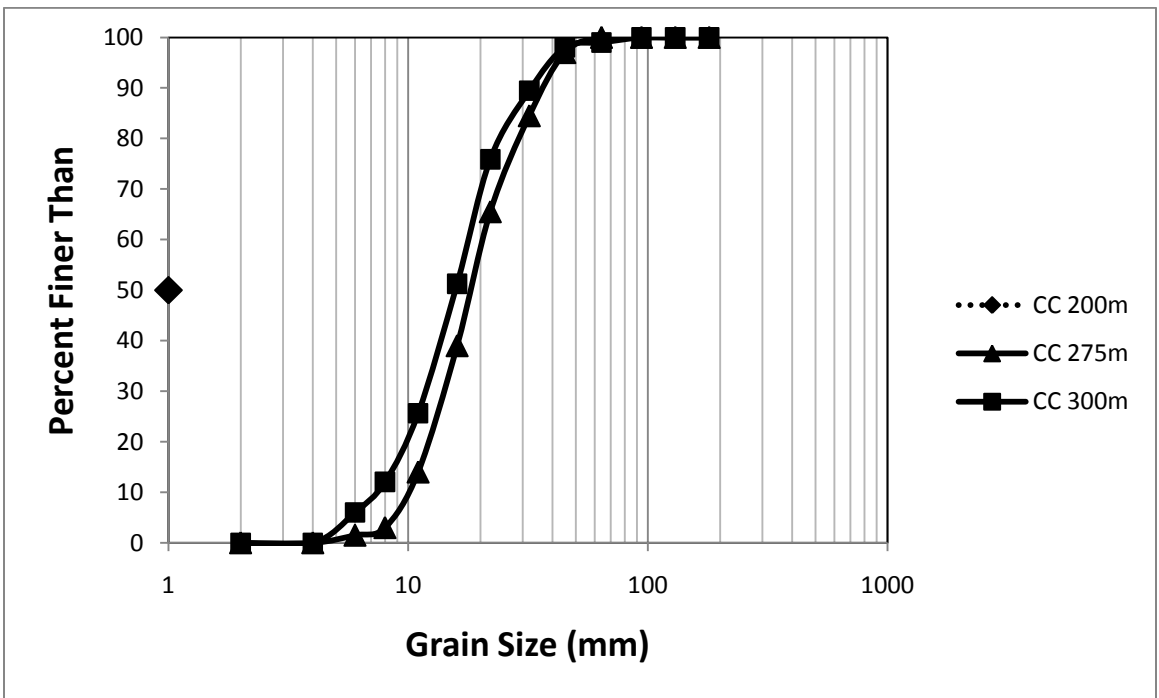


Figure 21. Sediment size distribution graph for Cabin Creek. Grain sizes measured at the piezometer at 200 m were very low relative to the mean value for the stream due to a large woody debris jam. At this site,  $D_{50}$  was estimated to be 1 mm. Data collected January 2011.

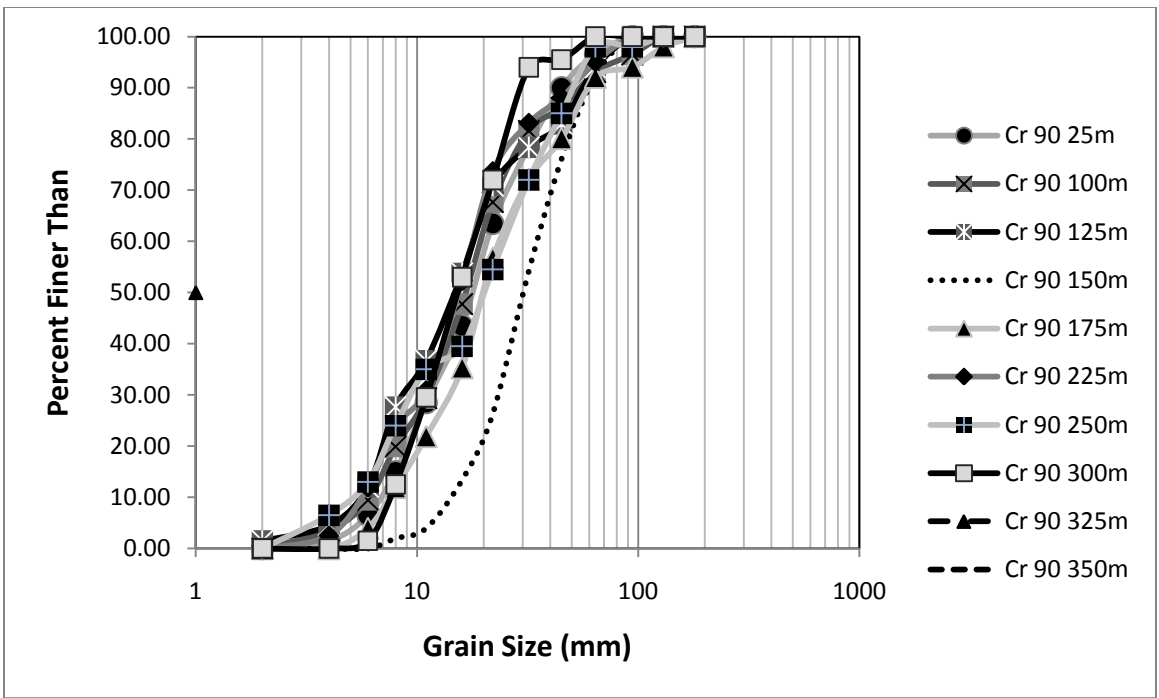


Figure 22. Sediment size distribution graph for Creek 90. Site 150 m had the highest  $D_{50}$  value where a small debris jam blocked fine sediment accumulation (30 mm). Similar to Cabin Creek, there were two sites along Creek 90 (325 m and 350 m) where  $D_{50}$  was estimated to be 1 mm. Data collected January 2011.

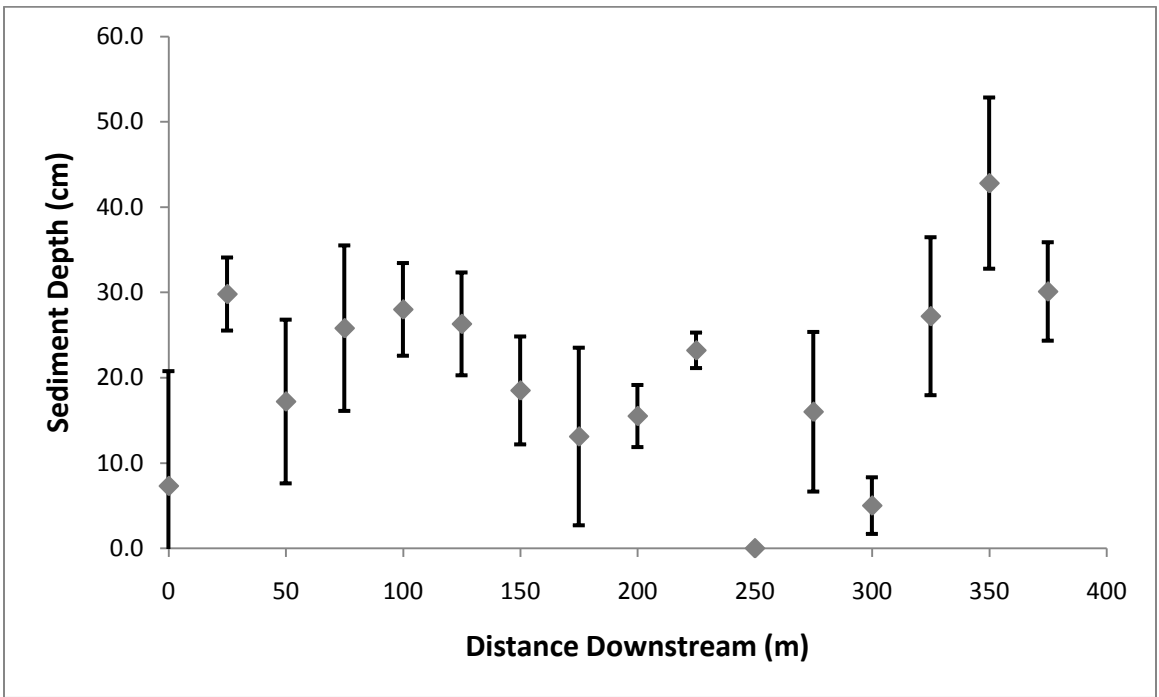


Figure 23. Sediment depth – downstream distance plot for Deep Creek. Sediment depth peaks at 350 m. Sediment depths influenced by the large woody debris jam are visible at and around 100 m. Measured on 7/19/2010.



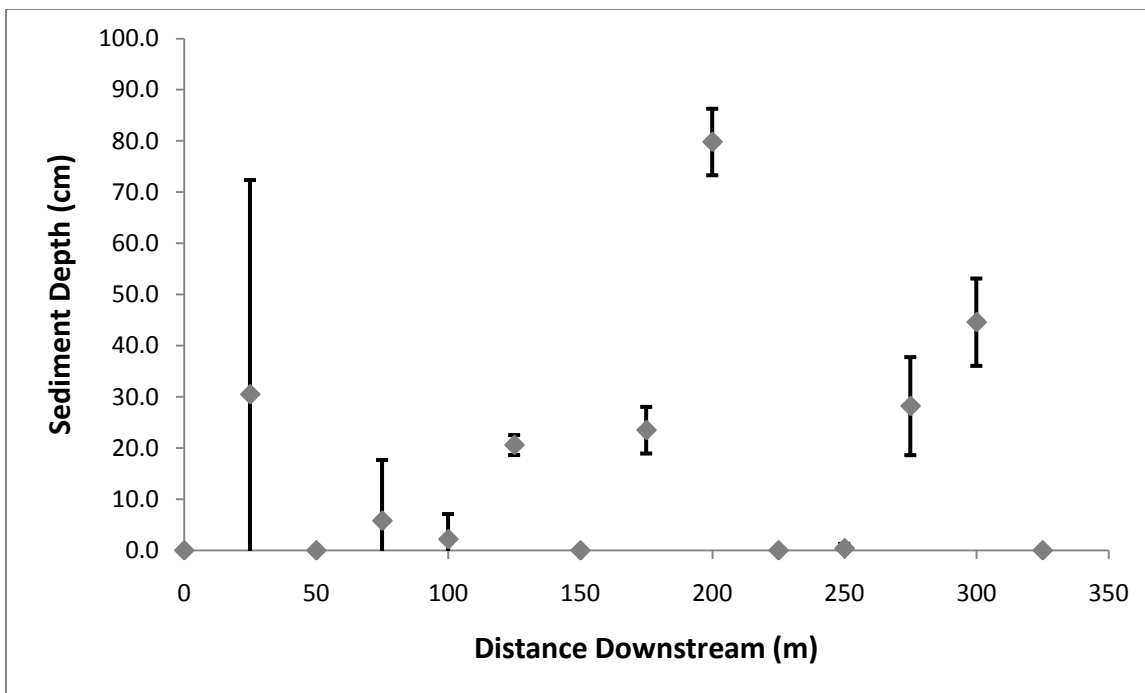


Figure 24. Sediment depth versus downstream distance plot for Cabin Creek highlights the lack of sediment at many of the repeat measurement sites. Bedrock dominates much of this creek, as indicated by the 'zero' depth sediment values. Sediment depth is thickest at 200 m where a large woody debris jam blocks the channel. Measured on 7/19/2010.

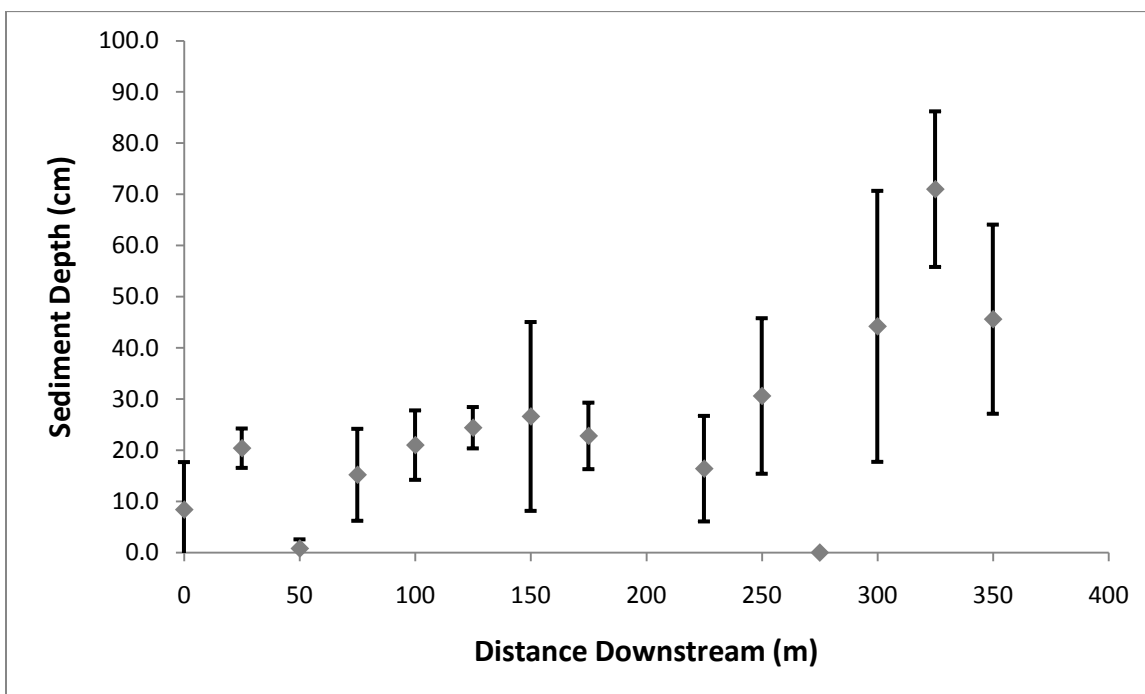


Figure 25. Sediment depth versus downstream distance plotted for Creek 90 show a peak in depth at the second to last site where the valley becomes wider and briefly takes on the appearance of a swampy area. Sediment depth generally increases in the downstream direction. Measured on 7/20/2010.

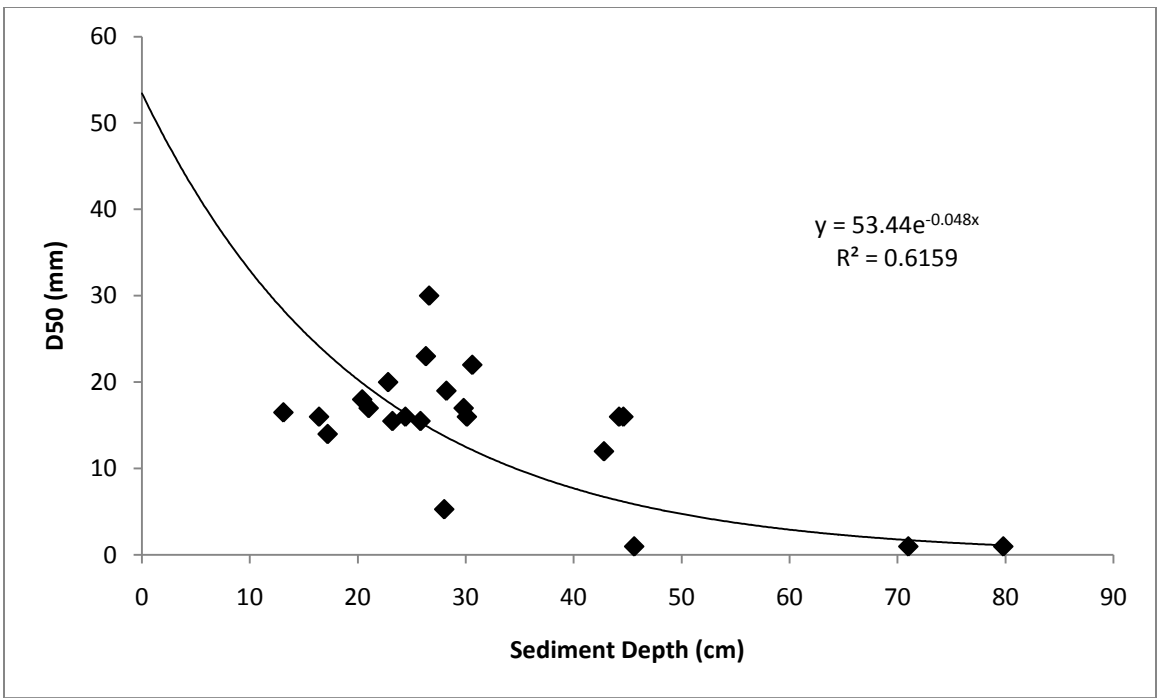


Figure 26. A statistically significant trend between sediment depth and  $D_{50}$  values was measured. In general as sediment depth increases  $D_{50}$  appears to decrease. ( $p = 0.000719$ ). This is a correlative association and not a causal relationship because it is likely that  $D_{50}$  and sediment depth are both influenced by slope. When the three estimated values are removed the trend is no longer significant.

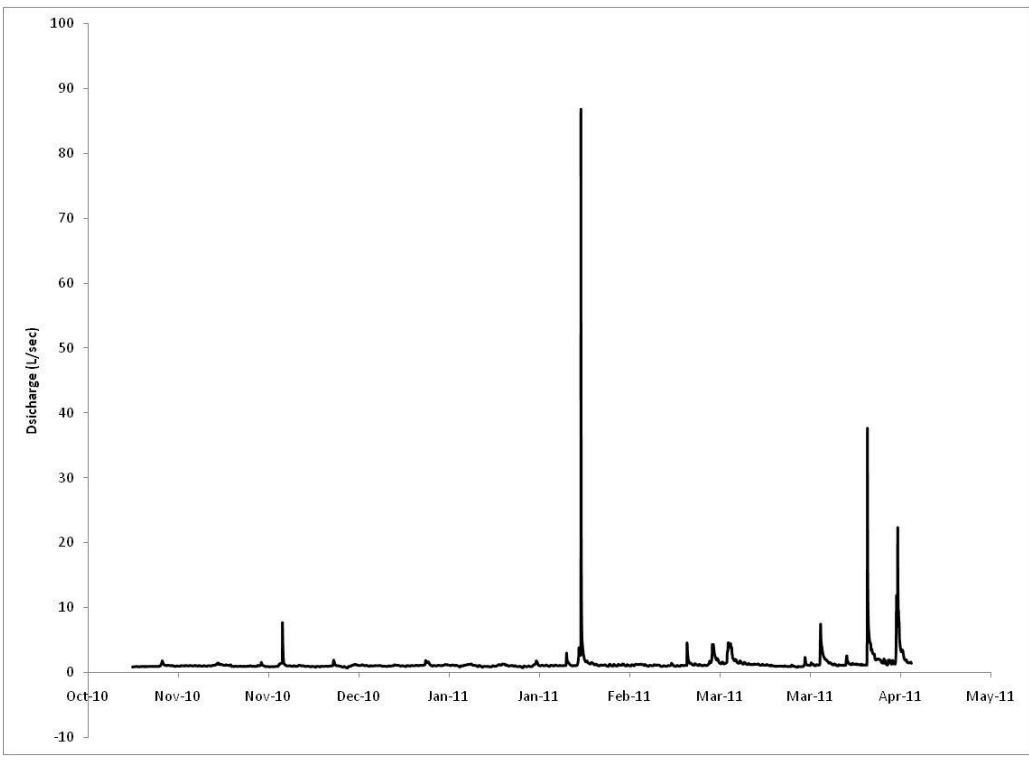


Figure 27. Hydrograph of Deep Creek from October 28, 2010 to April 3, 2011.

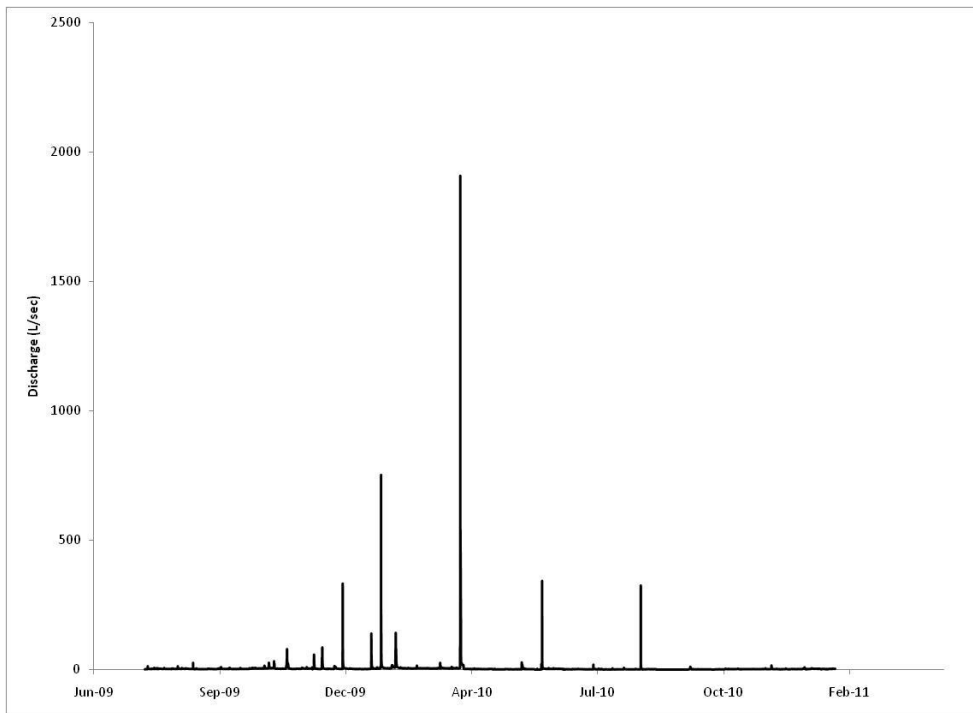


Figure 28. Hydrograph of Cabin Creek from July 27, 2009 to January 21, 2011. Baseflow values were higher during the summer of 2009 than in 2010. Baseflow increased during the winter. Hydrograph ends in January as opposed to April like Deep Creek due to a malfunction of the Odyssey data logger.

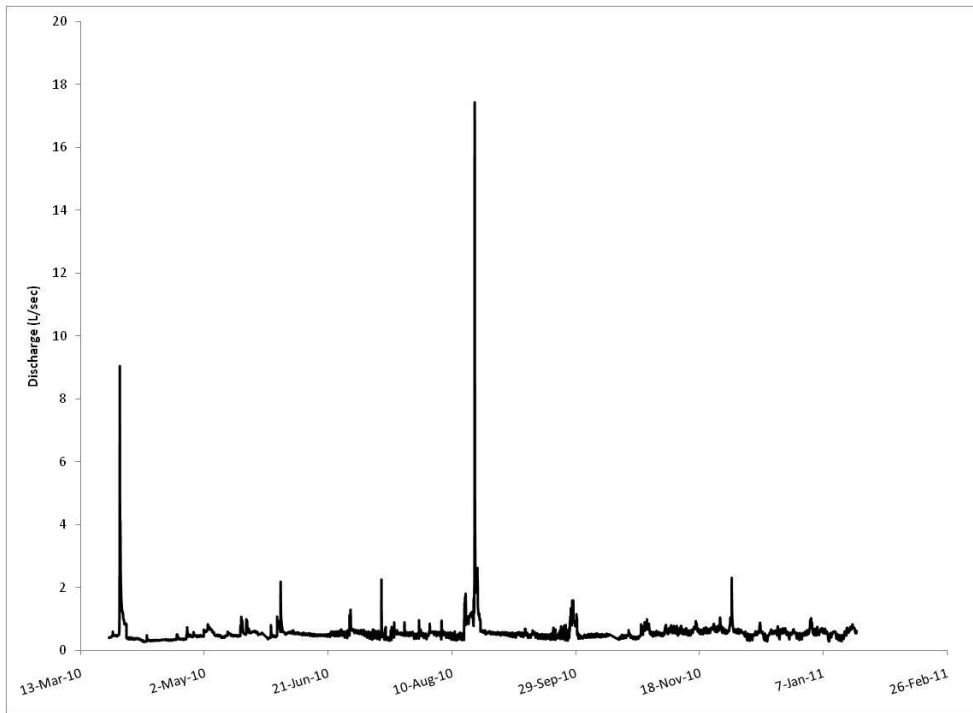


Figure 29. Hydrograph of Creek 90 from March 3, 2010 to January 21, 2011. Hydrograph ends in January as opposed to April like Deep Creek due to a malfunction of the Odyssey data logger.

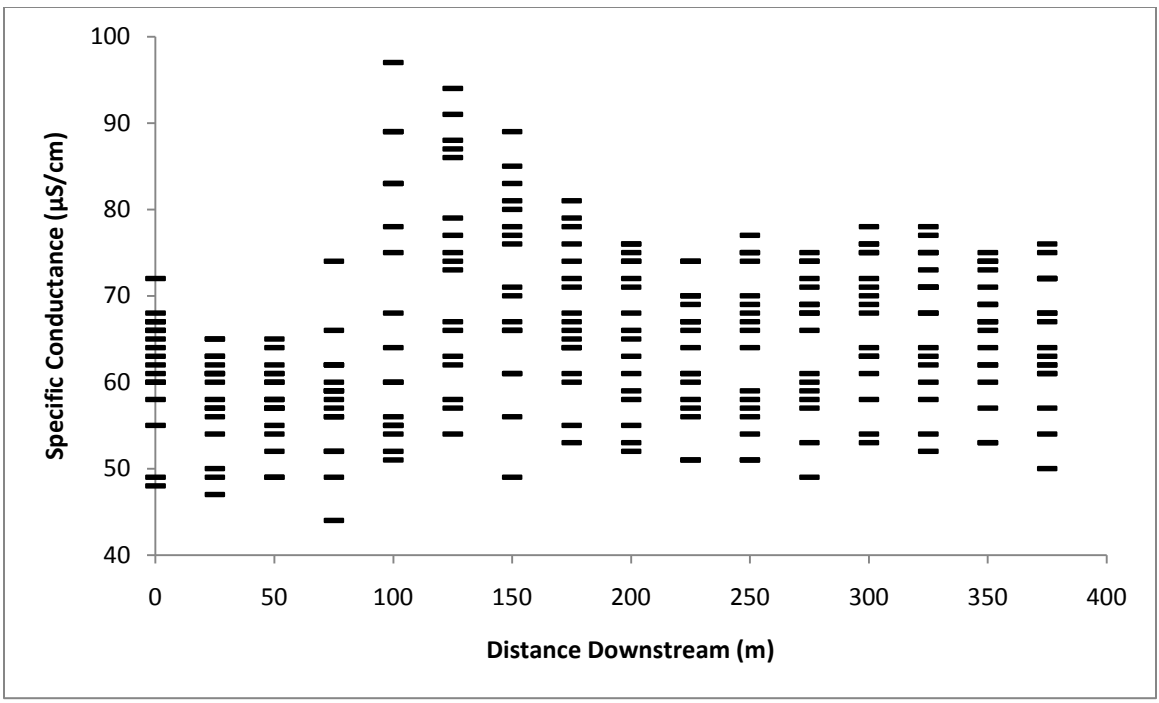


Figure 30. Relationship between specific conductance and distance downstream for Deep Creek. Notice that specific conductance consistently peaks at 125 m.

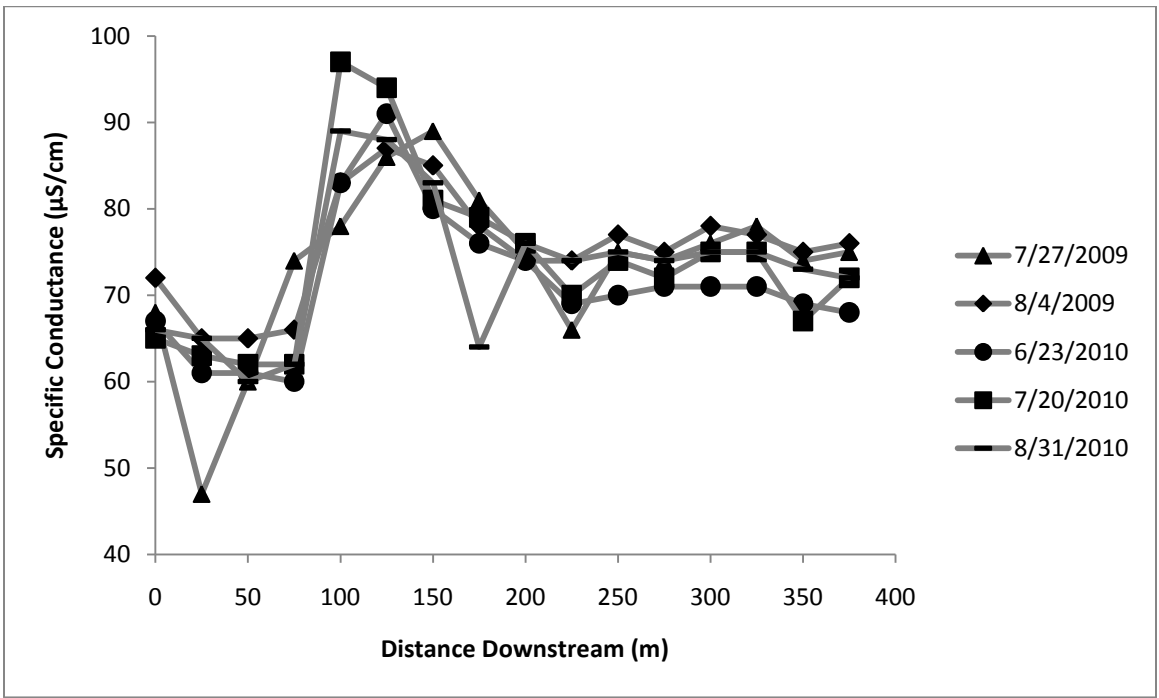


Figure 31. Relationship between specific conductance and distance downstream for Deep Creek during summer months only. A 30 – 40 μS/cm increase in specific conductance occurs at 125 m .

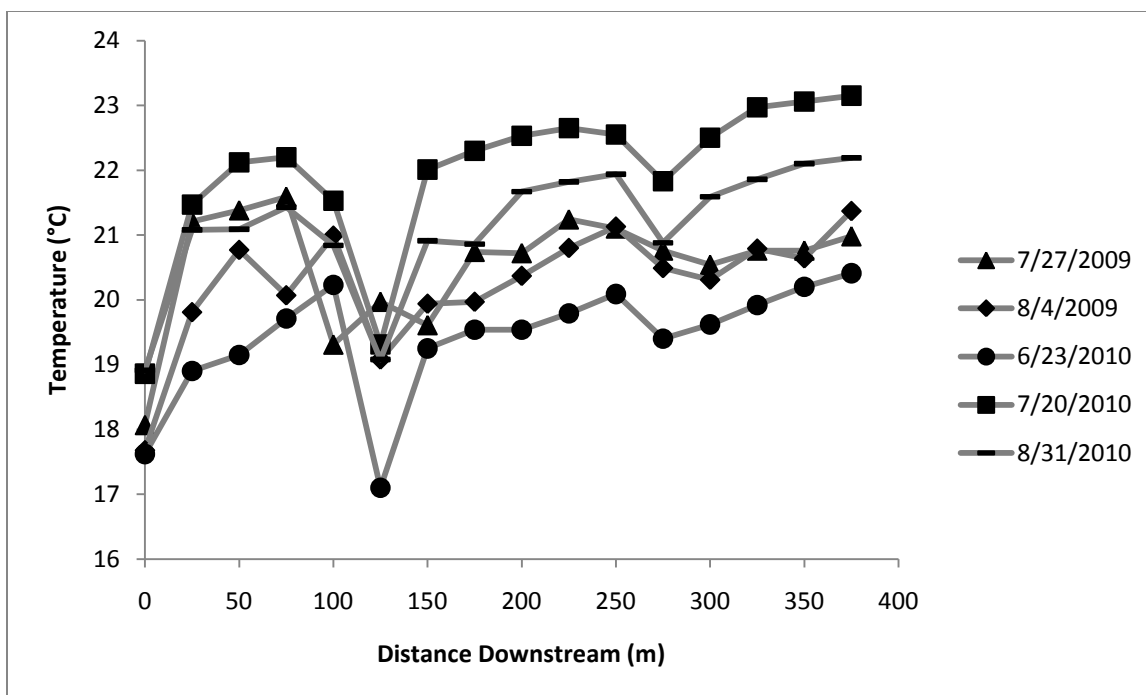


Figure 32. Plotting temperature vs. distance downstream for Deep Creek during summer months reveals a sharp drop of 2 – 3 °C at 125 m, as well as a very distinctly lower temperature (2 °C) at the upstream most point compared to the 25 m point. A small temperature decrease is seen at 275 m.

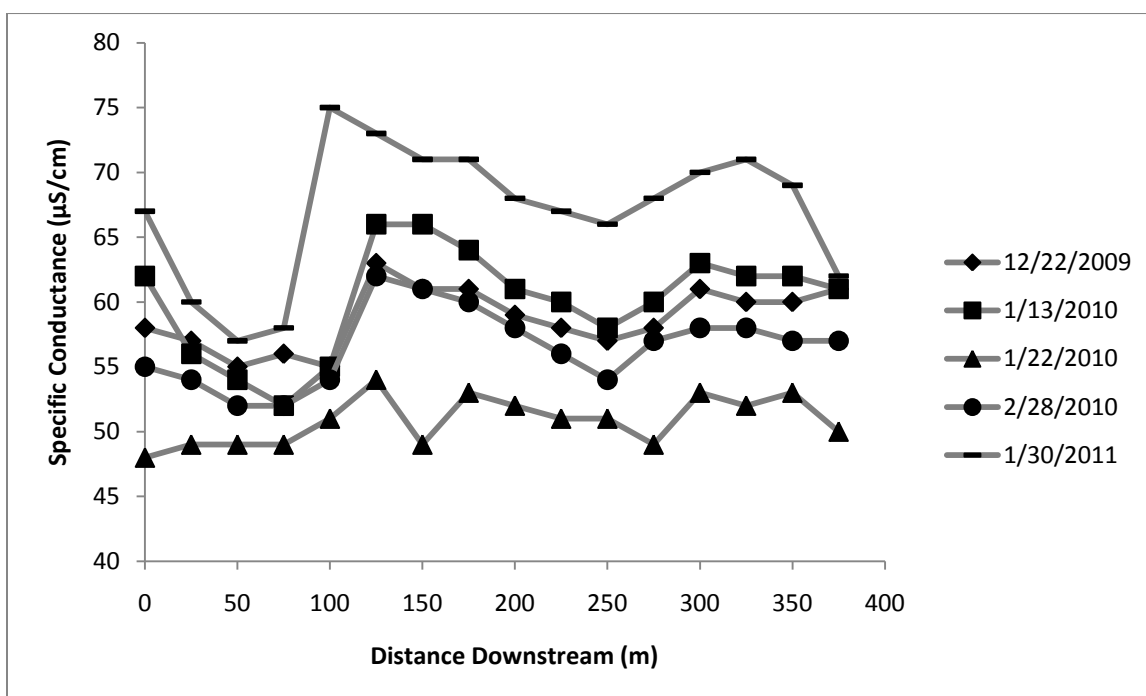


Figure 33. Specific conductance vs. distance downstream for Deep Creek during the winter months only. Elevated conductance at 125 m is less pronounced than is seen during the summer, with increases only ranging between 5 – 15 µS/cm.

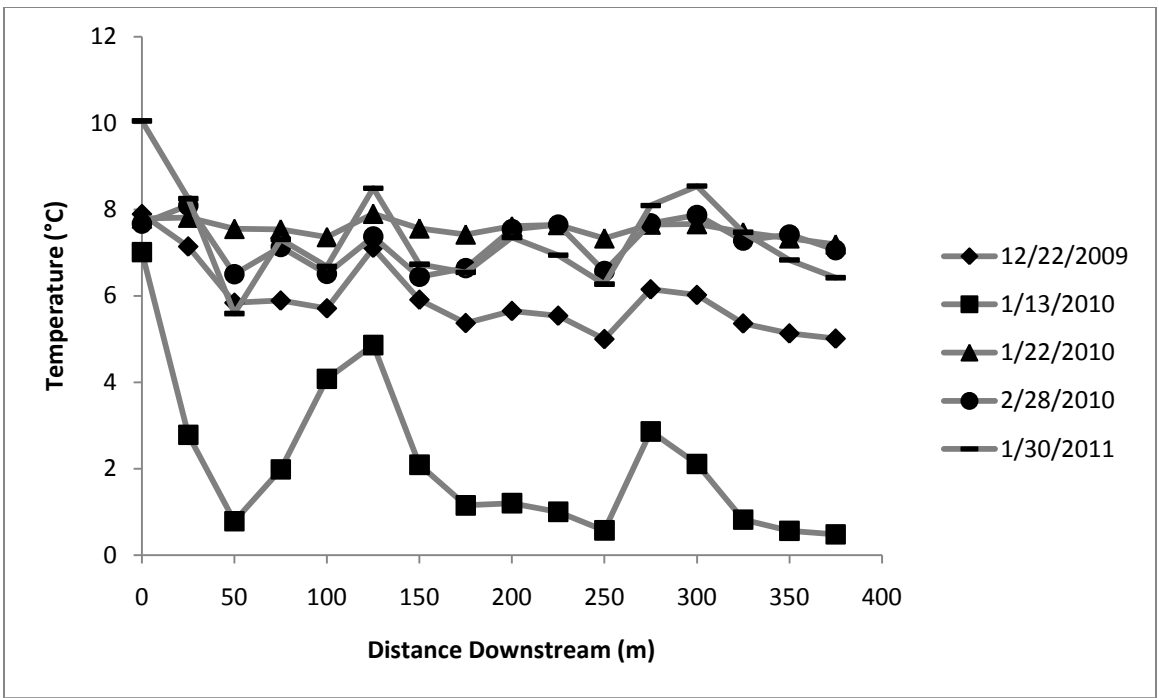


Figure 34. Temperature vs. downstream distance for Deep Creek during winter months shows a reversal of the trend seen in the summer. In terms of air temperature, one of the coldest weeks during the study period occurred during the week leading up to and including the measurements taken on 1/13/2010. During this week mean air temperature was -1 °C.

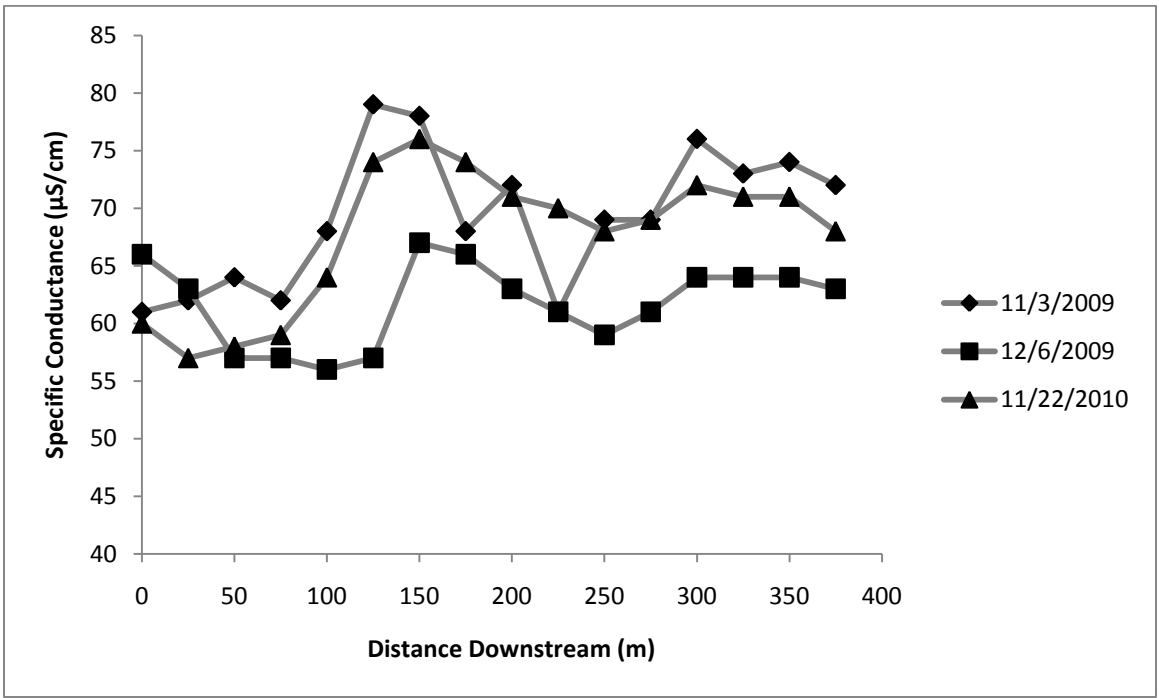


Figure 35. Specific conductance vs. distance downstream for Deep Creek during the fall months only. Conductance signatures were slightly more elevated (10 – 15 µS/cm) at 125 m during the fall than the winter.

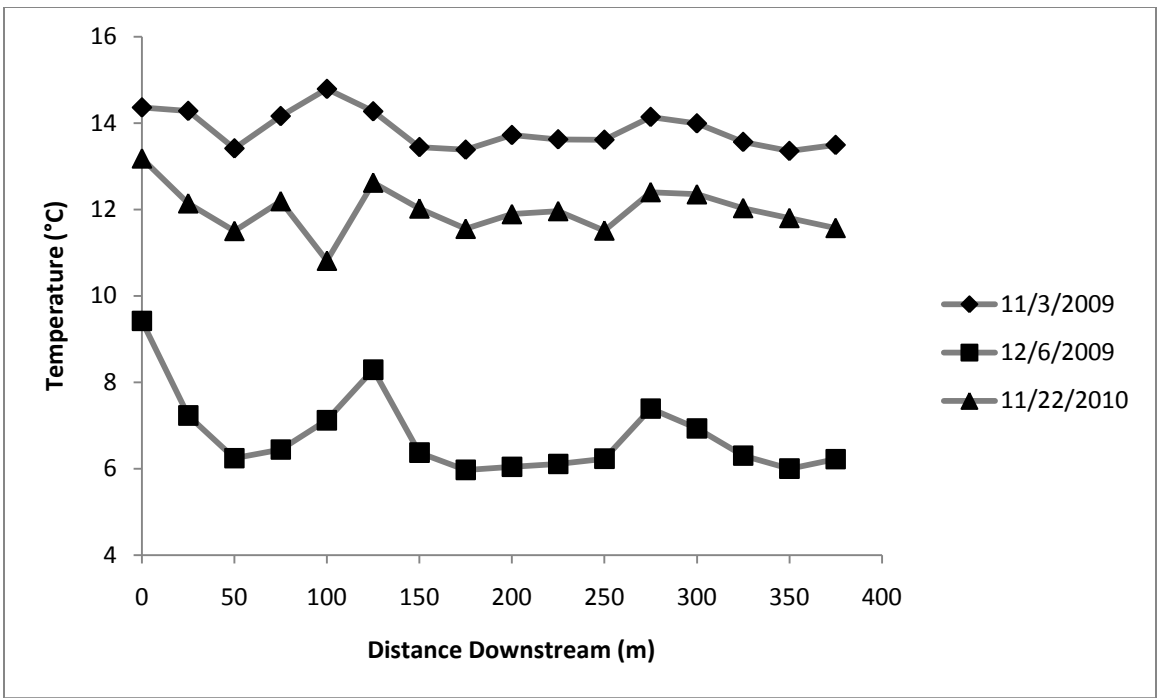


Figure 36. Temperature vs. downstream distance for Deep Creek during the fall clearly shows overall stream temperature declining as the season progresses closer to winter. Small perturbations in temperature can be seen at 100 m during measurements taken in November. A clearer signature emerges in December when baseline stream temperatures drop sufficiently to see the warmer upwelling groundwater.

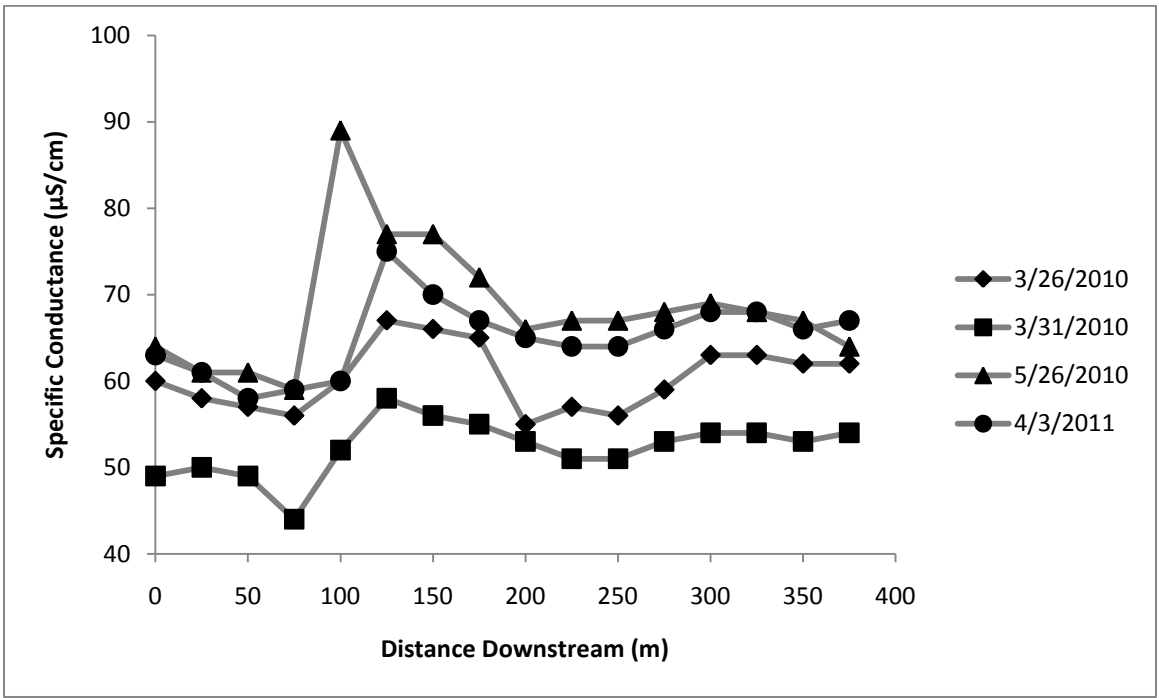


Figure 37. Specific conductance vs. distance downstream for Deep Creek for spring months. Specific conductance increases range from 10 – 15 µS/cm and in one case decreases (5/26/2010) by 12 µS/cm.

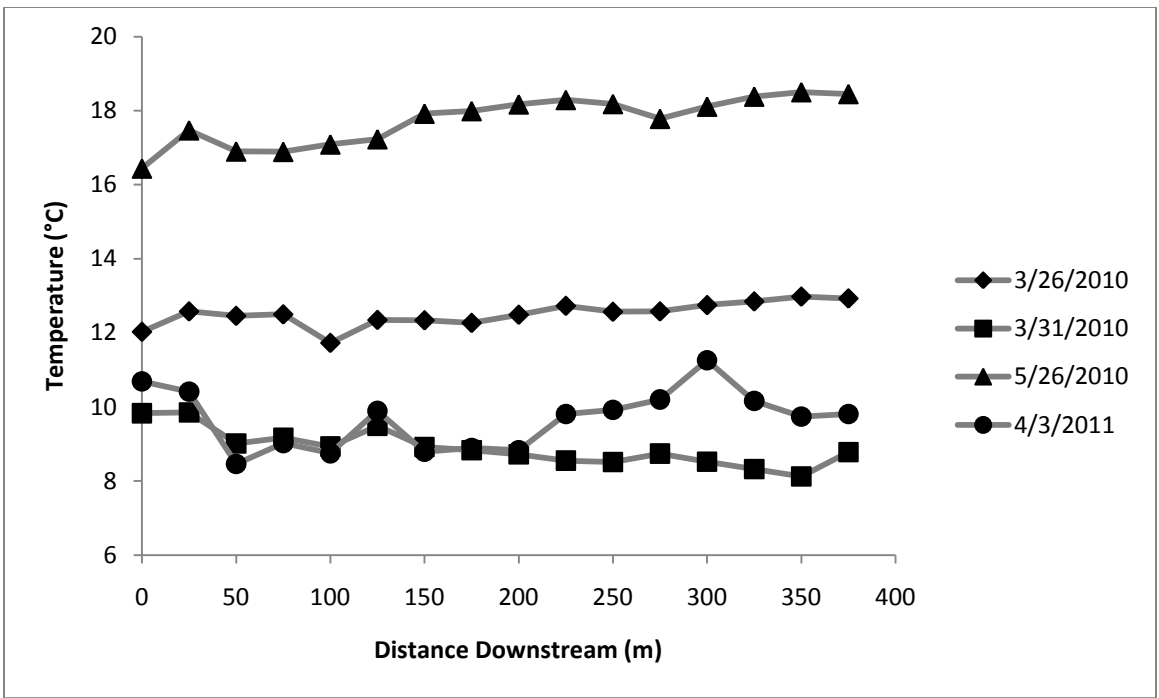


Figure 38. Temperature vs. distance downstream for Deep Creek during the spring shows few marked perturbations in temperature. This is to be expected if groundwater temperature is very close to ambient stream temperature at this time of year.

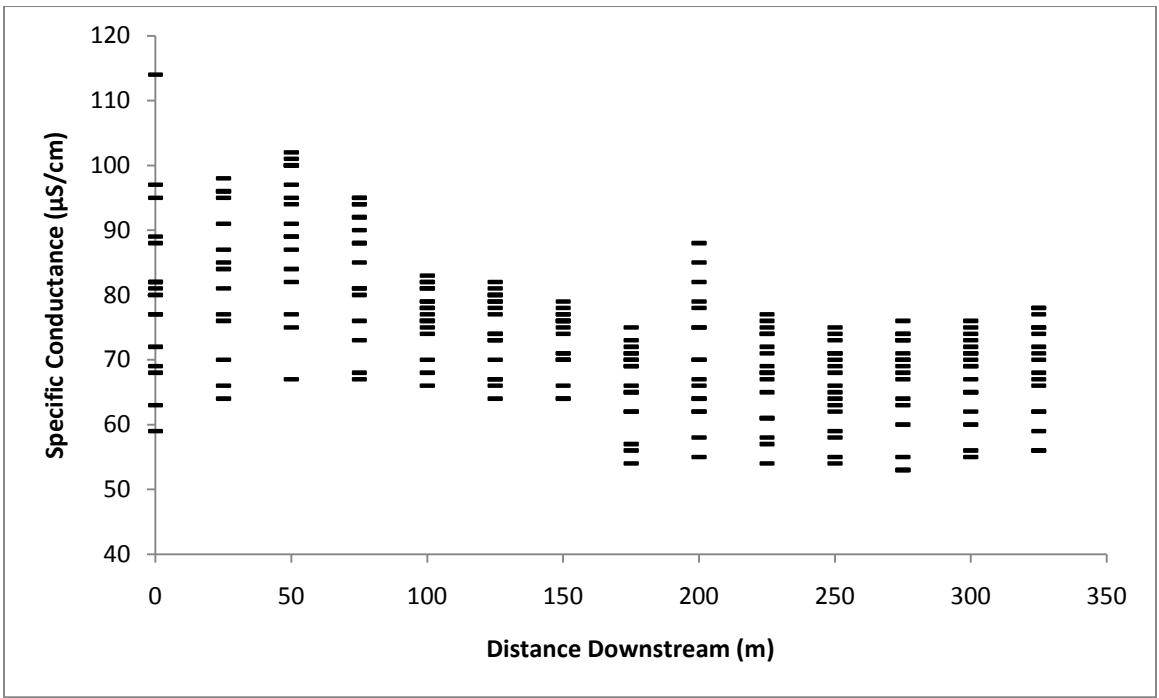


Figure 39. Cumulative plot of all specific conductance measurements for Cabin Creek vs. downstream distance. Elevated specific conductance is seen most frequently at 50 m and 200 m with the general trend being an overall gradual decrease in conductance from the first measurement point to the last.



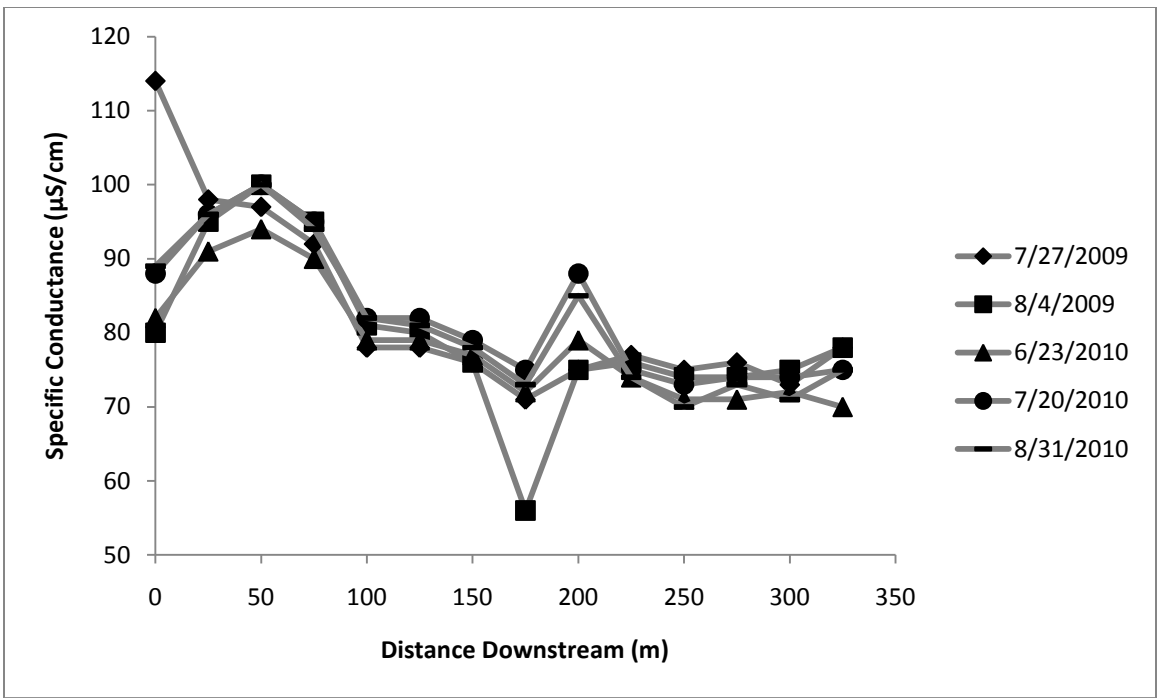


Figure 40. Relationship between specific conductance and downstream distance for Cabin Creek during summer months. Potential groundwater discharge zones are seen at 50 m and 200 m.

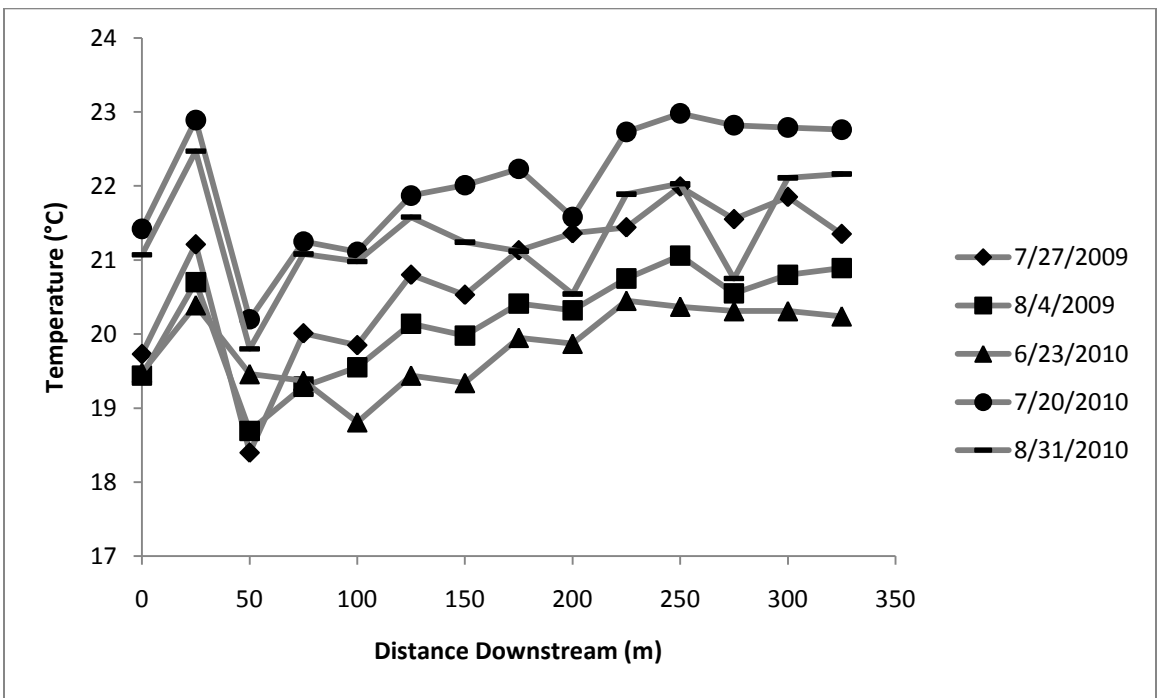


Figure 41. Summer relationships of temperature vs. downstream distance for Cabin Creek support possible groundwater discharge at 50 m and 200 m. A strong cooling signature can be seen at 50 m and a weaker one is present at 200 m.

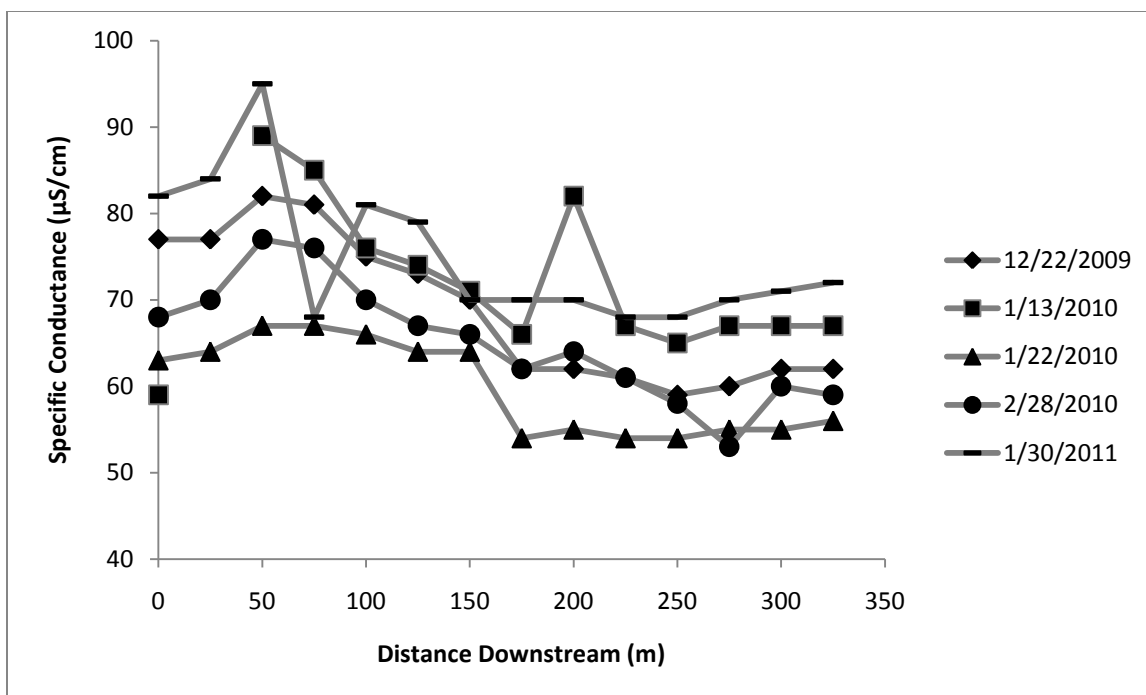


Figure 42. Specific conductance vs. downstream distance for Cabin Creek during winter shows the 50 m point having a distinctly elevated conductance and a relatively small spike at 200 m.

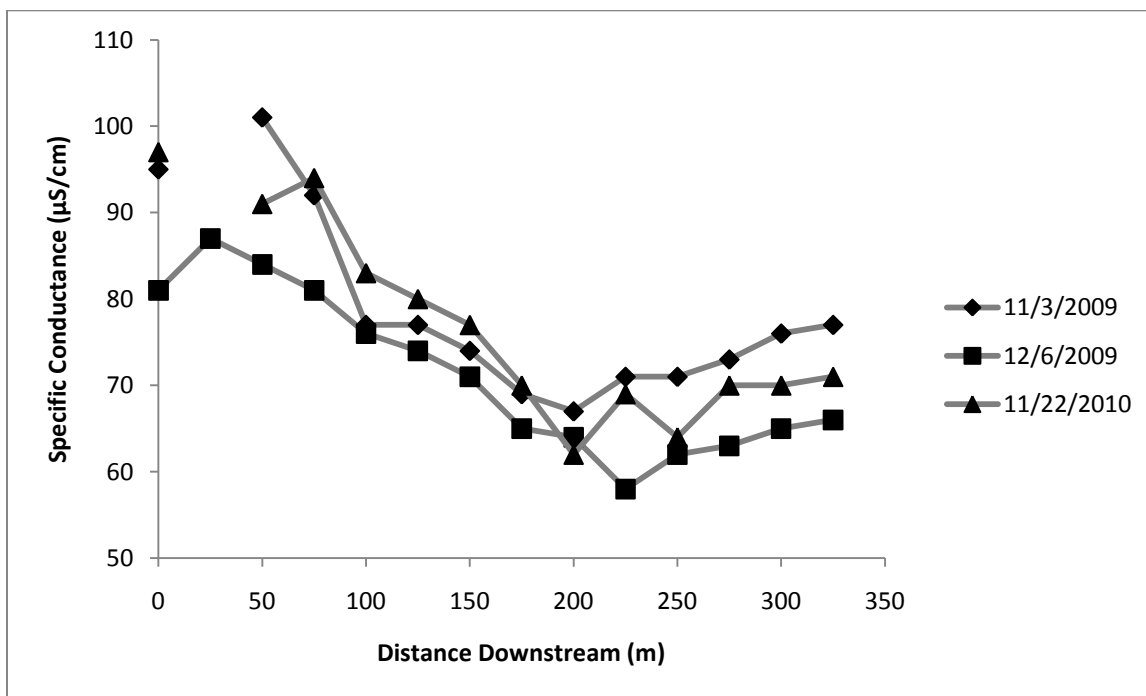


Figure 43. Fall trends in specific conductance vs. downstream distance in Cabin Creek show conductance rising at the 25 – 50 m point and decreasing until 225 m. After 225 m conductance gradually increases over the remaining length of the creek. No water was present at 25 m on 11/6/09 and 11/22/09.

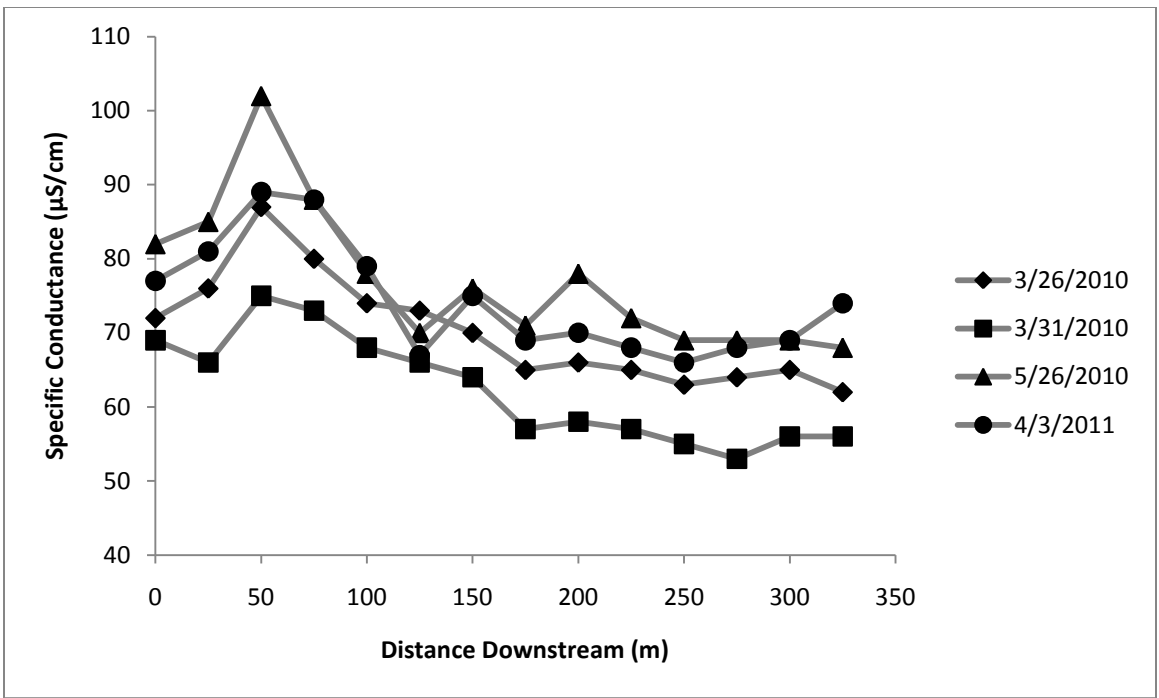


Figure 44. Specific conductance vs. downstream distance for Cabin Creek in the spring shows the reappearance of clearly elevated conductance at 50 m and a slight elevation at 200 m.

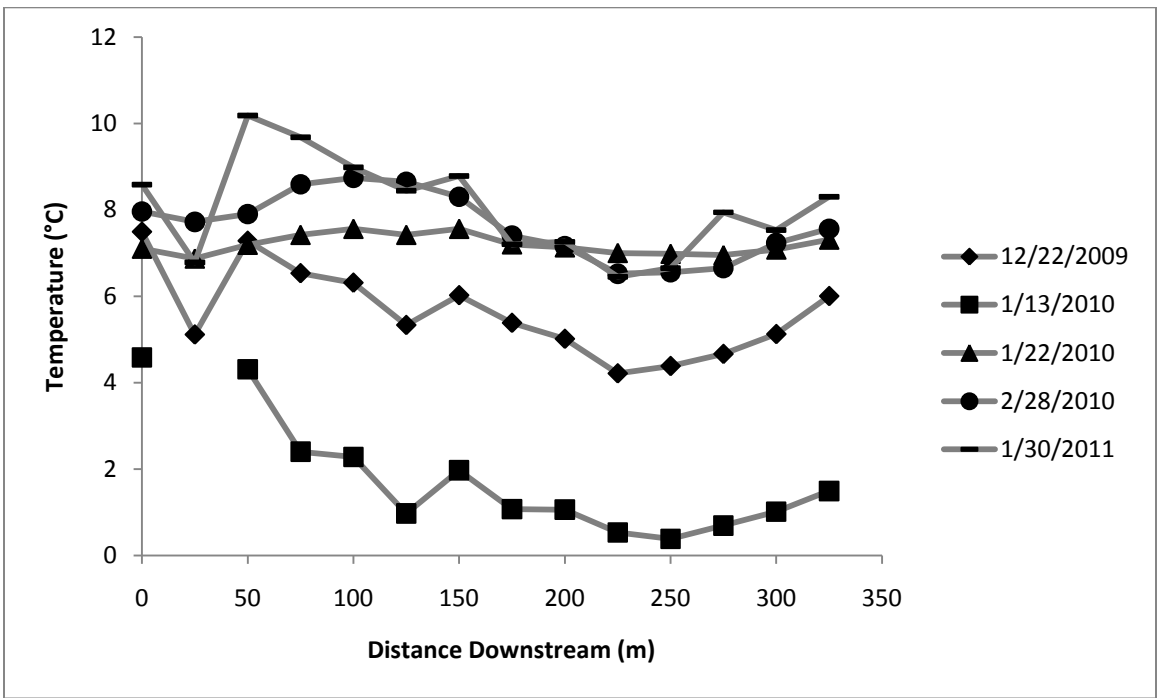


Figure 45. Plotting temperature vs. distance downstream in Cabin Creek during winter months shows a noticeable rise in water temperature at 50 m and no apparent perturbation at 200 m.

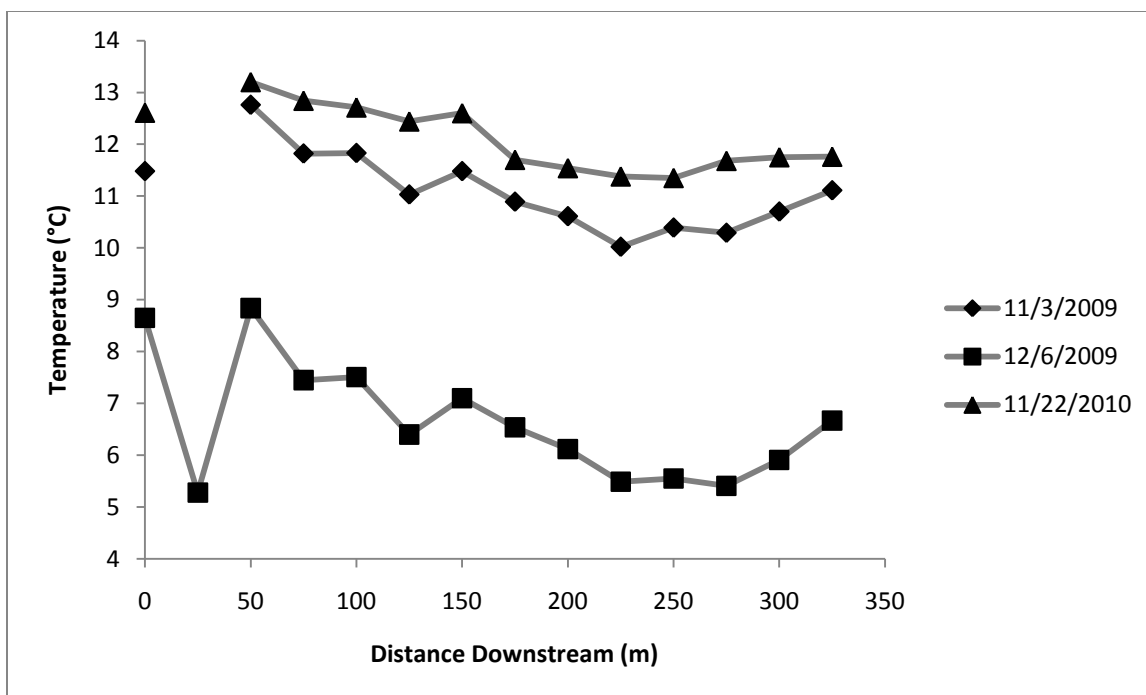


Figure 46. Temperature vs. downstream distance on Cabin Creek for fall measurements shows a large (3 °C) drop in temperature at 25 m during the 12/6/09 round of data collection. Water was not present here during the other two measurement rounds, indicating that there may be a losing reach upstream of that point.

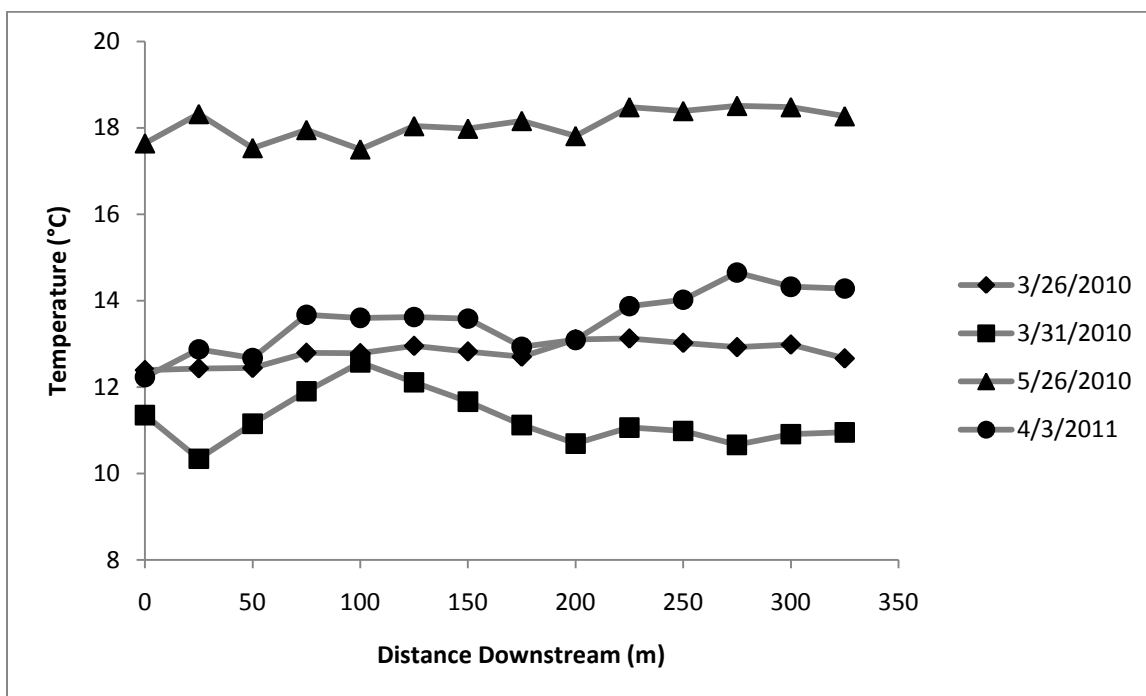


Figure 47. Temperature vs. downstream distance along Cabin Creek in the spring does not show any clear trend with regards to the two points (50 m and 200 m) of possible groundwater discharge. So signatures are typical for spring when average air temperature is close to average groundwater temperature.

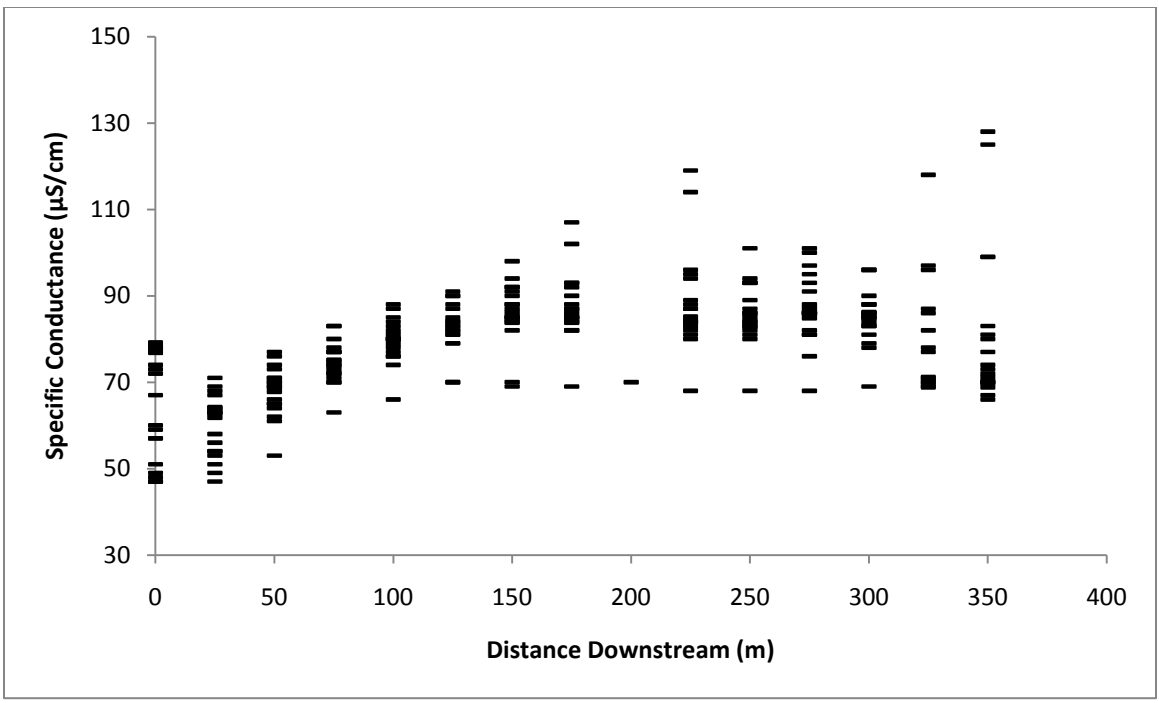


Figure 48. Cumulative plot of all specific conductance measurements in relation to downstream distance for Creek 90. Specific conductance tends to increase in the downstream direction, usually peaking at some point between 150 m and 275 m. Conductance values decline after 275 m. Water was only recorded once in the ephemeral section at 200 m.

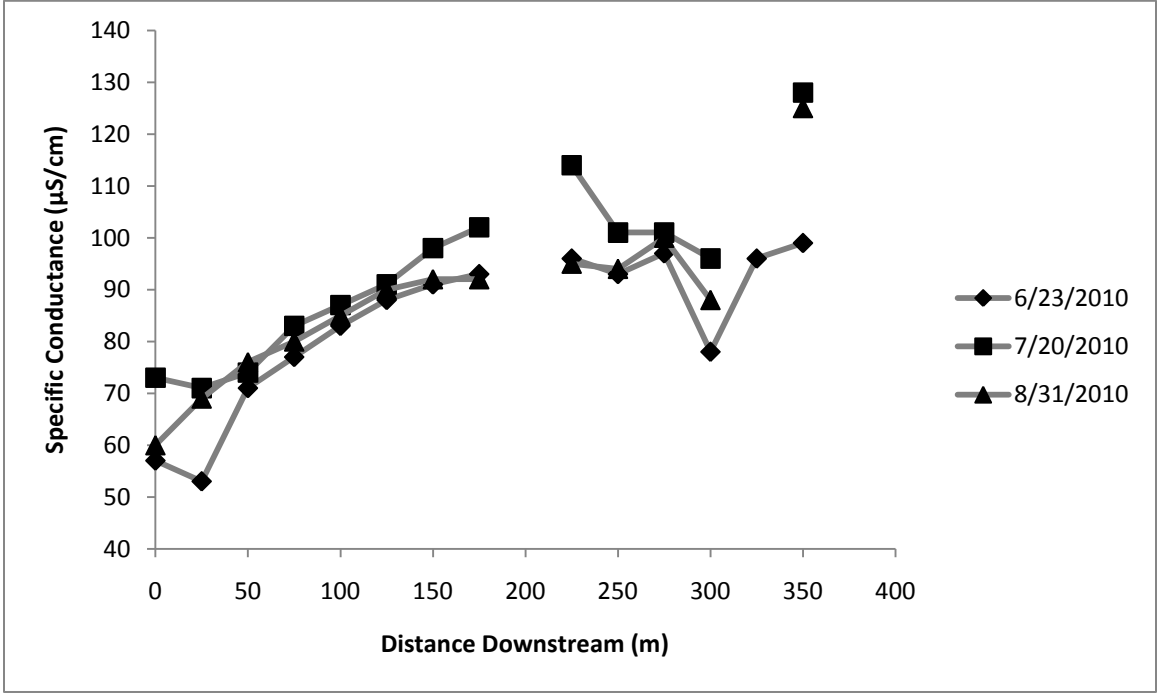


Figure 49. Specific conductance vs. downstream distance for Creek 90 in the summer did not show an overall decrease in conductance over the final third of the creek. A decrease in conductance was seen during winter, spring, and fall.

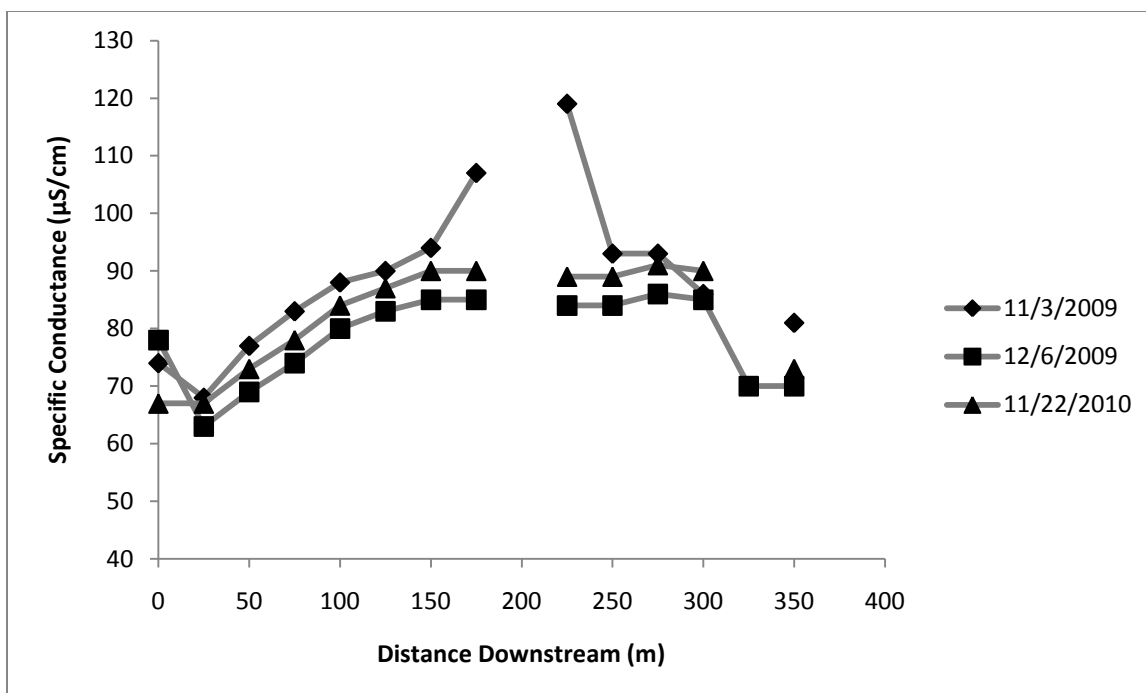


Figure 50. Specific conductance measurements during the fall at Creek 90 show conductance values dropped by 5 – 15  $\mu\text{S}/\text{cm}$  over the final 75 m relative to the middle reaches of the stream. This trend was present during three of four seasons.

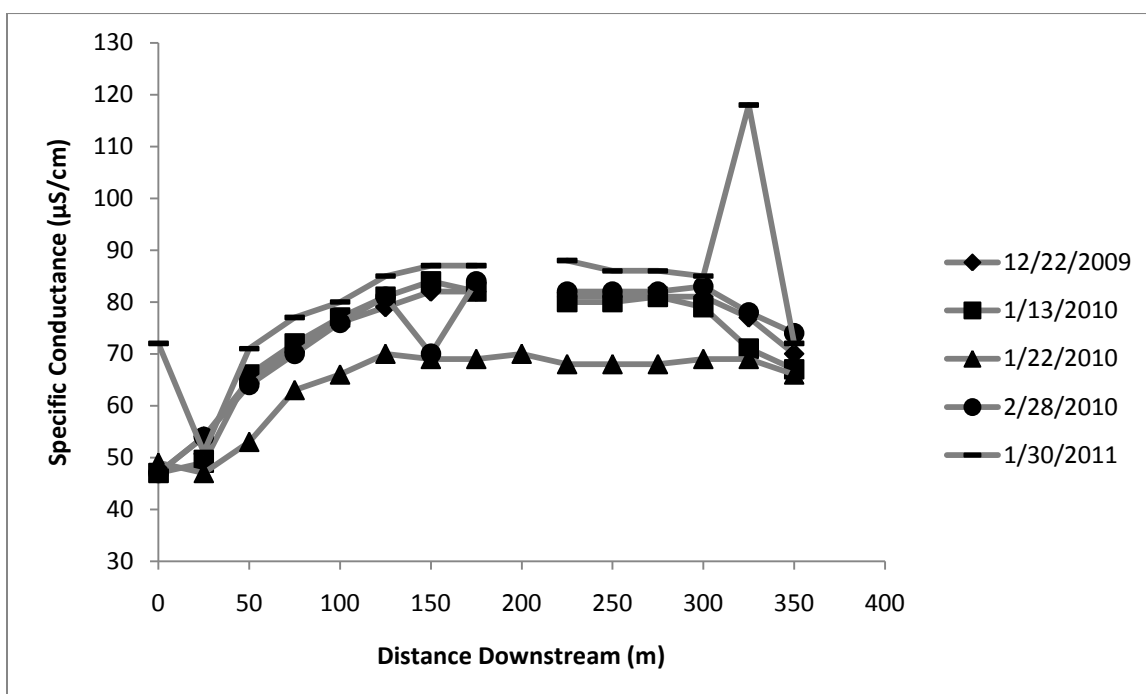


Figure 51. The general trend for winter specific conductance values at Creek 90 showed the typical 5 – 15  $\mu\text{S}/\text{cm}$  drop in conductance over the final few reaches of the creek. Although one outlier seemed to defy this trend at 325 m on 1/30/2011, conductance quickly diminished to normal baseline levels by 350 m.

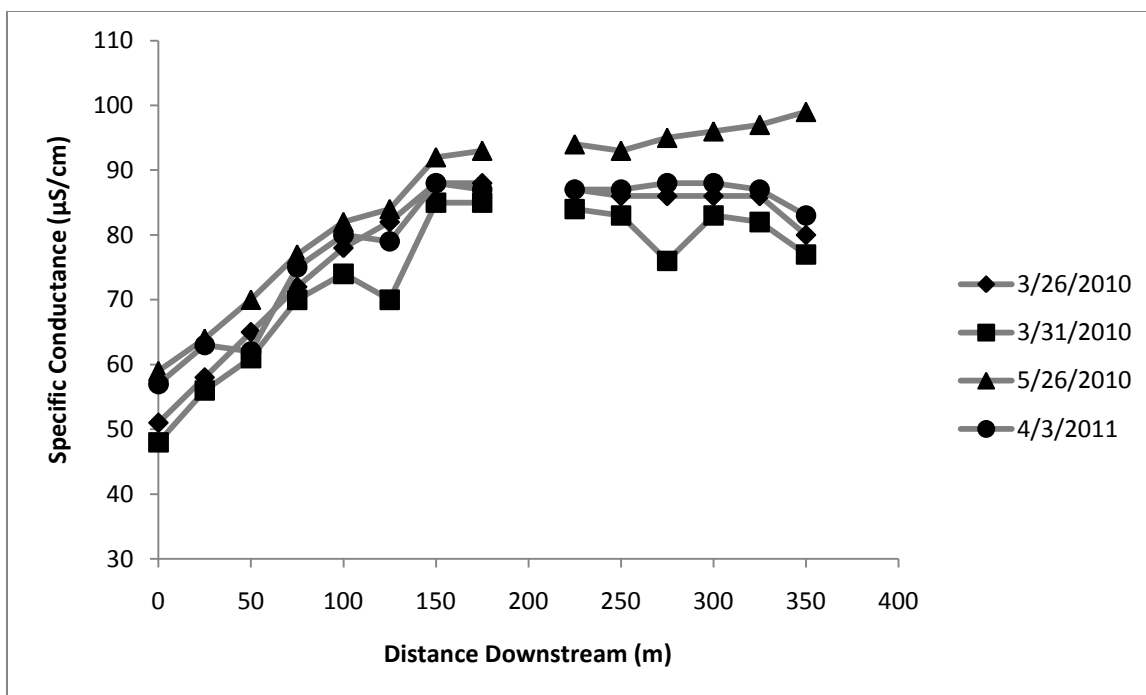


Figure 52. The trend that dominated fall and winter conductance values over the final third of the creek appeared again in the spring with conductance dropping by 5 – 15  $\mu\text{S}/\text{cm}$  in the last three reaches. A progression to a summer pattern may be in the beginning stages during measurements taken on 5/26/2010, where conductance increases by 5  $\mu\text{S}/\text{cm}$  over the last three measurement points.

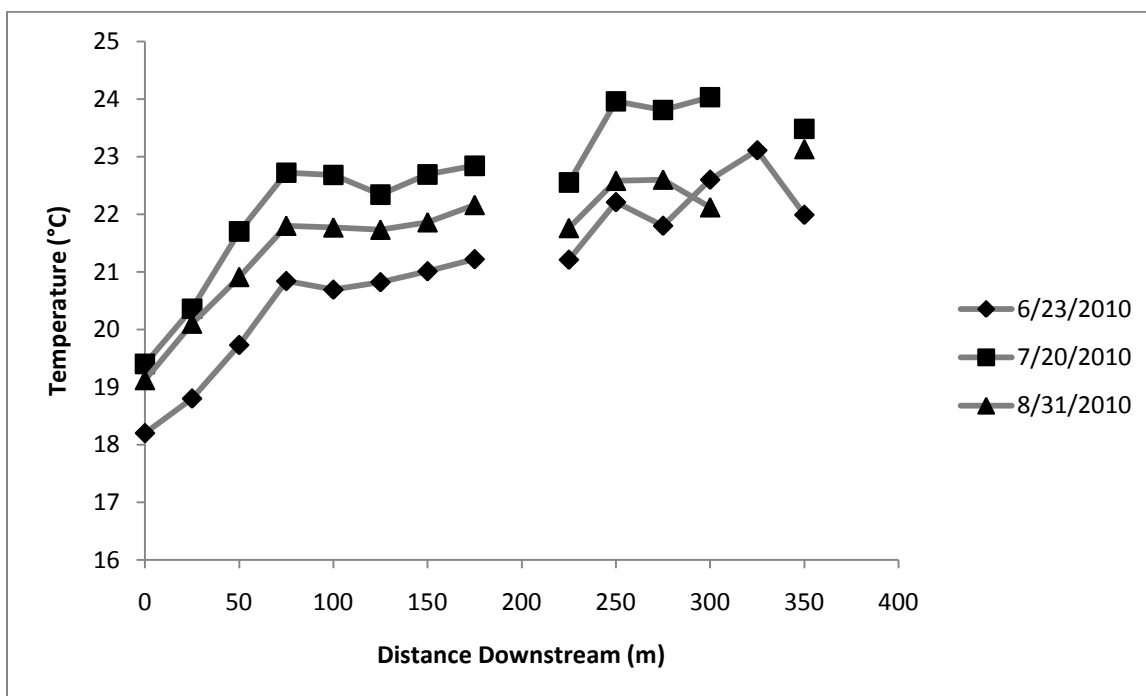


Figure 53. Summer temperature patterns at Creek 90 show a similar trend to specific conductance, with a steady increase in temperature up to 75 m before an abrupt leveling off occurs.

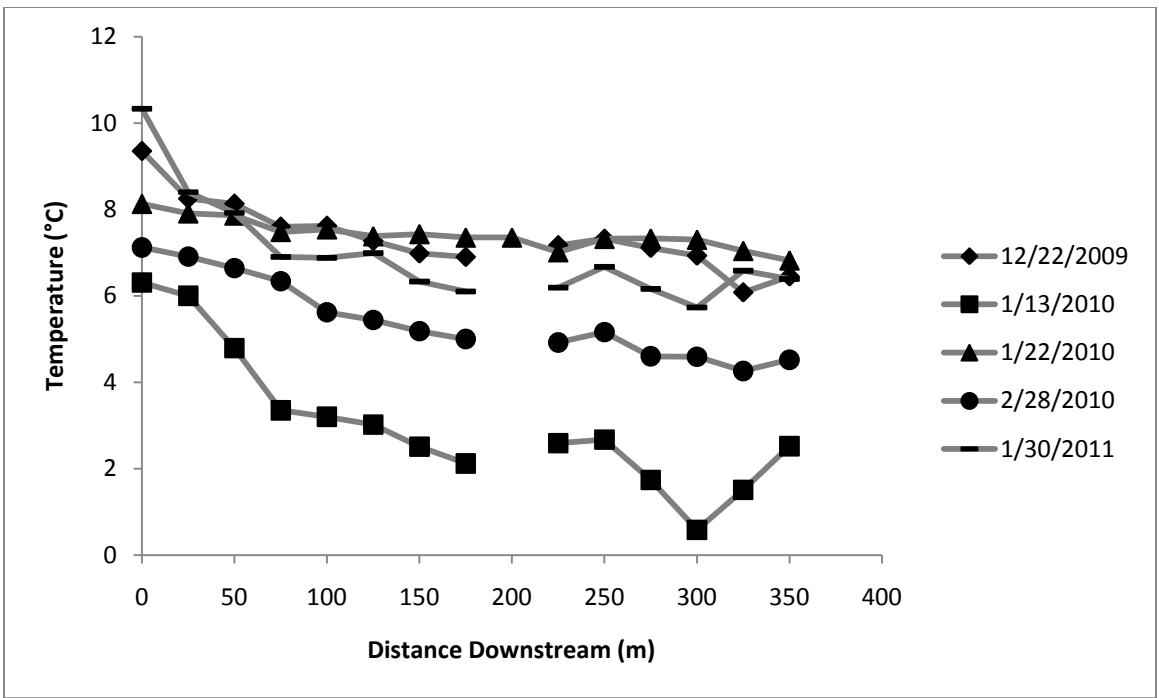


Figure 54. Winter stream temperatures at Creek 90 decline quickly to 75 m and continue on a more gradual decline thereafter.

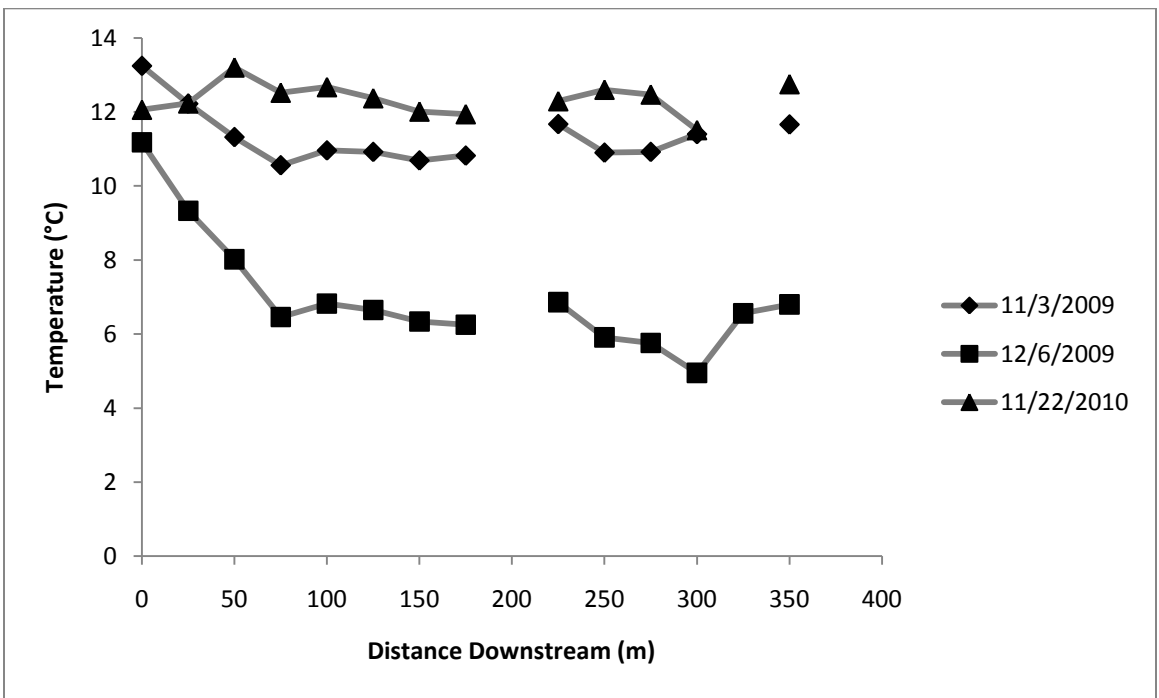


Figure 55. Water temperature for two sampling dates in the fall showed a rapid decrease to 75 m followed by an abrupt plateau. Water temperature on 11/22/2010 was influenced more by unusually high air temperature (21 °C) that is more typical of late October.



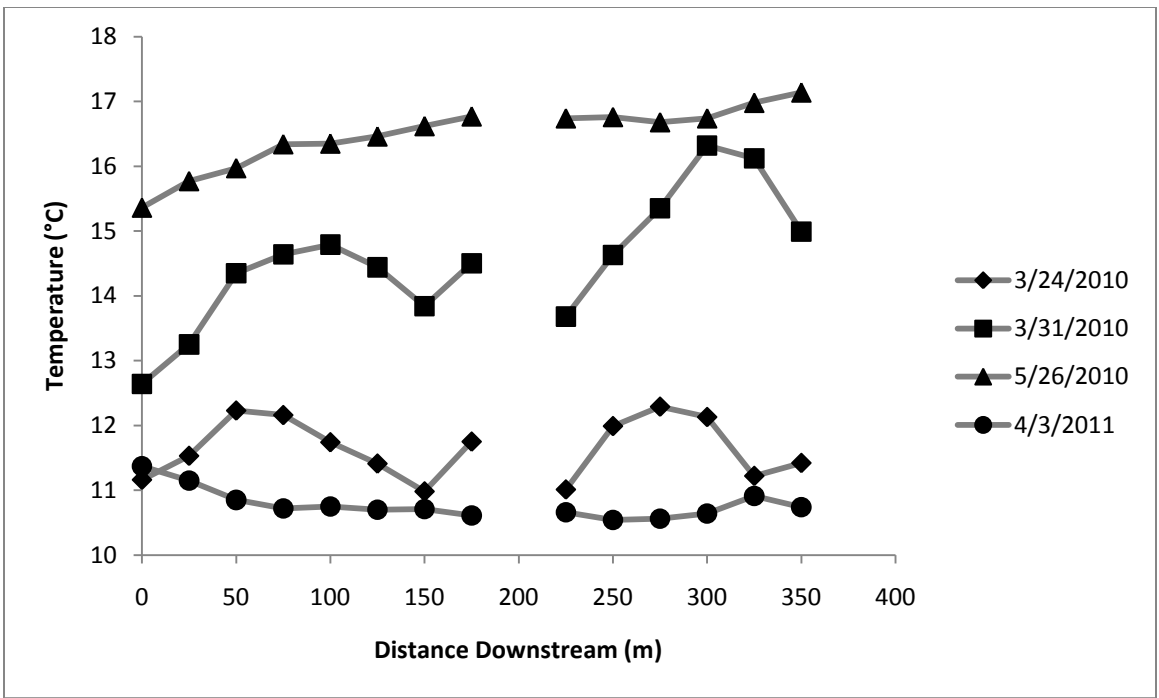


Figure 56. Breaks in stream temperature at 75 m can be seen in the spring at Creek 90, though variable air temperatures tend to make the overall trend more chaotic.

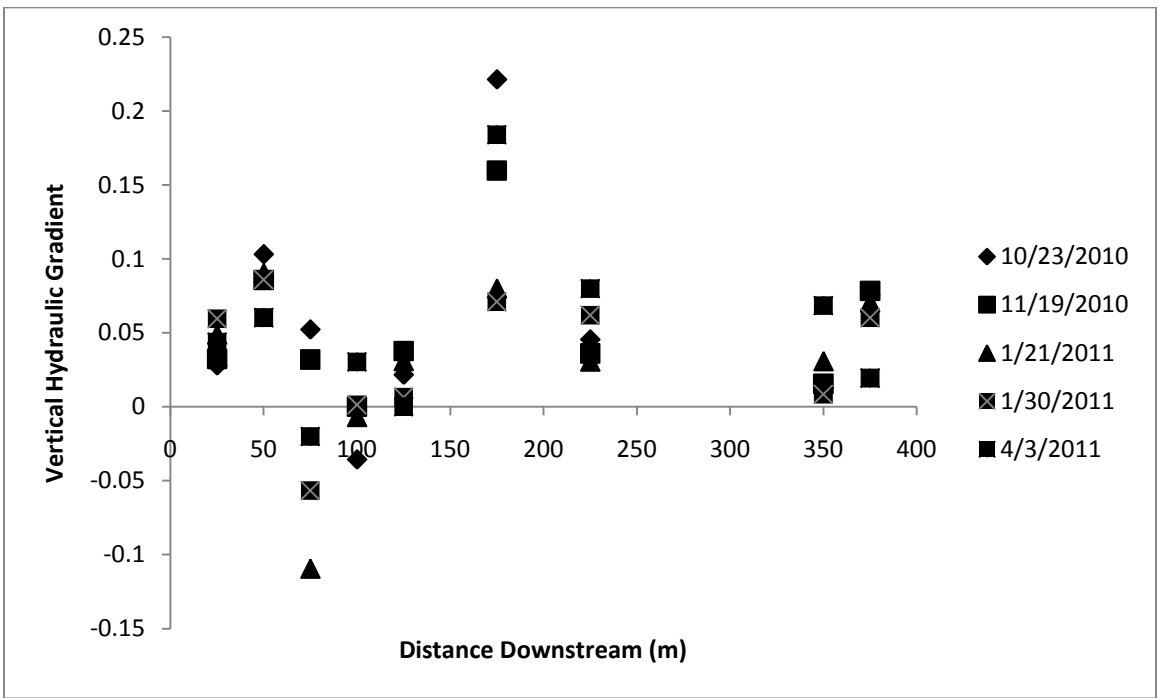


Figure 57. Graph showing variations in vertical hydraulic gradient as a function of downstream distance for Deep Creek.

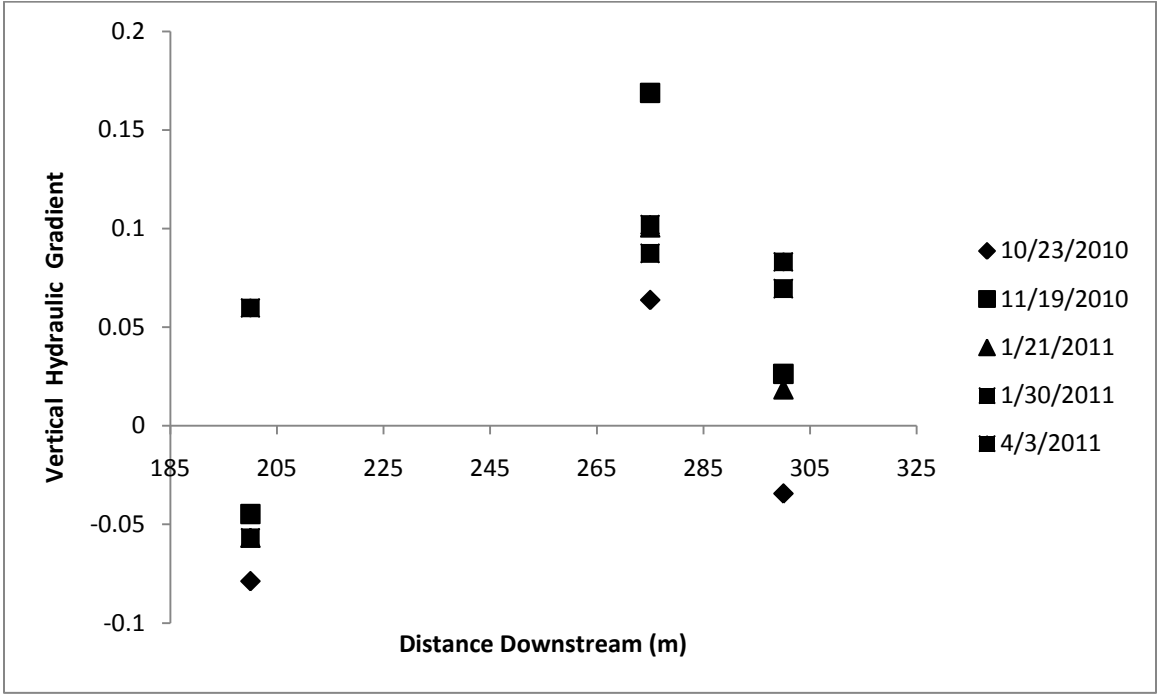


Figure 58. Graph showing vertical hydraulic gradient as a function of distance downstream for Cabin Creek.

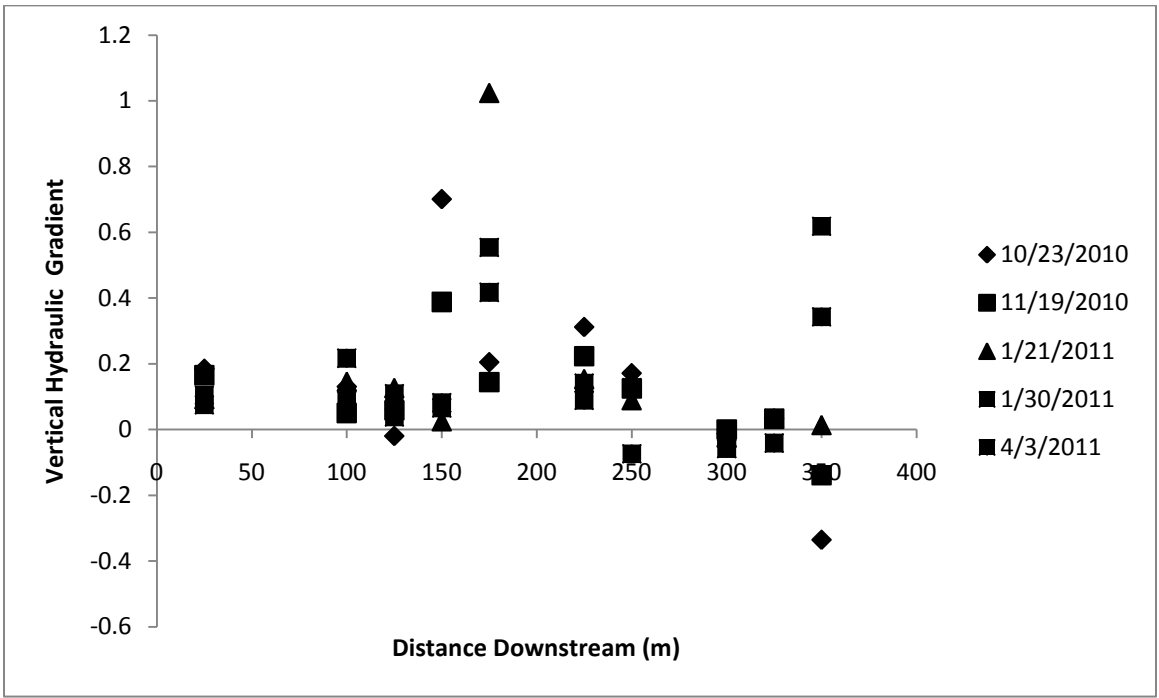


Figure 59. Graph showing vertical hydraulic gradient as a function of distance downstream for Creek 90.

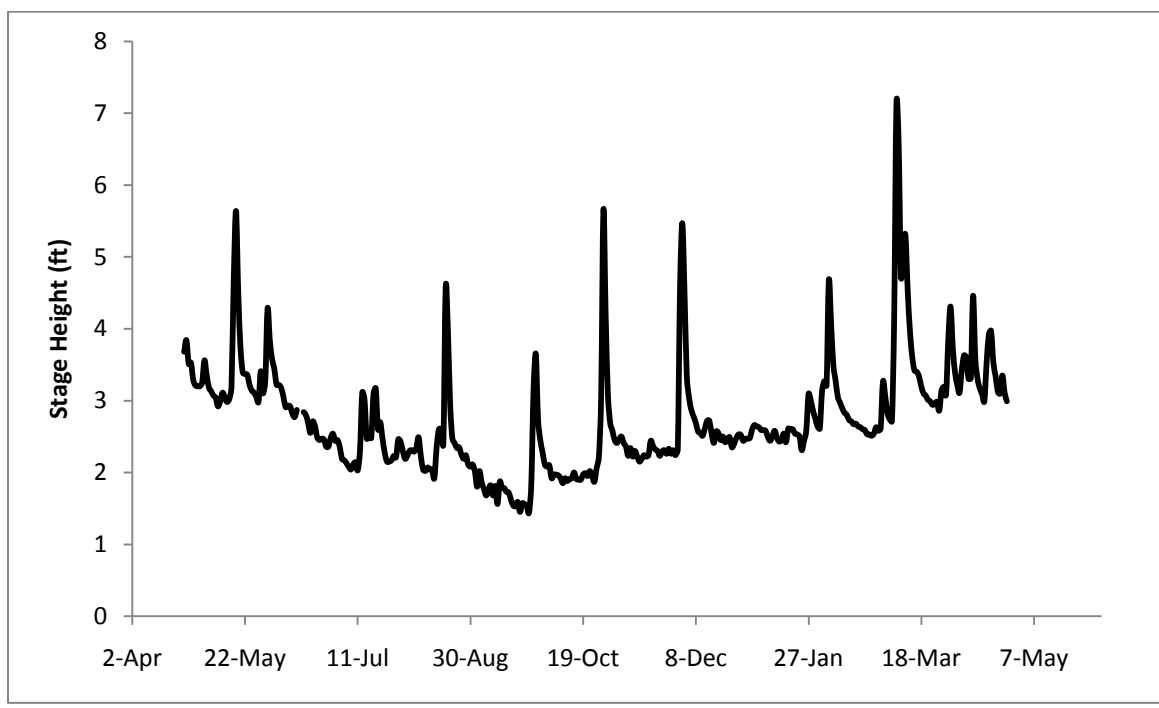


Figure 60. Stage height values for the South Fork of the Catawaba River show stage reaching its lowest level during late September/early October and rising steadily into winter. Head gradient values at Creek 90 350 m mirror this pattern by their most negative values in October before rising into January.

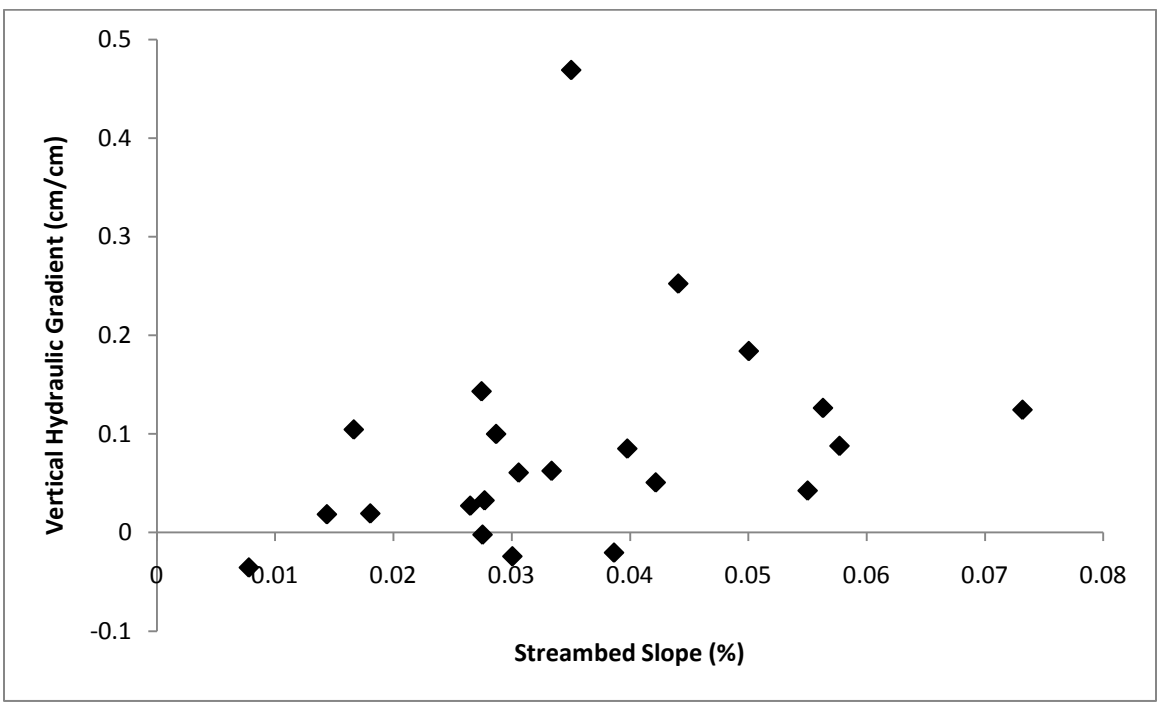


Figure 61. Relationship between streambed slope and vertical hydraulic gradient. Although a statistically significant relationship was not seen, visual correlation suggests a positive correlation between slope and vertical gradient ( $p$ -value = 0.10).







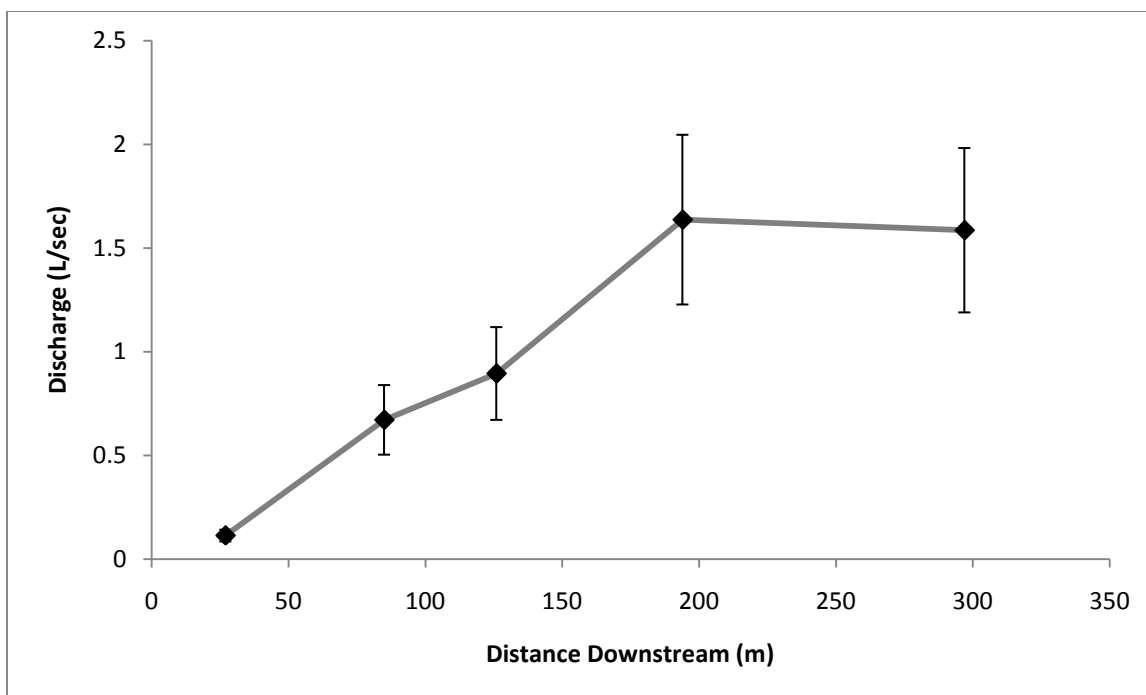


Figure 68. Longitudinal discharge measurements at Cabin Creek show a pattern of steadily increasing discharge from the 27 m measurement point down to 197 m, after which discharge appears to abruptly level off. Data collected on 6/15/2010.

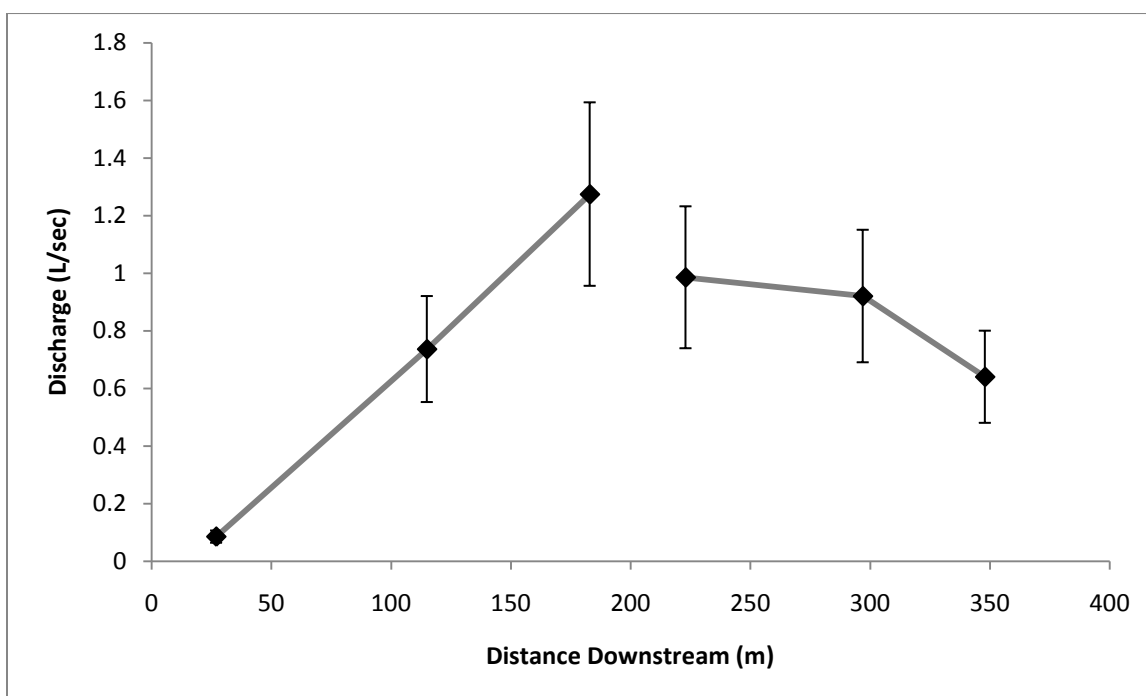


Figure 69. Longitudinal discharge measurements for Creek 90 show discharge peaking just before the creek disappears beneath the 27 m long sediment wedge. Data collected on 6/15/2010.

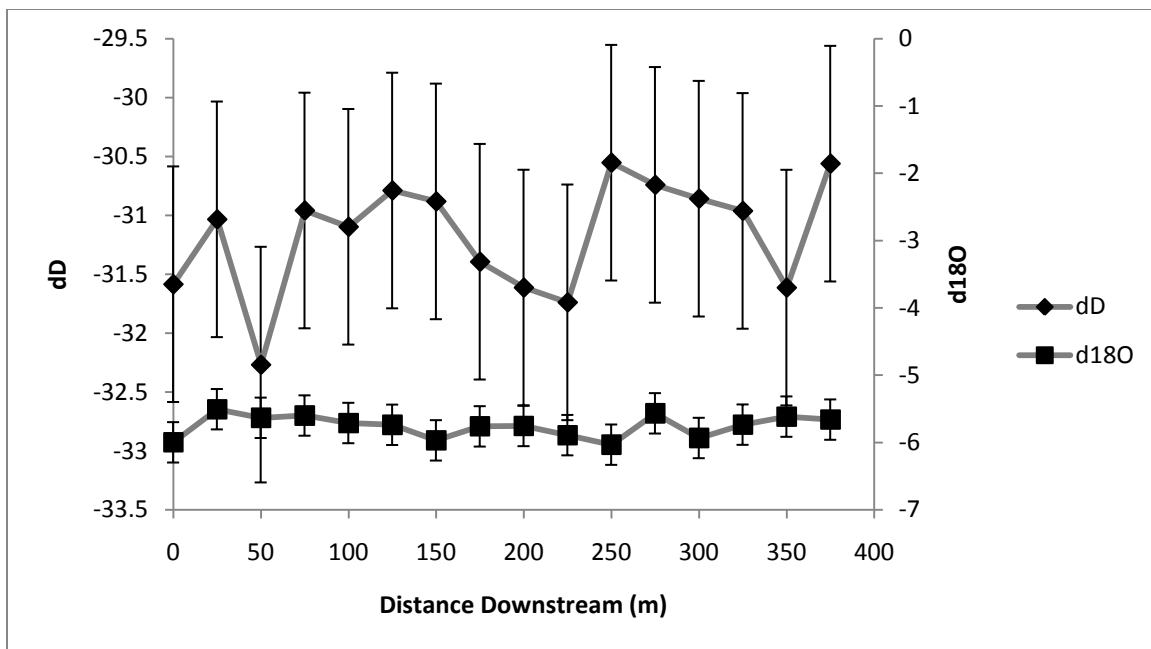


Figure 70. Stable isotope data for Deep Creek show no prominent trends that would suggest water is coming from multiple sources. Data collected 8/31/10.

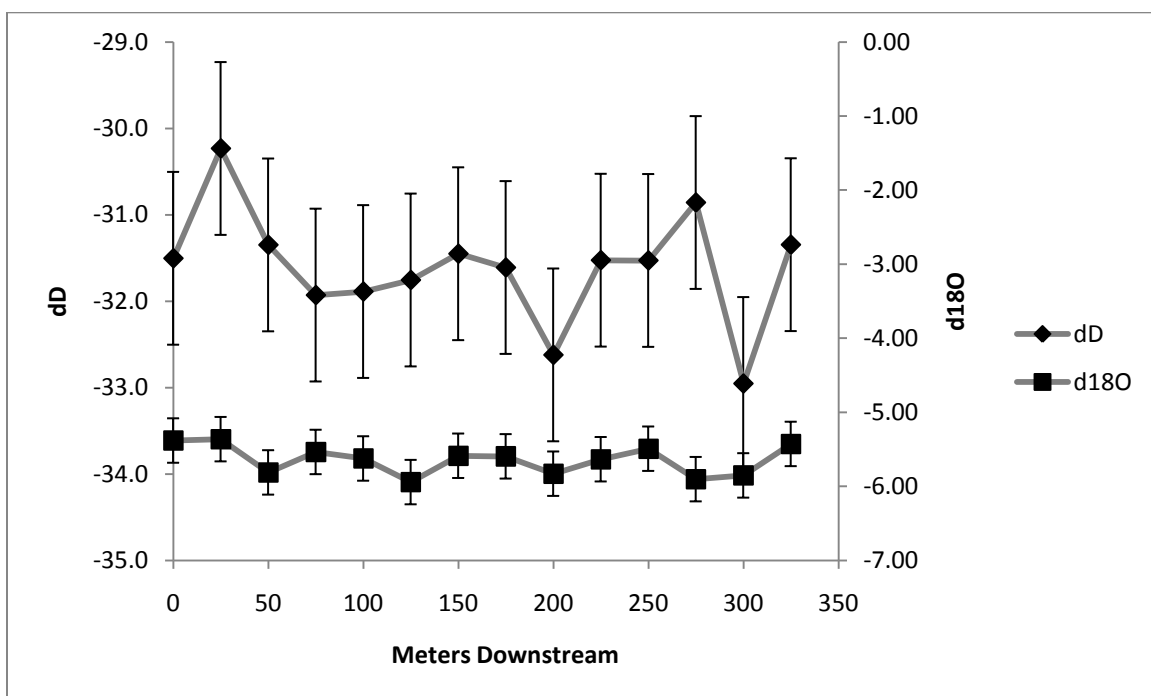


Figure 71. Stable isotope data at Cabin Creek show no trends that indicate water might be coming from multiple sources. Data collected on 8/31/10.



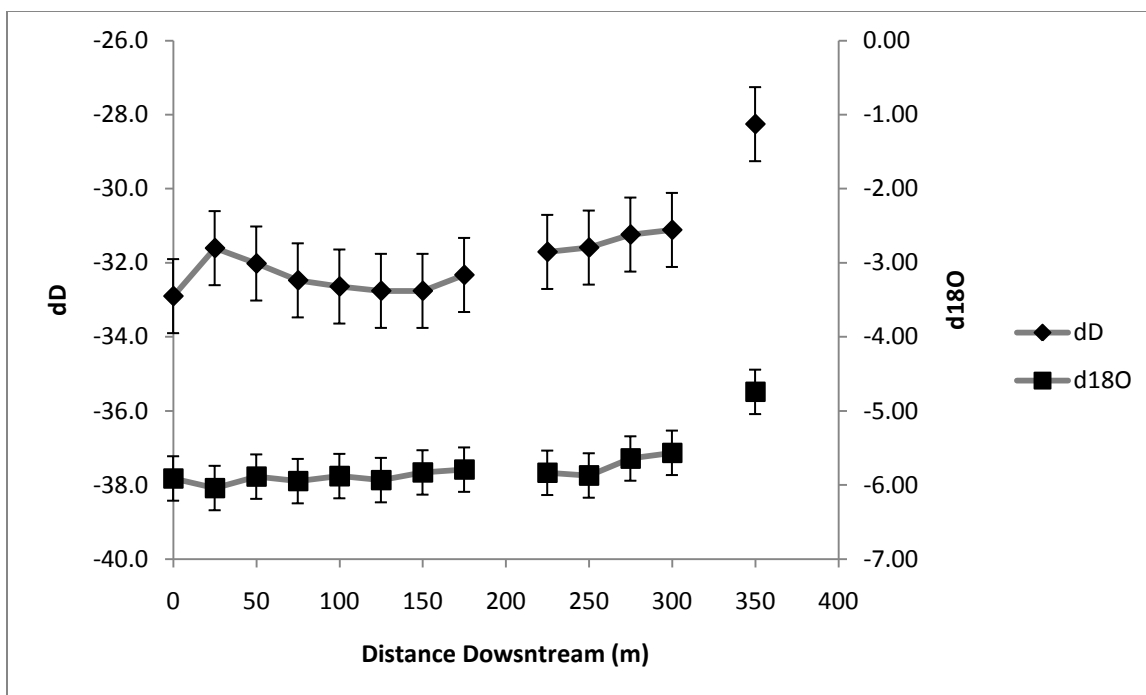


Figure 72. Stable isotope data for Creek 90 show little variation except for Creek 90 350 m, where isotope ratios trend toward higher concentrations of heavier isotopes. Data collected on 8/31/2010.

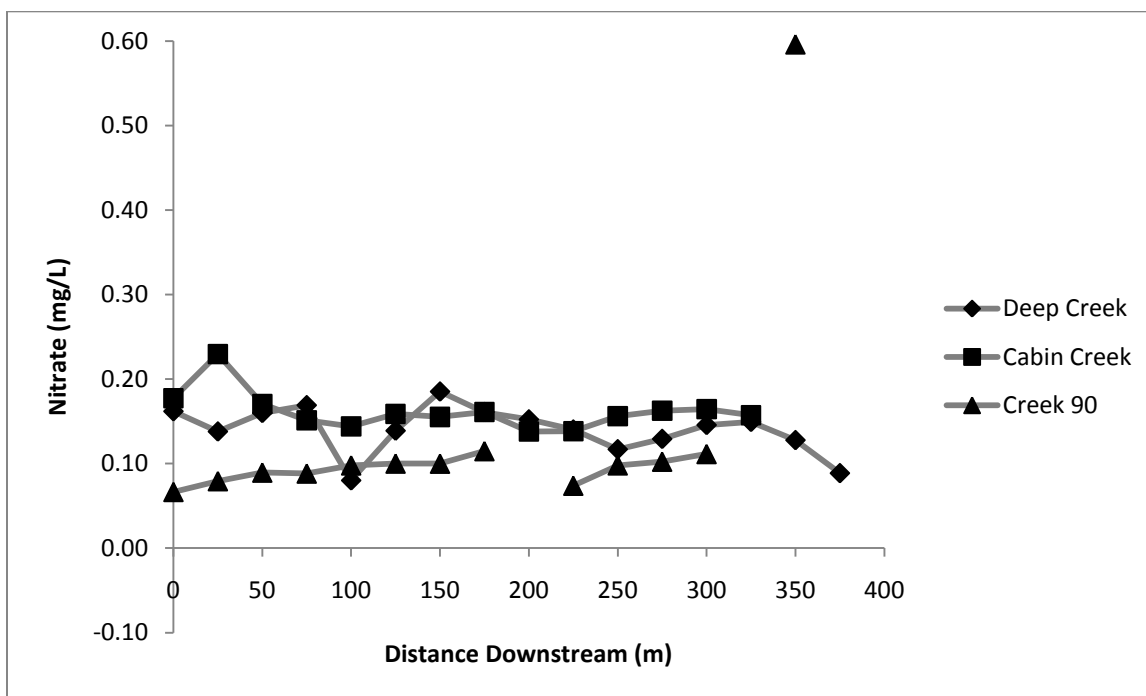


Figure 73. Nitrate concentration in the study creeks is quite low and peak at 0.60 mg/L at Creek 90, likely a cause of local interaction with the South Fork of the Catawba River. Data collected on 8/31/2010.

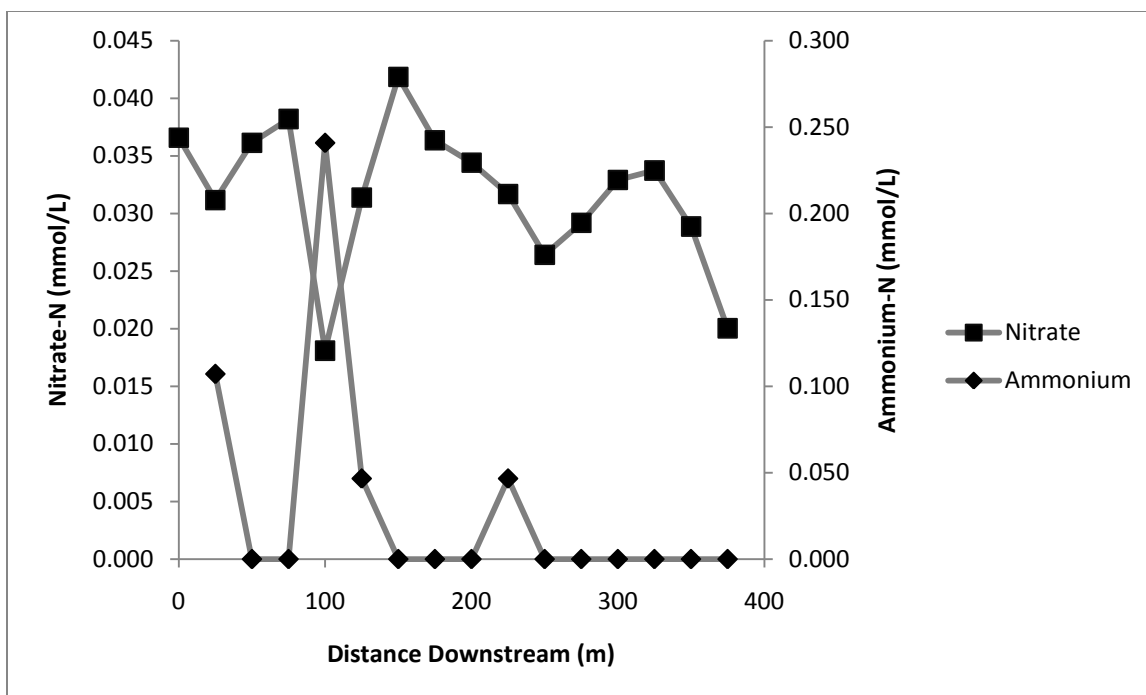


Figure 74. Nitrate versus ammonium concentrations at Deep Creek suggest several significant hyporheic flowpaths, the most prominent of which appears at 100 m. Error is estimated at 0.43% and 7.75% deviation from accepted value for nitrate and ammonium, respectively. Data collected on 8/31/2010.

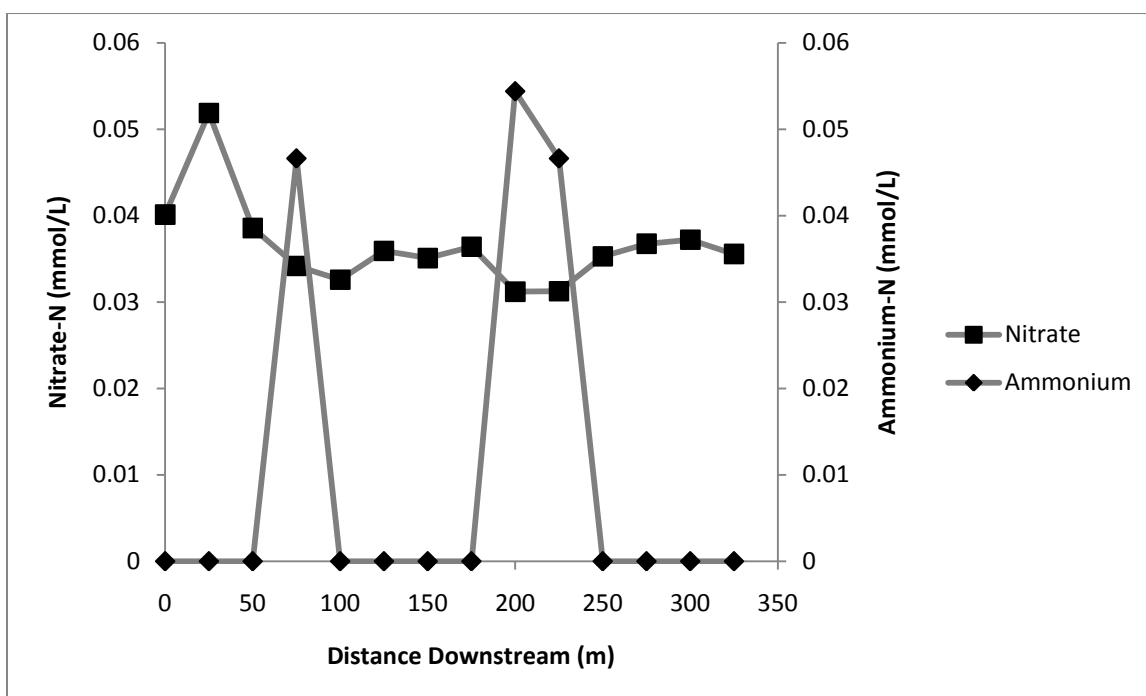


Figure 75. Nitrate versus ammonium concentrations for Cabin Creek elevated ammonium concentrations occurring with lower nitrate concentrations as a consequence of probable upwelling and downwelling. Error is estimated at 0.43% and 7.75% deviation from accepted value for nitrate and ammonium, respectively. Data collected on 8/31/2010.

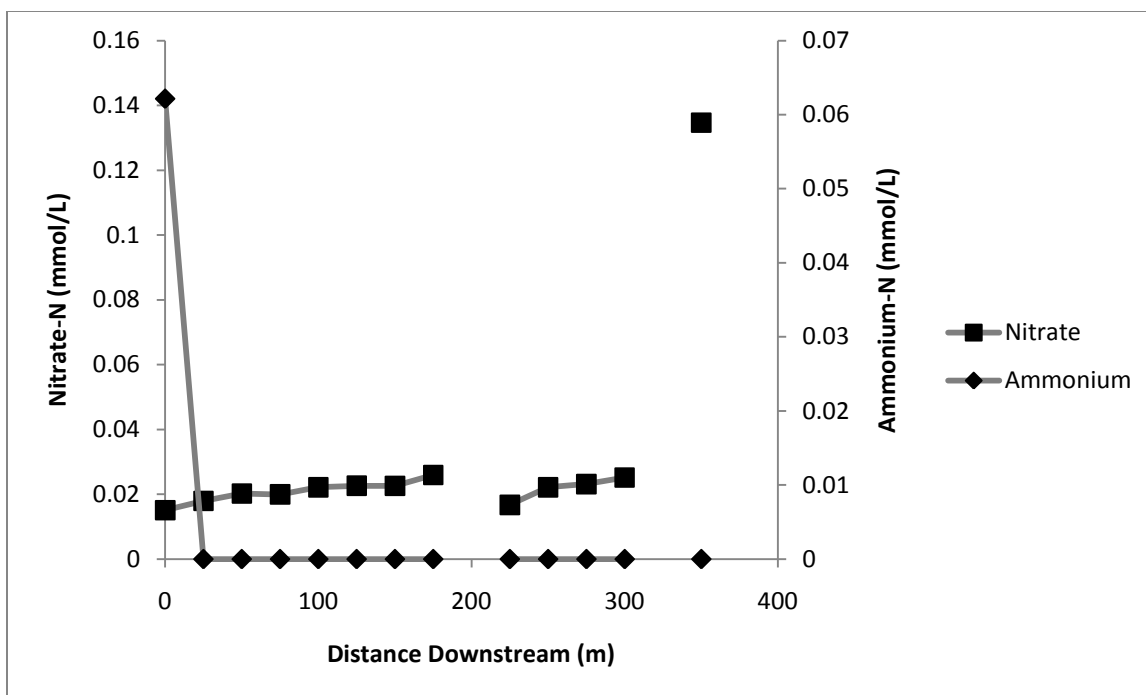


Figure 76. Nitrate versus ammonium concentrations at Creek 90 show little interpretable variation, which is in agreement with the belief that few large scale upwelling zones exist here. Error is estimated at 0.43% and 7.75% deviation from accepted value for nitrate and ammonium, respectively. Data collected on 8/31/2010.

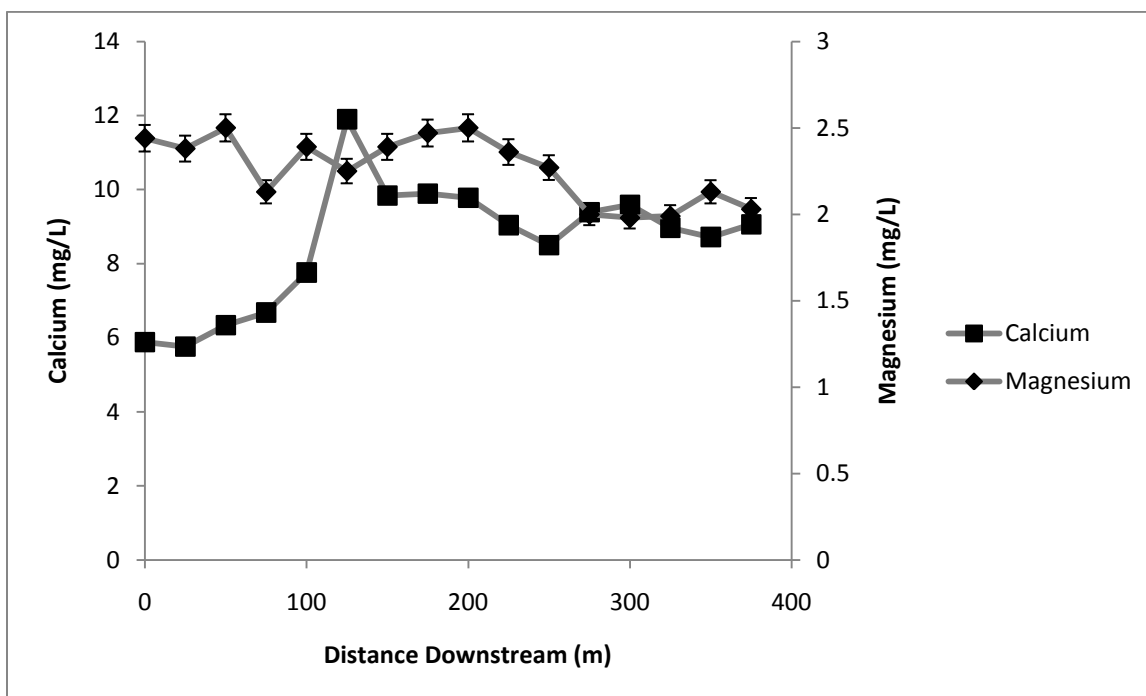


Figure 77. Calcium versus magnesium concentrations at Deep Creek show little interpretable variation in Magnesium. However, an elevated calcium signature is seen from 100 – 125 m where probable upwelling is thought to be occurring. Error is estimated at 0.28% and 3.15% deviation from accepted value for calcium and ammonium, respectively. Data collected on 8/31/2010.

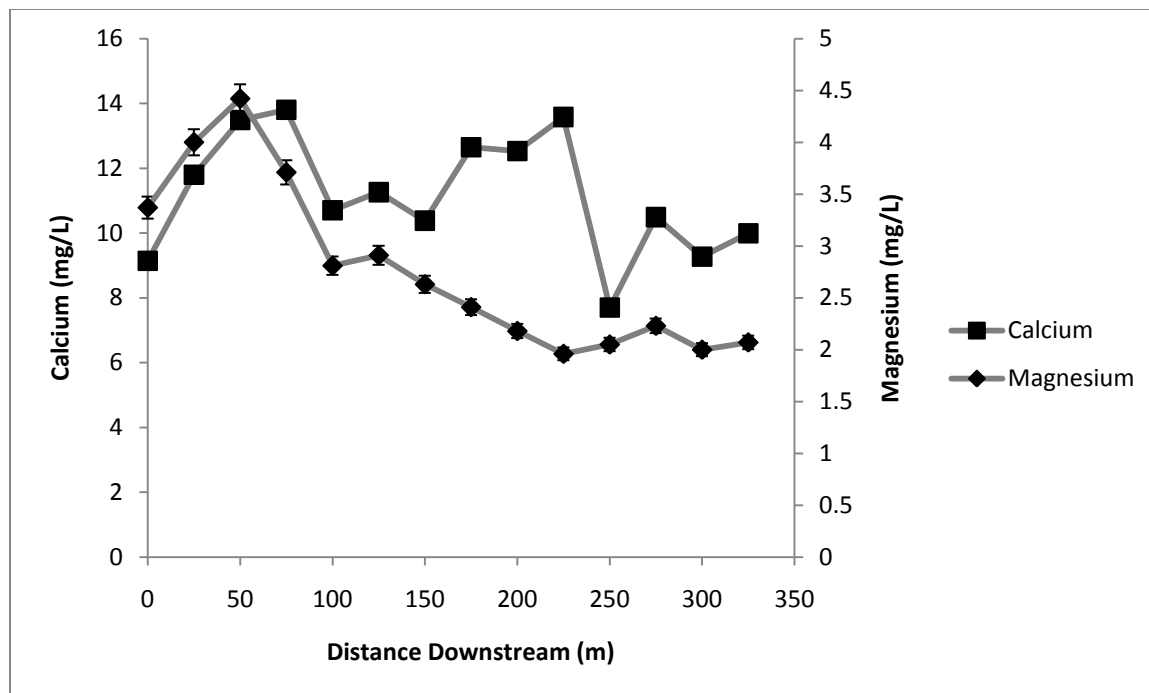


Figure 78. Calcium versus magnesium concentrations at Cabin Creek show elevated magnesium and calcium at 50 m, with an additional elevation in calcium concentrations in the upwelling and downwelling zone at 200 m. Error is estimated at 0.28% and 3.15% deviation from accepted value for calcium and ammonium, respectively. Data collected on 8/31/2010.

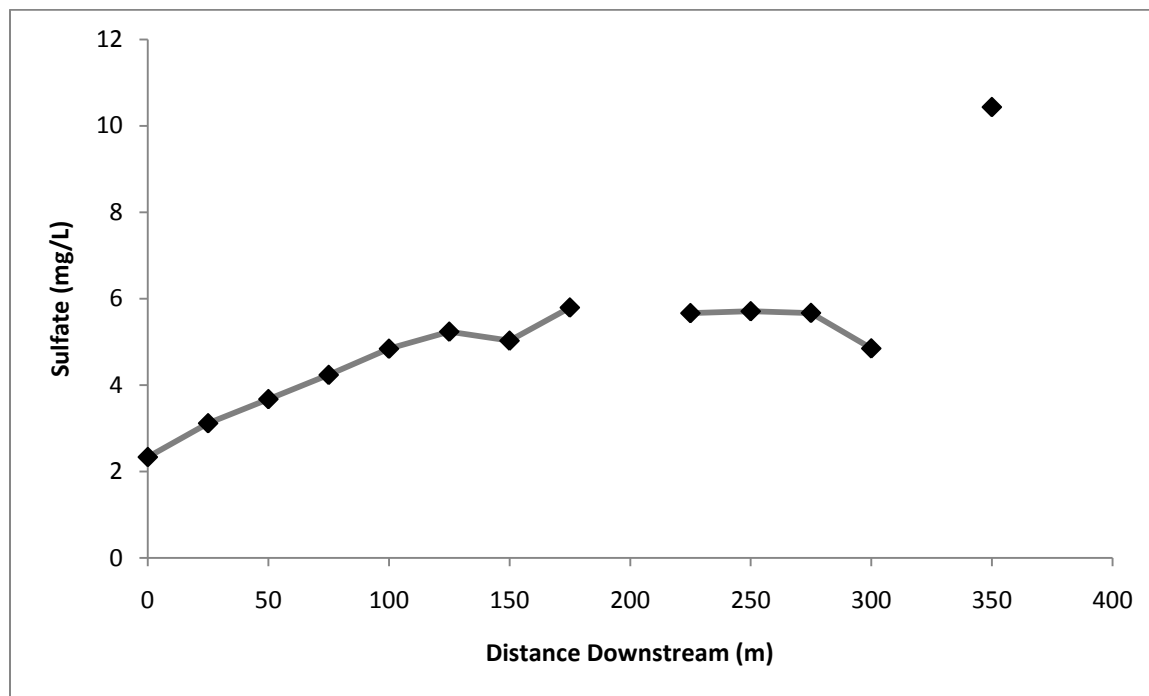


Figure 79. Sulfate concentrations are between two and five times higher than levels observed at Deep Creek or Cabin Creek, likely a product of pyrite and hematite in the quartz-sericite schist that is the dominant lithology of Creek 90. Error is estimated at 1.91% deviation from accepted value. Data collected on 8/31/2010.

Table 1. Temperature and specific conductance record days and precipitation characteristics for the days leading up to them.

<b>Measurement Date</b>	<b>Days Since Last Precipitation</b>	<b>Last Precipitation Amount (cm)</b>	<b>Deep Creek Discharge (L/sec)</b>	<b>Cabin Creek Discharge (L/sec)</b>	<b>Creek 90 Discharge (L/sec)</b>
07/27/2009	4	2.8	NA	4.53	NA
08/04/2009	2	0.5	NA	4.47	NA
11/03/2009	2	1.5	NA	5.07	NA
12/06/2009	4	3.9	NA	4.04	NA
12/22/2009	4	2.2	NA	4.85	NA
01/13/2010	15	0.4	NA	3.98	NA
01/22/2010	1	0.3	NA	8.21	NA
02/28/2010	4	0.3	NA	6.45	NA
03/26/2010	1	0.2	NA	7.38	0.47
03/31/2010	2	0.7	NA	4.77	0.82
05/26/2010	2	0.4	NA	3.18	0.52
06/23/2010	6	0.9	NA	3.45	0.59
07/20/2010	2	1.2	NA	2.68	0.56
08/31/2010	12	3.1	NA	3.03	0.54
11/22/2010	6	0.3	0.93	3.93	0.69
01/30/2011	4	0.8	1.10	NA	0.61
04/03/2011	4	2.7	1.14	NA	NA

Table 2. Cumulative sediment depth data for every 25 m measurement point showing distance downstream, average sediment depth at each 25 m measurement point, as well as standard deviation.

<b>Creek</b>	<b>Downstream Distance (m)</b>	<b>Average Sediment Depth (cm)</b>	<b>Standard Deviation (cm)</b>
Cabin Creek	0	0.0	0.0
Cabin Creek	25	30.5	41.9
Cabin Creek	50	0.0	0.0
Cabin Creek	75	5.8	11.9
Cabin Creek	100	2.2	4.9
Cabin Creek	125	20.6	1.9
Cabin Creek	150	0.0	0.0
Cabin Creek	175	23.5	4.6
Cabin Creek	200	79.8	6.5
Cabin Creek	225	0.0	0.0
Cabin Creek	250	0.4	0.9
Cabin Creek	275	28.2	9.6
Cabin Creek	300	44.6	8.5
Cabin Creek	325	0.0	0.0
Deep Creek	0	7.3	13.5
Deep Creek	25	29.8	4.3
Deep Creek	50	17.2	9.6
Deep Creek	75	25.8	9.7
Deep Creek	100	28.0	5.4
Deep Creek	125	26.3	6.0
Deep Creek	150	18.5	6.3
Deep Creek	175	13.1	10.4
Deep Creek	200	15.5	3.6
Deep Creek	225	23.2	2.1
Deep Creek	250	0.0	0.0
Deep Creek	275	16.0	9.4
Deep Creek	300	5.0	3.3
Deep Creek	325	27.2	9.3
Deep Creek	350	42.8	10.0
Deep Creek	375	30.1	5.8
Creek 90	0	8.4	9.3
Creek 90	25	20.4	3.8
Creek 90	50	0.8	1.8
Creek 90	75	15.2	9.0
Creek 90	100	21.0	6.8
Creek 90	125	24.4	4.0
Creek 90	150	26.6	18.4
Creek 90	175	22.8	6.5

Creek 90	225	16.4	10.3
Creek 90	250	30.6	15.2
Creek 90	275	0.0	0.0
Creek 90	300	44.2	26.5
Creek 90	325	71.0	15.2
Creek 90	350	45.6	18.5

Table 3. Table showing all point discharge measurements for each of the three study creeks.

<b>Location</b>	<b>Date/Time</b>	<b>Method</b>	<b>Discharge (L/sec)</b>	<b>Stage Height (cm)</b>
Deep Creek	11/11/2009 16:30	Swoffer	9.47	28.0
Deep Creek	06/17/2010 12:39	Swoffer	1.13	22.2
Deep Creek	07/10/2010 14:20	Swoffer	1.02	22.3
Deep Creek	02/28/2010 10:45	Salt Dilution	0.65	23.3
Deep Creek	02/28/2010 09:00	Swoffer	1.80	23.3
Deep Creek	12/15/2010 12:30	Swoffer	0.49	22.2
Deep Creek	02/05/2011 10:20	Swoffer	10.41	31.3
Deep Creek	02/05/2011 10:47	Swoffer	8.79	30.5
Deep Creek	02/05/2011 12:38	Swoffer	6.19	29.8
Deep Creek	04/03/2011 13:15	Swoffer	1.21	23.9
Cabin Creek	11/11/2009 17:10	Swoffer	18.17	18.0
Cabin Creek	02/28/2010 11:38	Salt Dilution	5.03	14.4
Cabin Creek	02/28/2010 13:00	Swoffer	9.20	14.4
Cabin Creek	04/25/2010 17:00	Swoffer	1.58	11.5
Cabin Creek	06/18/2010 13:25	Swoffer	1.59	9.1
Cabin Creek	07/10/2010 15:40	Swoffer	1.94	9.6
Cabin Creek	04/03/2011 17:00	Swoffer	1.03	13.2
Cabin Creek	02/05/2011 11:30	Swoffer	15.01	17.3
Cabin Creek	02/05/2011 11:48	Swoffer	12.32	16.8
Cabin Creek	02/05/2011 12:04	Swoffer	10.57	16.6
Creek 90	04/06/2010 11:45	Swoffer	0.42	9.0
Creek 90	02/02/2010 12:10	Salt Dilution	9.74	17.8
Creek 90	02/02/2010 13:00	Swoffer	6.70	17.8
Creek 90	06/15/2010 09:45	Swoffer	0.62	11.0
Creek 90	07/10/2010 11:15	Swoffer	0.105	10.6
Creek 90	08/19/2010 08:45	Swoffer	6.73	17.2
Creek 90	08/19/2010 17:15	Swoffer	5.80	14.0
Creek 90	02/05/2011 08:40	Swoffer	11.50	25.5
Creek 90	02/05/2011 14:00	Swoffer	9.96	21.5
Creek 90	04/03/2011 09:00	Swoffer	1.03	12.0



Table 4: Unit discharge for summer baseflow in the three study creeks.

<b>Creek</b>	<b>Summer '09 Baseflow (L/sec/km<sup>2</sup>)</b>	<b>Summer '10 Baseflow (L/sec/km<sup>2</sup>)</b>
Deep Creek	NA	NA
Cabin Creek	23.2	17.4
Creek 90	NA	5.43

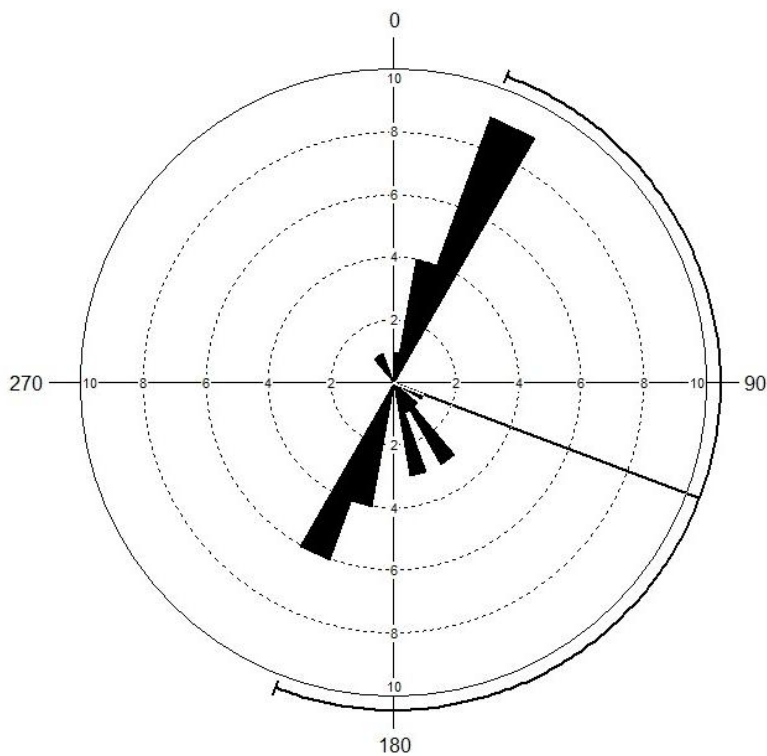
Table 5: Unit peak flow data for a selected high discharge event. Table also shows time taken to attain peak flow from the beginning of the precipitation event.

<b>Creek</b>	<b>Date</b>	<b>Peak Flow (L/sec/km<sup>2</sup>)</b>	<b>Time to Peak Flow (min)</b>
Deep Creek	12/1/2010	58.62	45
Cabin Creek	12/1/2010	106.38	30
Creek 90	12/1/2010	54.33	90

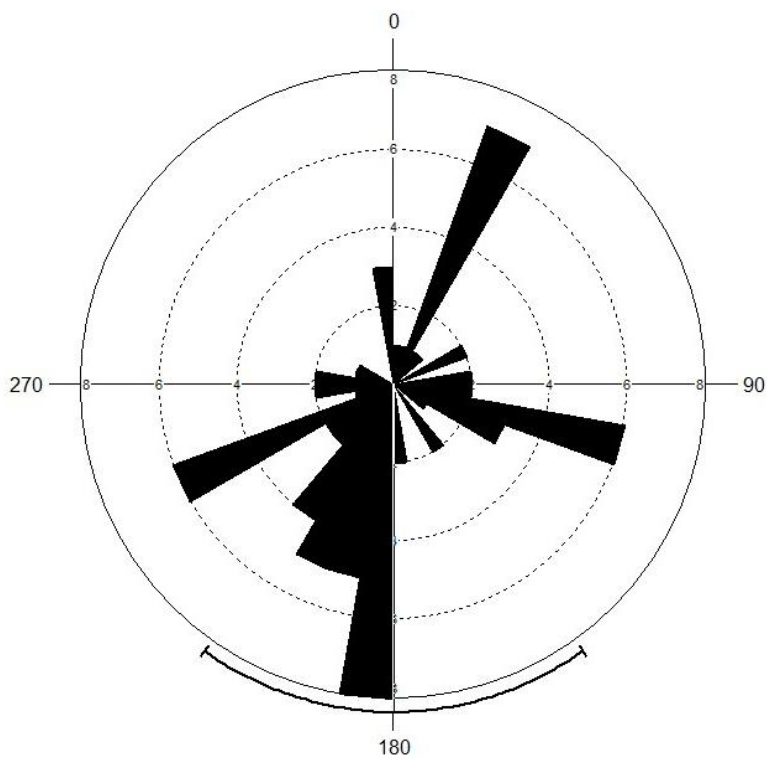
Table 6: Average unit discharge for water year 2010 and 2011 shows Cabin Creek having the largest values from available data sets in 2010 and 2011.

<b>Creek</b>	<b>Average Water Year 2010 Discharge (L/sec/km<sup>2</sup>)</b>	<b>Data Available for Average Water Year 2011 (L/sec/km<sup>2</sup>)</b>
Deep Creek	NA	10.04
Cabin Creek	35.34	23.17
Creek 90	11.12	16.12

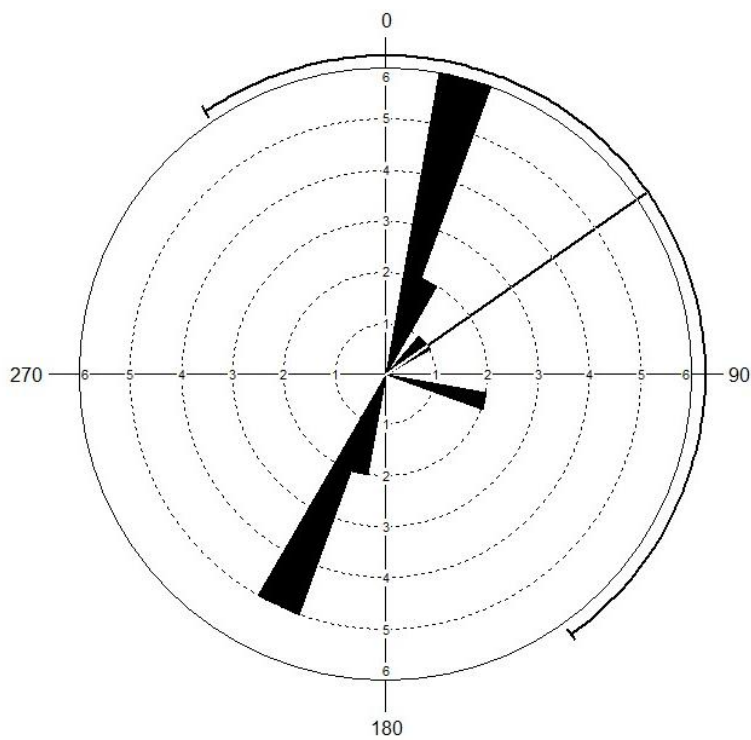
## Appendix



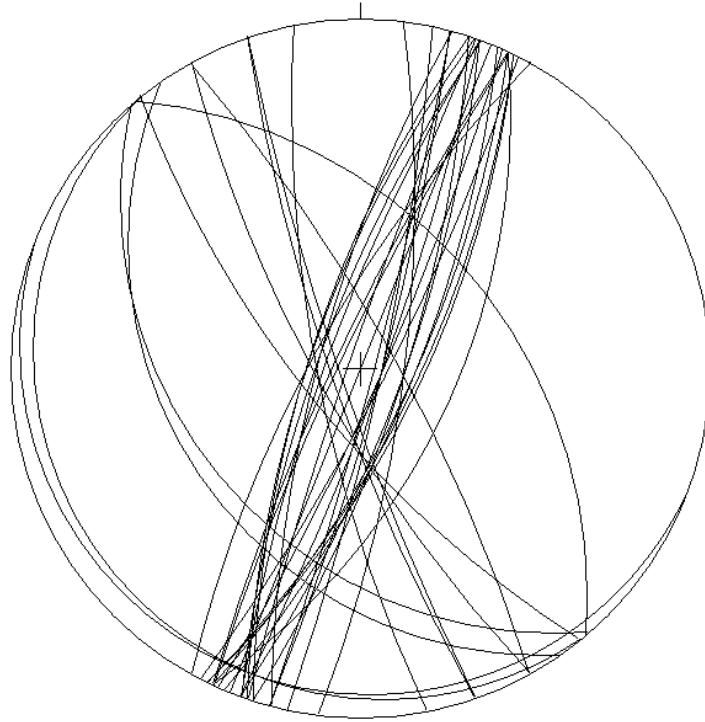
Appendix Figure 1: Rose diagram plot for Deep Creek showing orientation of 127 individual strike and dip measurements.



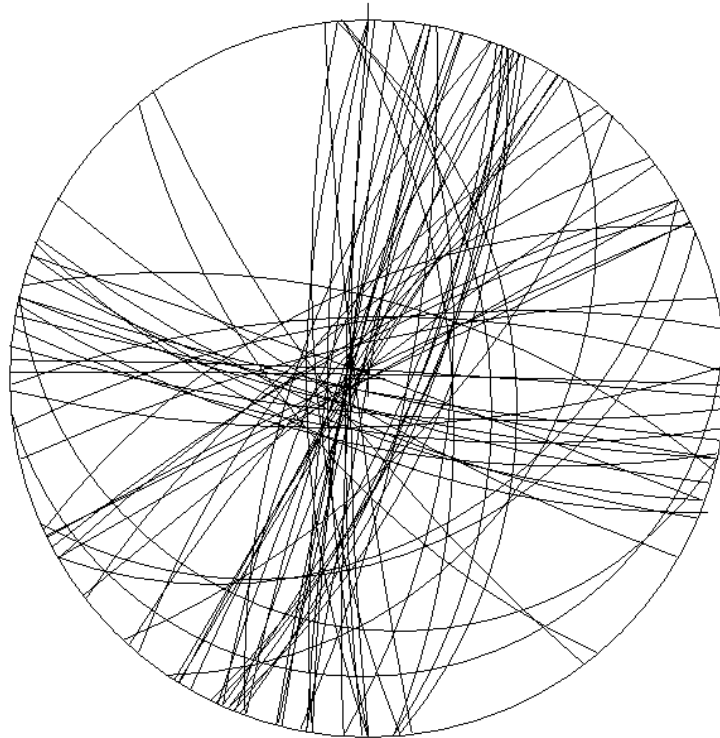
Appendix Figure 2: Rose diagram for Cabin Creek showing joint orientation for 73 strike measurements.



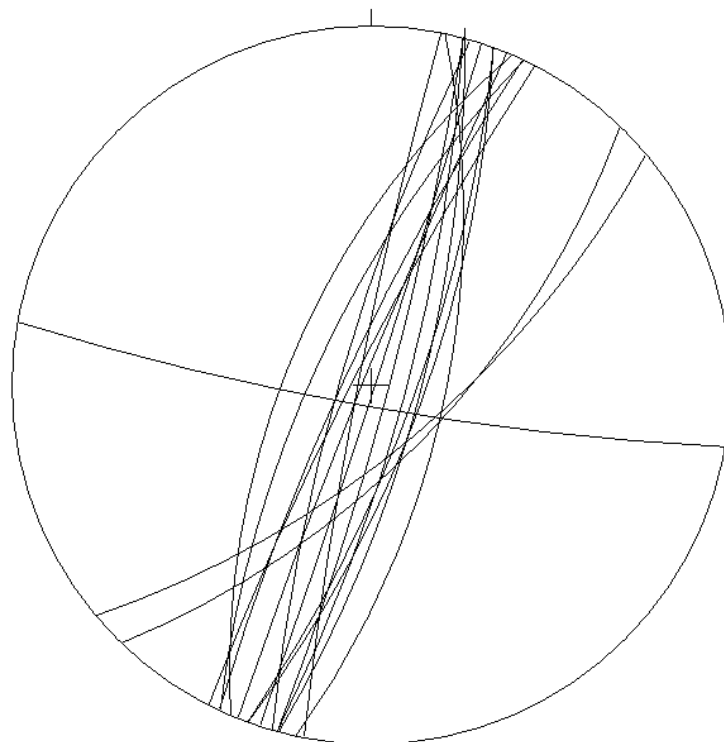
Appendix Figure 3: Rose diagram for Creek 90 showing joint orientation for 19 strike measurements.



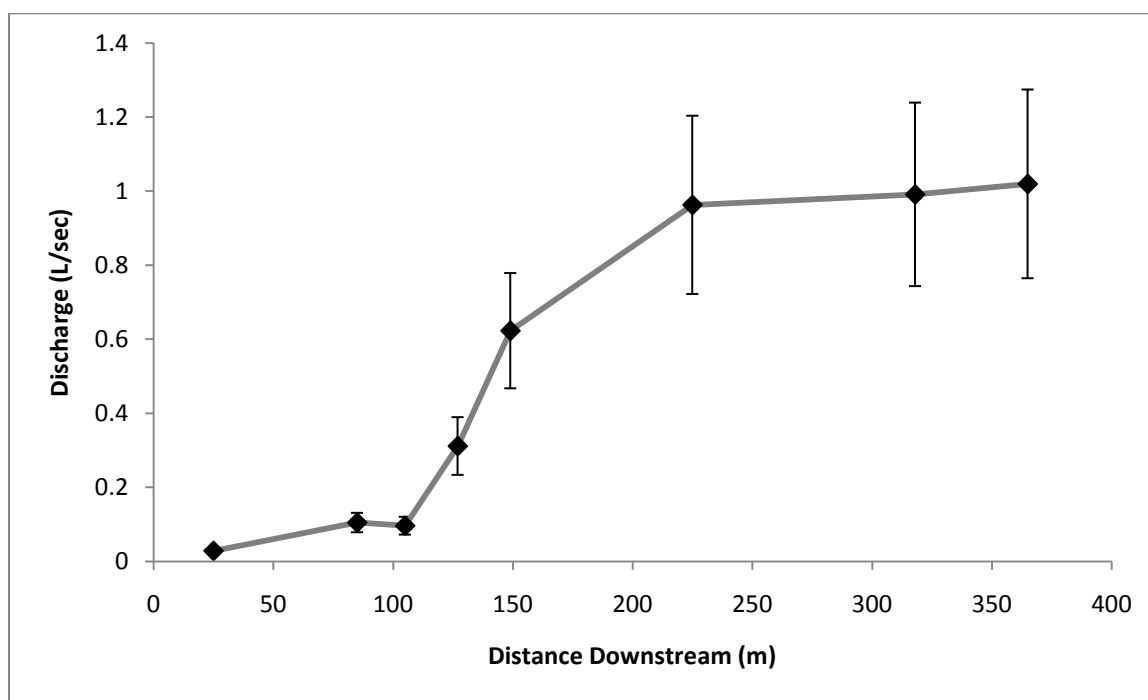
Appendix Figure 4: Stereonet of joint orientation for Deep Creek for the 35 strike and dip measurements.



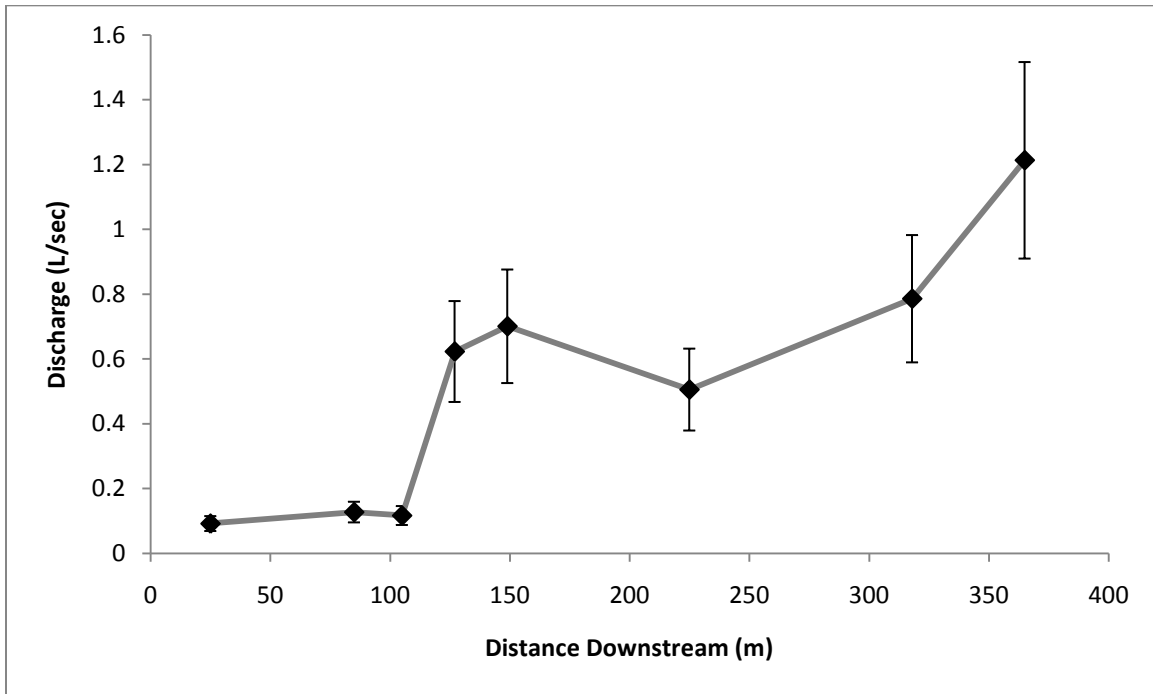
Appendix Figure 5: Stereonet of joint orientation for Cabin Creek for the 73 strike and dip measurements.



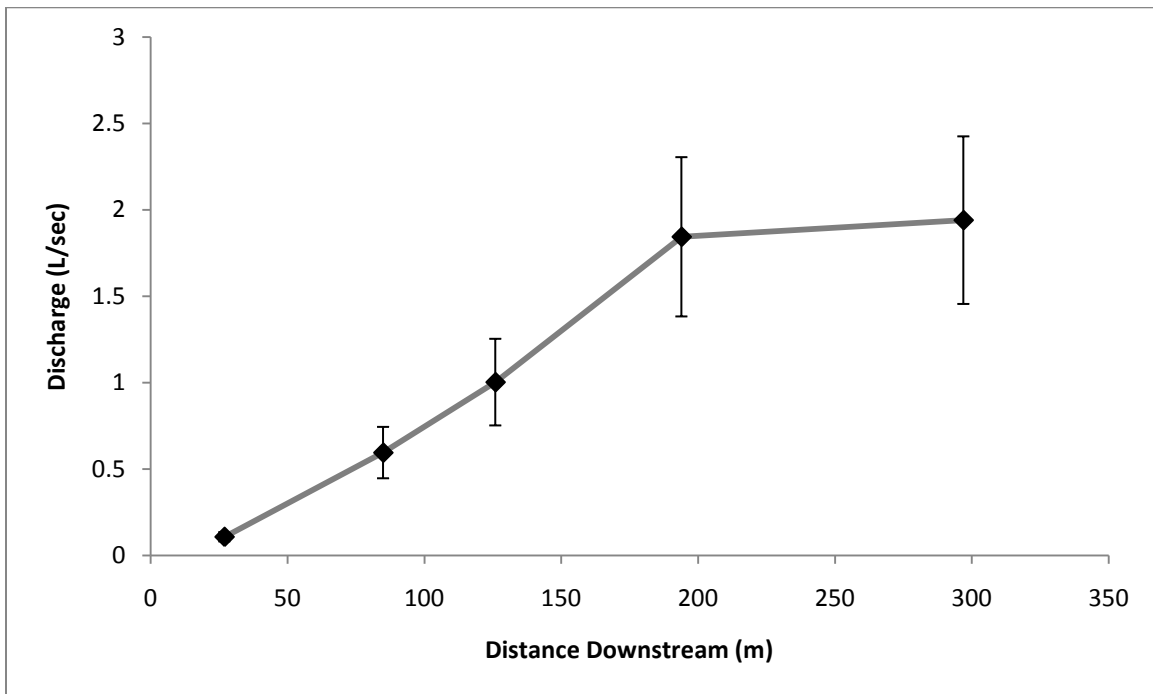
Appendix Figure 6: Stereonet of joint orientation for Creek 90 for the 19 strike and dip measurements.



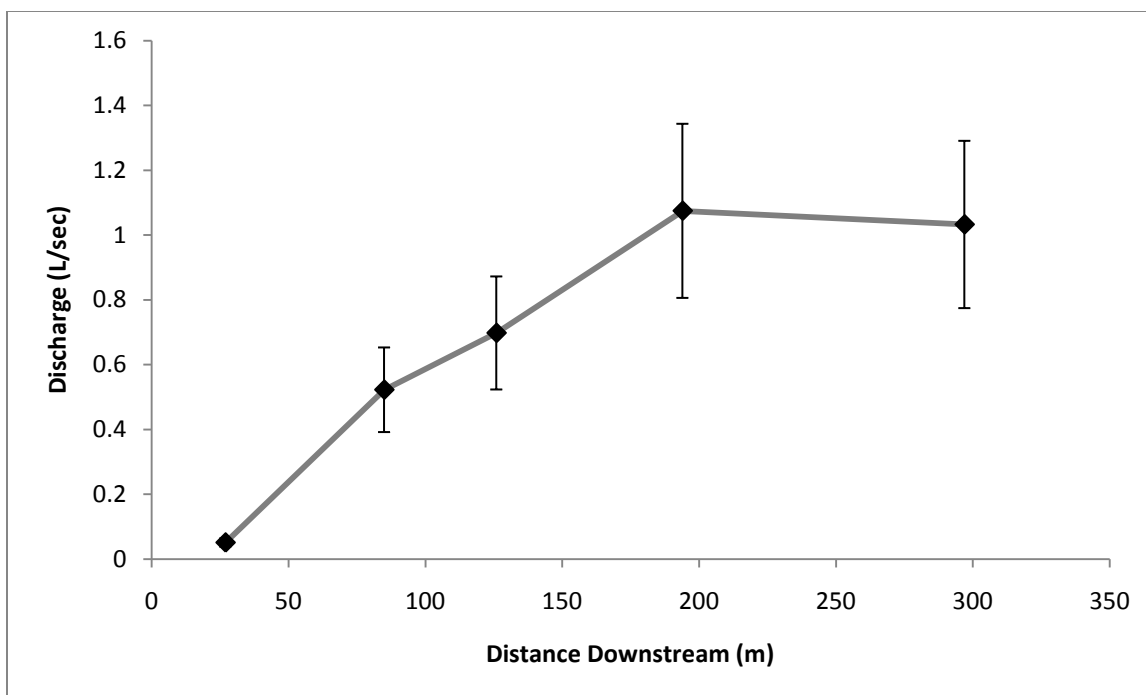
Appendix Figure 7: Deep Creek longitudinal discharge measurements. 7/10/2010.



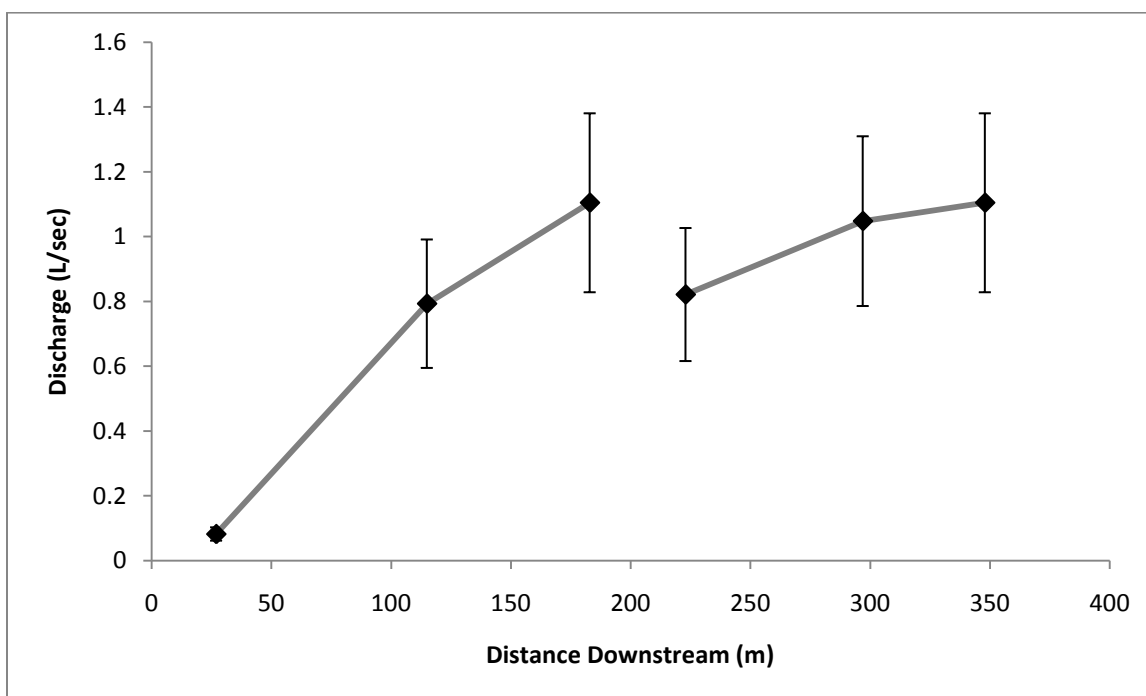
Appendix Figure 8: Deep Creek longitudinal discharge measurements. 4/3/2011.



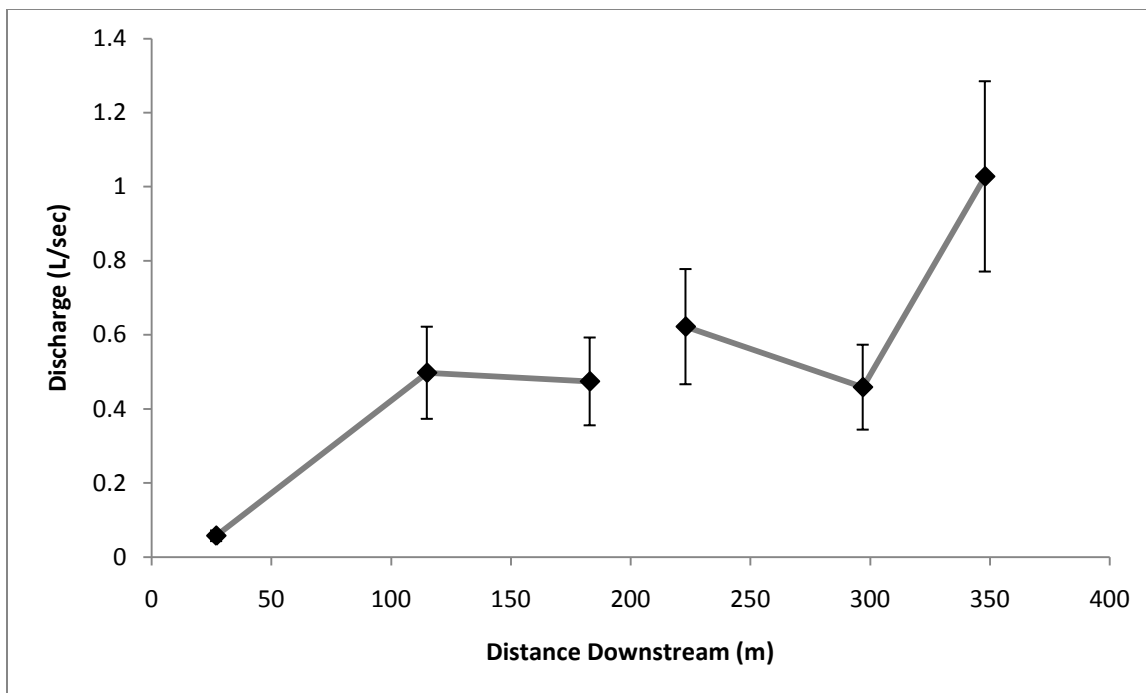
Appendix Figure 9: Cabin Creek longitudinal discharge measurements. 7/10/2010.



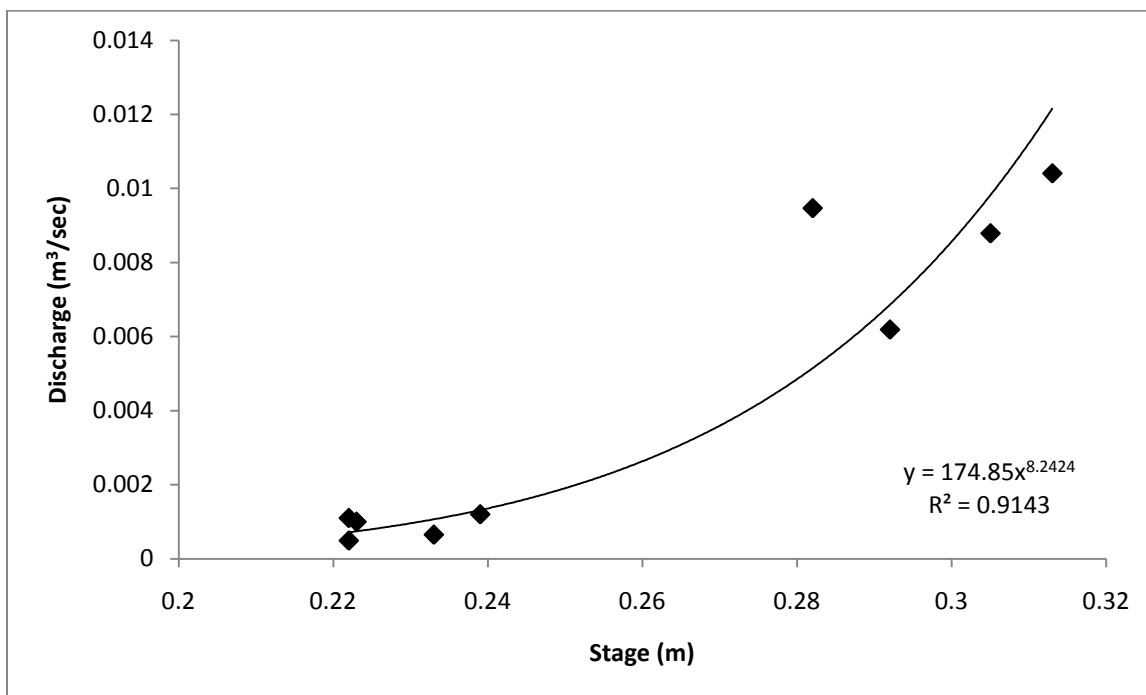
Appendix Figure 10: Cabin Creek longitudinal discharge measurements. 4/3/2011.



Appendix Figure 11. Creek 90 longitudinal discharge measurements. 7/10/2010.

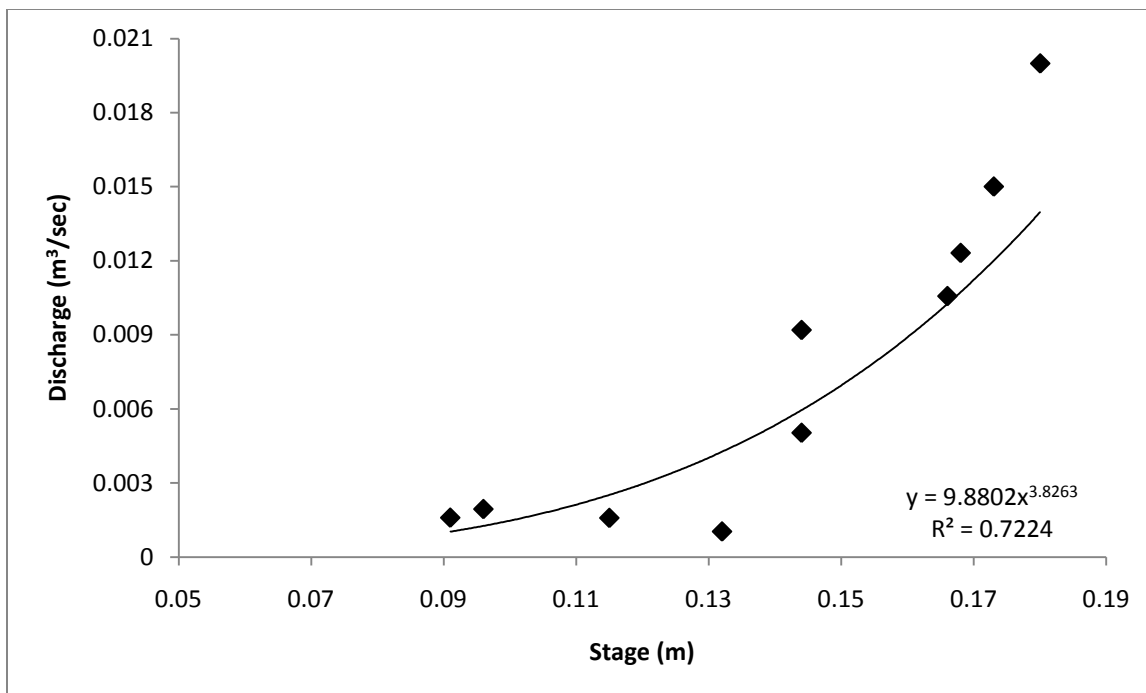


Appendix Figure 12. Creek 90 longitudinal discharge measurements. 4/3/2011.

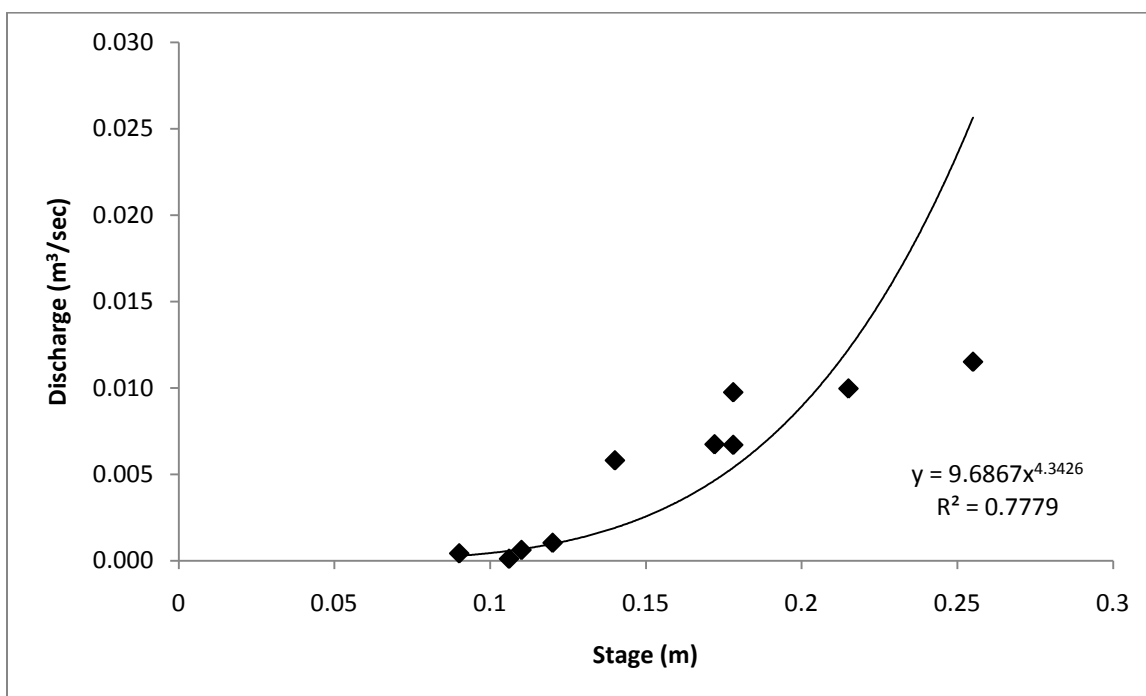


Appendix Figure 13. Deep Creek rating curve.

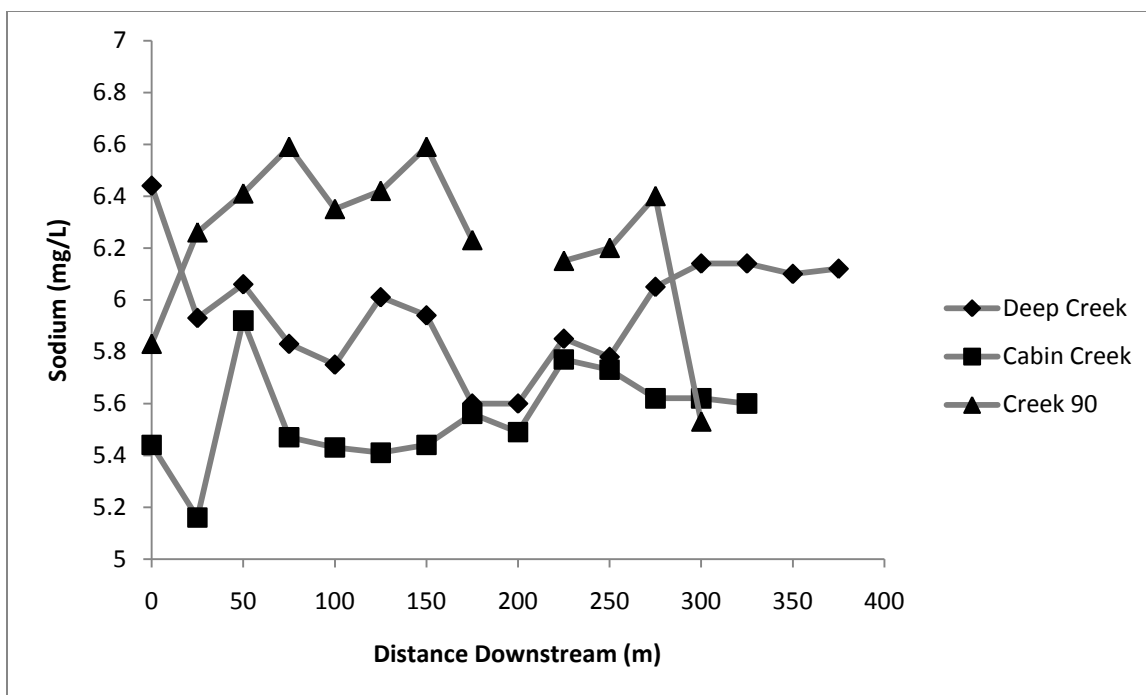




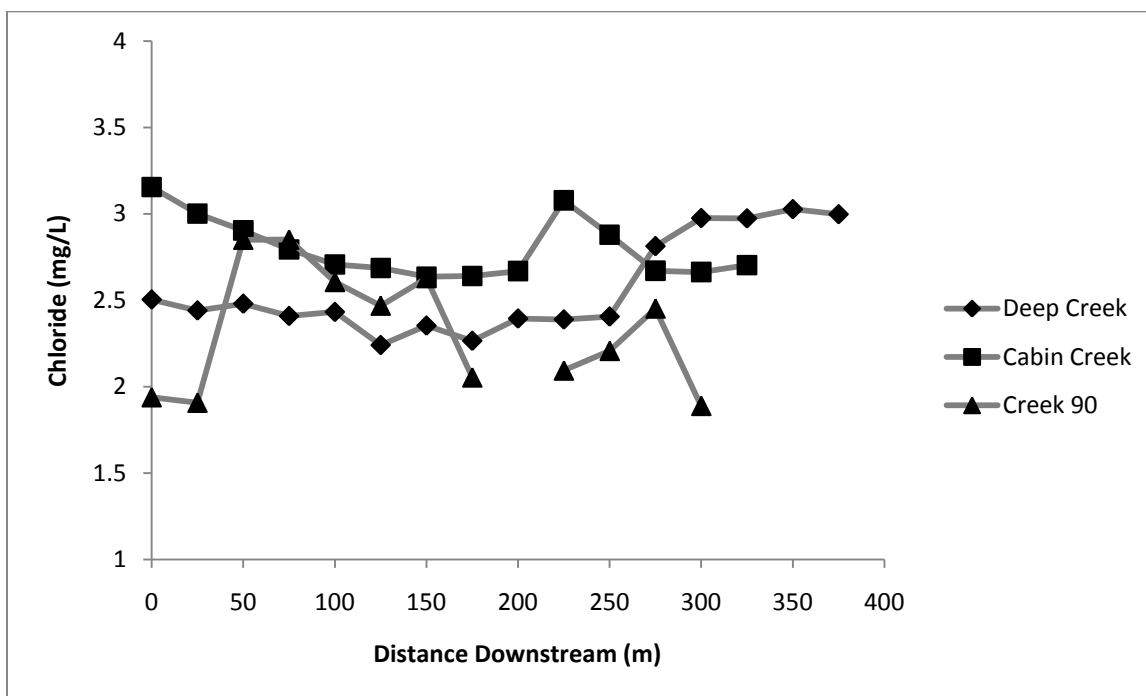
Appendix Figure 14. Cabin Creek rating curve.



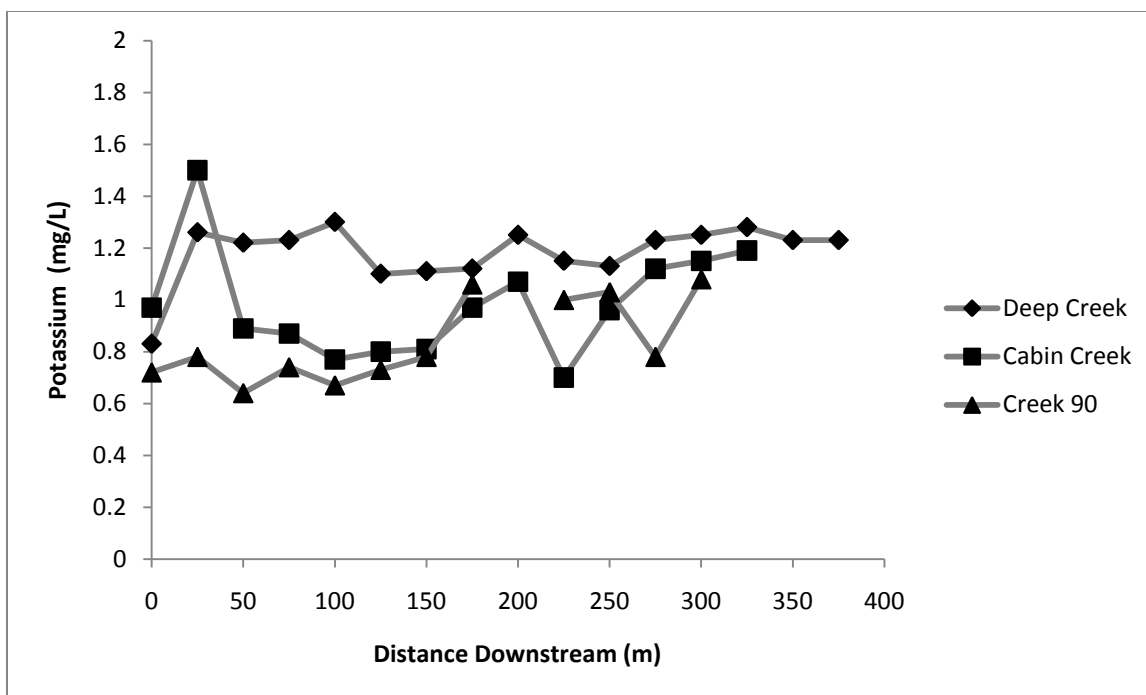
Appendix Figure 15. Creek 90 rating curve.



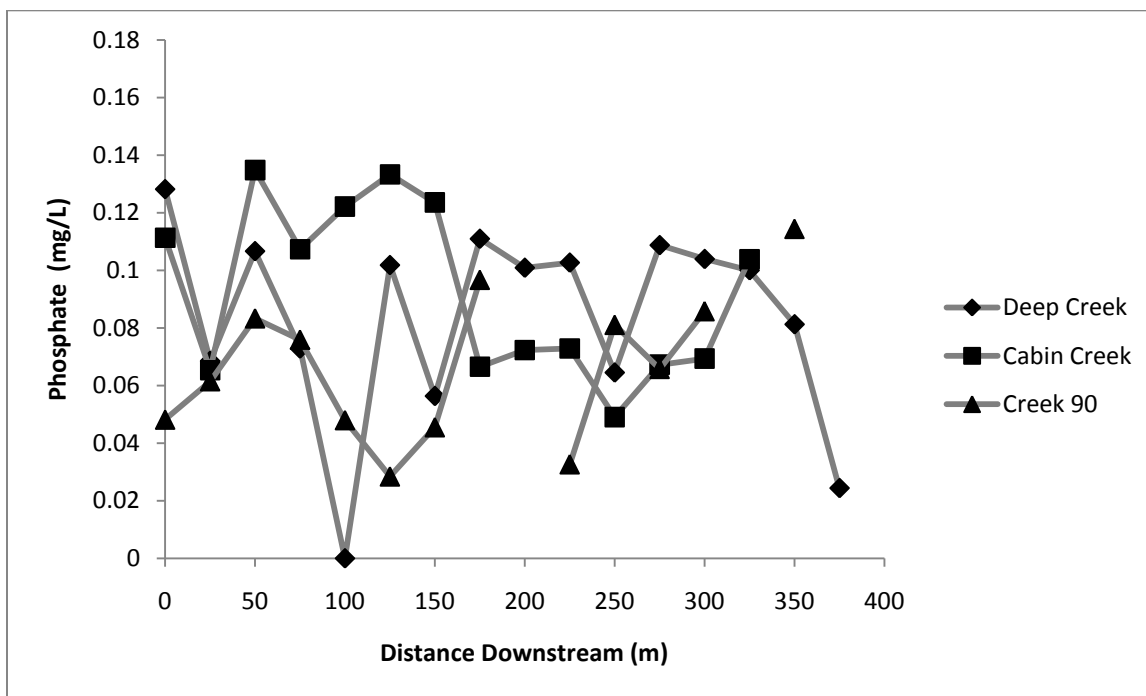
Appendix Figure 16. Sodium concentrations at the three study creeks. Creek 90 350 m was measured at 18 mg/L and is not included on this plot. Data collected 8/31/10.



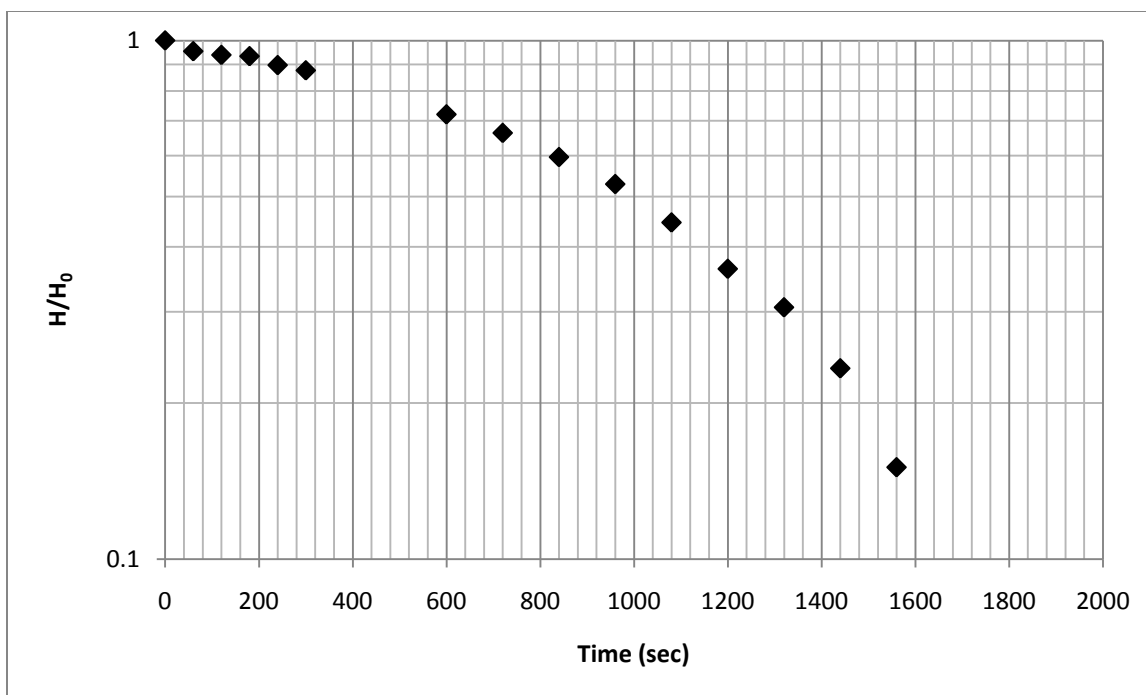
Appendix Figure 17. Chloride concentrations in the three study creeks in relation to downstream distance. Data collected 8/31/10.



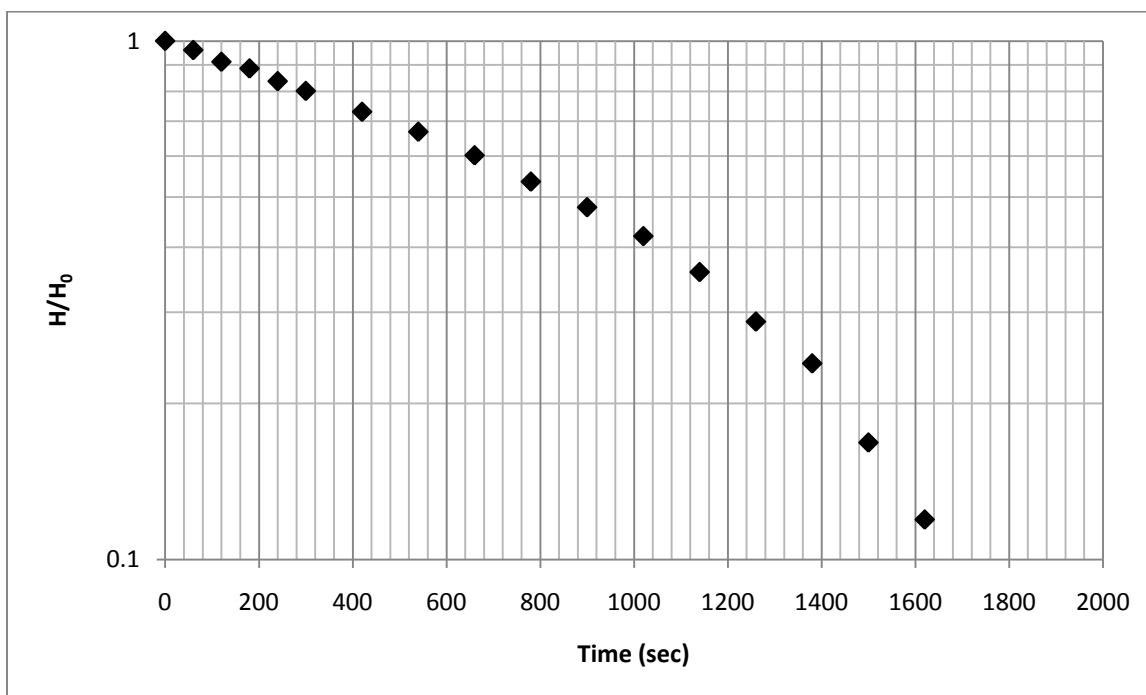
Appendix Figure 18. Potassium concentrations in the three study creeks. Creek 90 350 m was recorded at 2.81 mg/L. Data collected 8/31/2010.



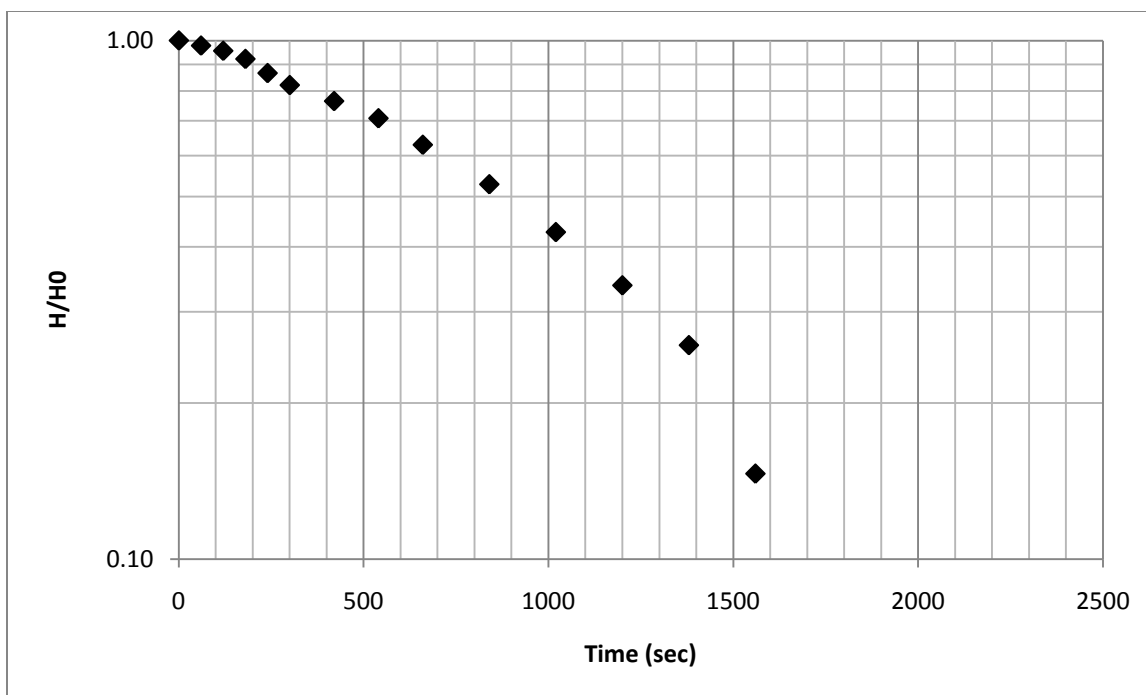
Appendix Figure 19. Phosphate concentrations in the three study creeks. Data collected 8/31/2010.



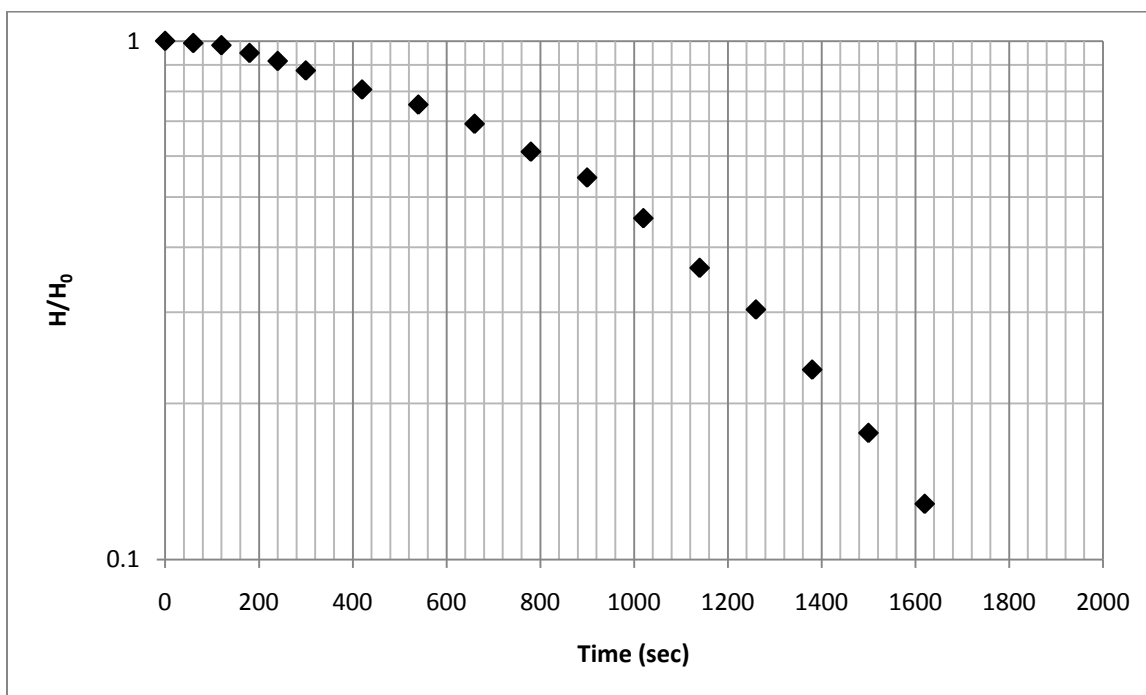
Appendix Figure 20. Hvorslev slug test for Deep Creek 25 m.



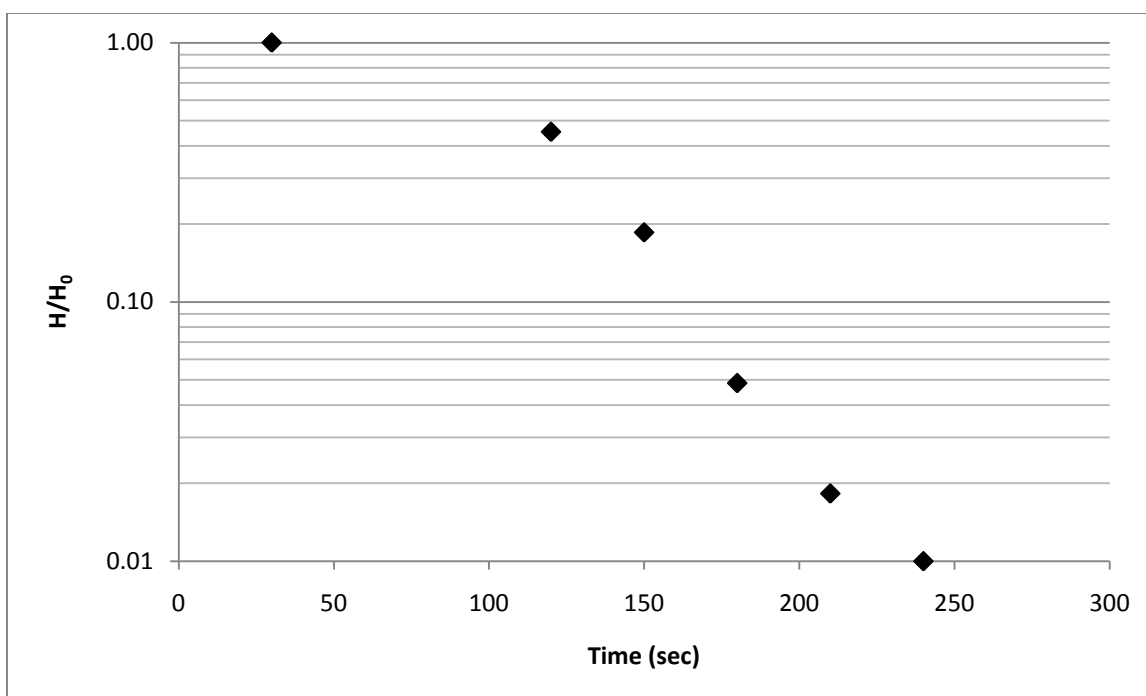
Appendix Figure 21. Hvorslev slug test for Deep Creek 50 m.



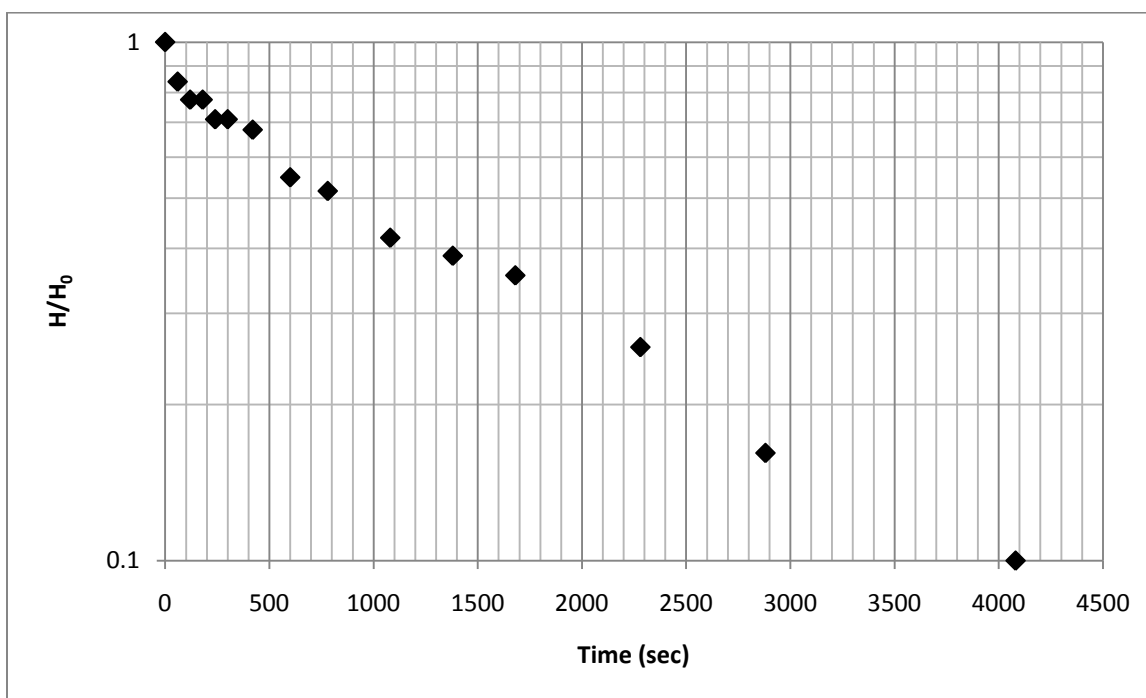
Appendix Figure 22. Hvorslev slug test for Deep Creek 75 m.



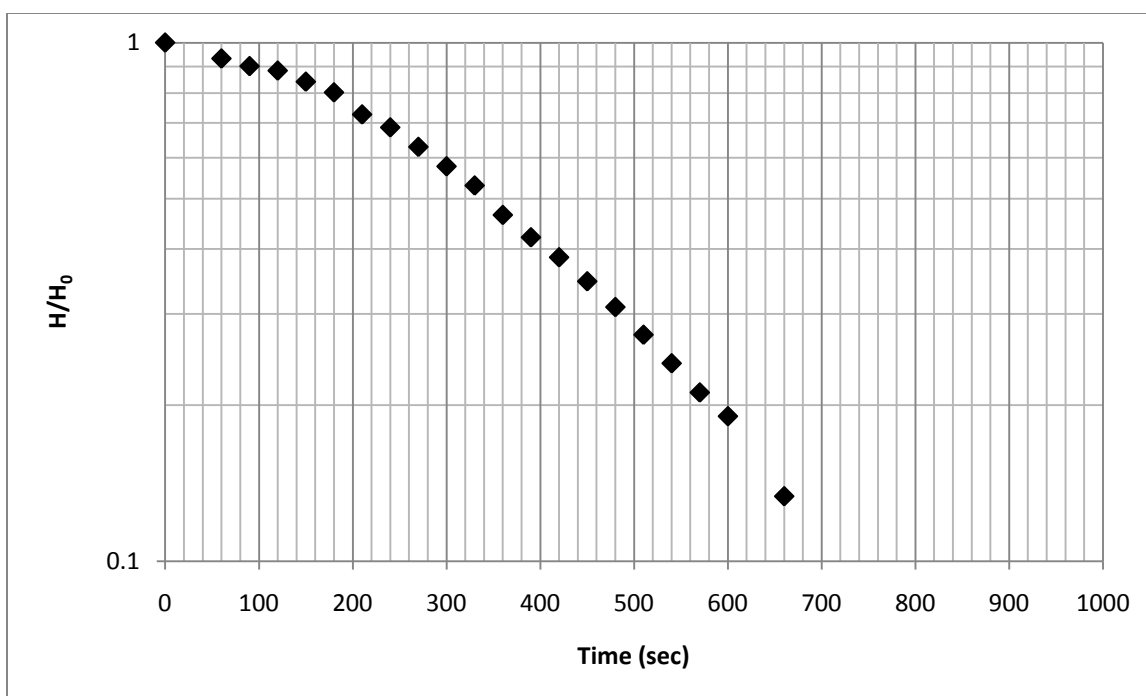
Appendix Figure 23. Hvorslev slug test for Deep Creek 100 m.



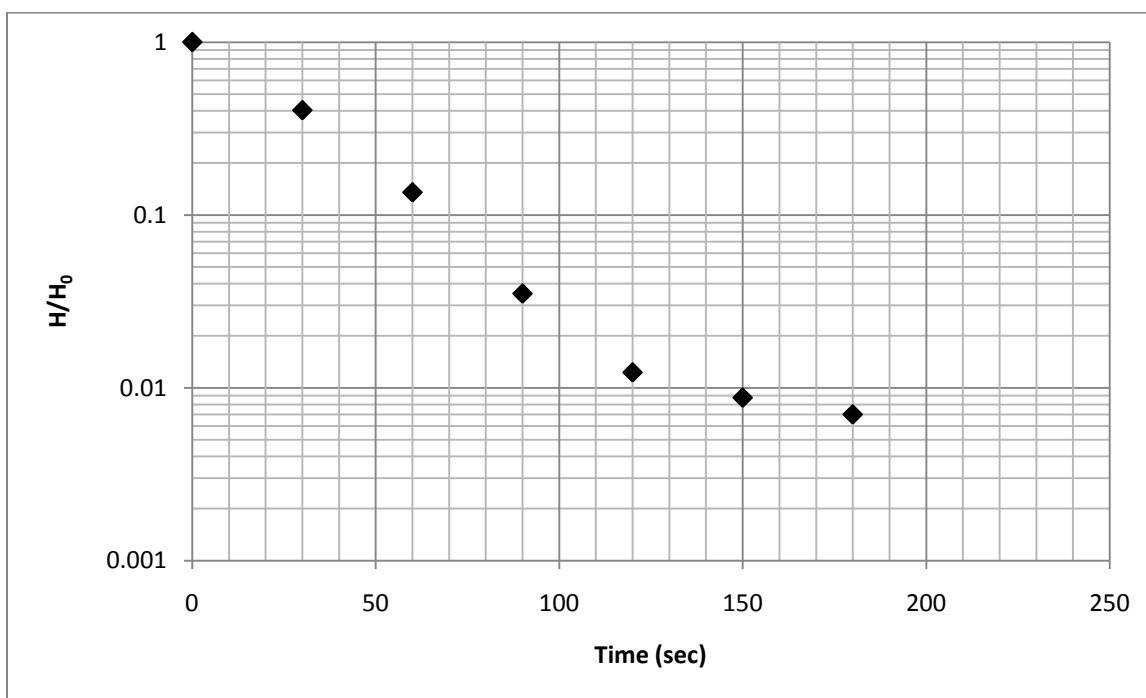
Appendix Figure 24. Hvorslev slug test for Deep Creek 125 m.



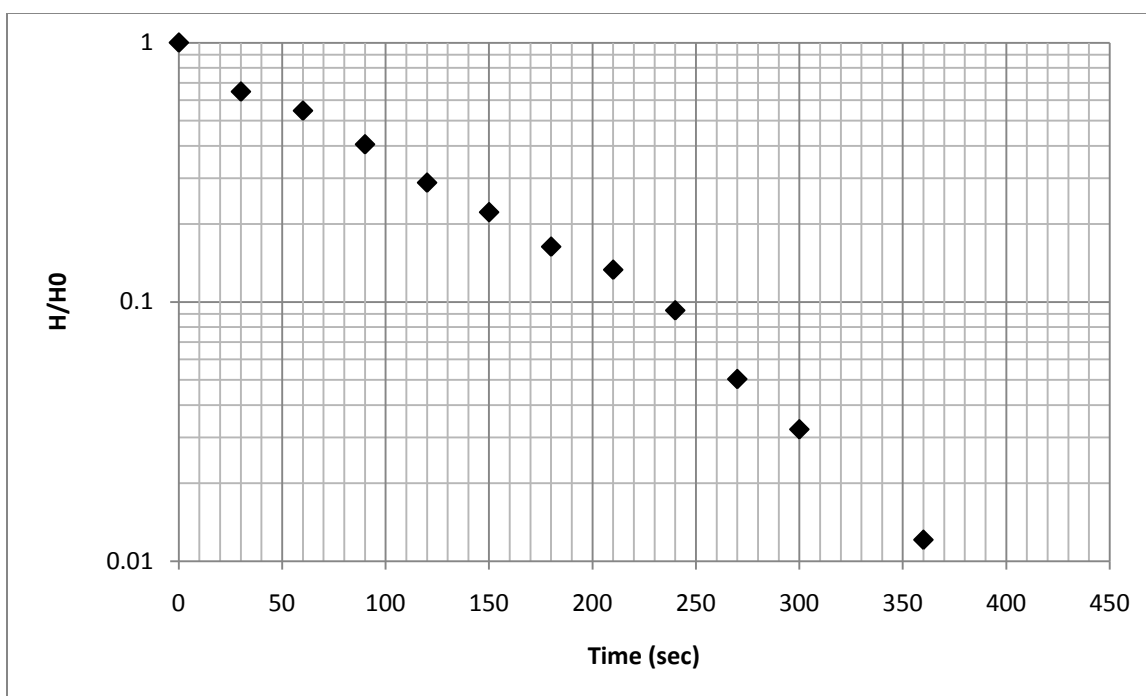
Appendix Figure 25. Hvorslev slug test for Deep Creek 175 m.



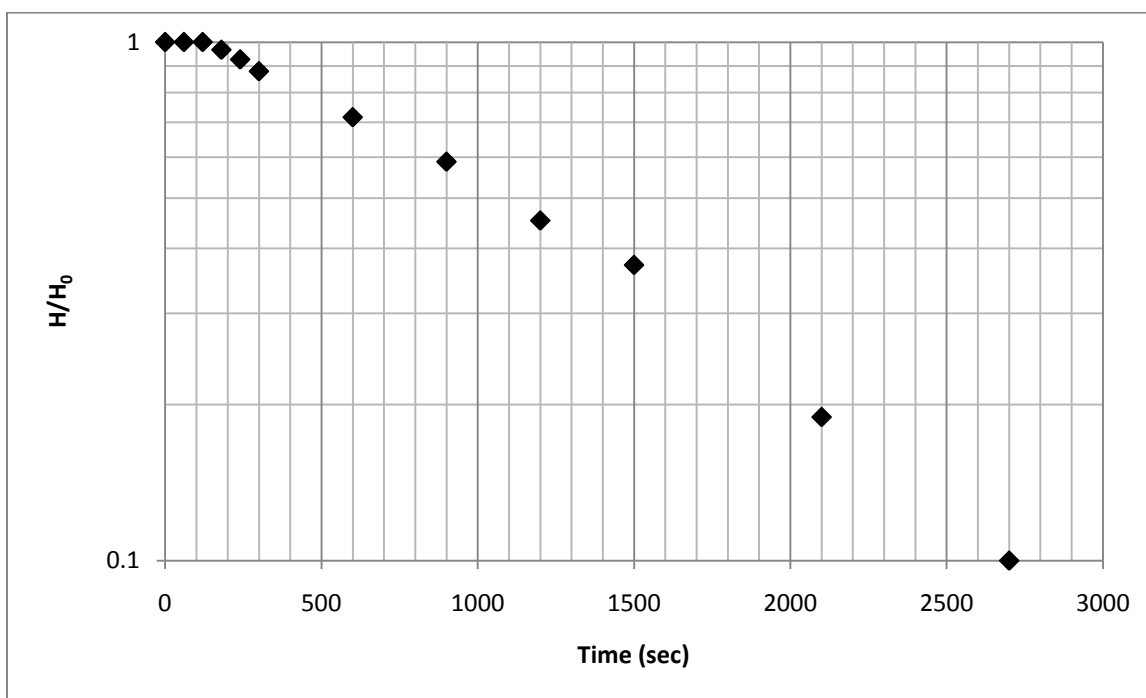
Appendix Figure 26. Hvorslev slug test for Deep Creek 225 m.



Appendix Figure 27. Hvorslev slug test for Deep Creek 350 m.

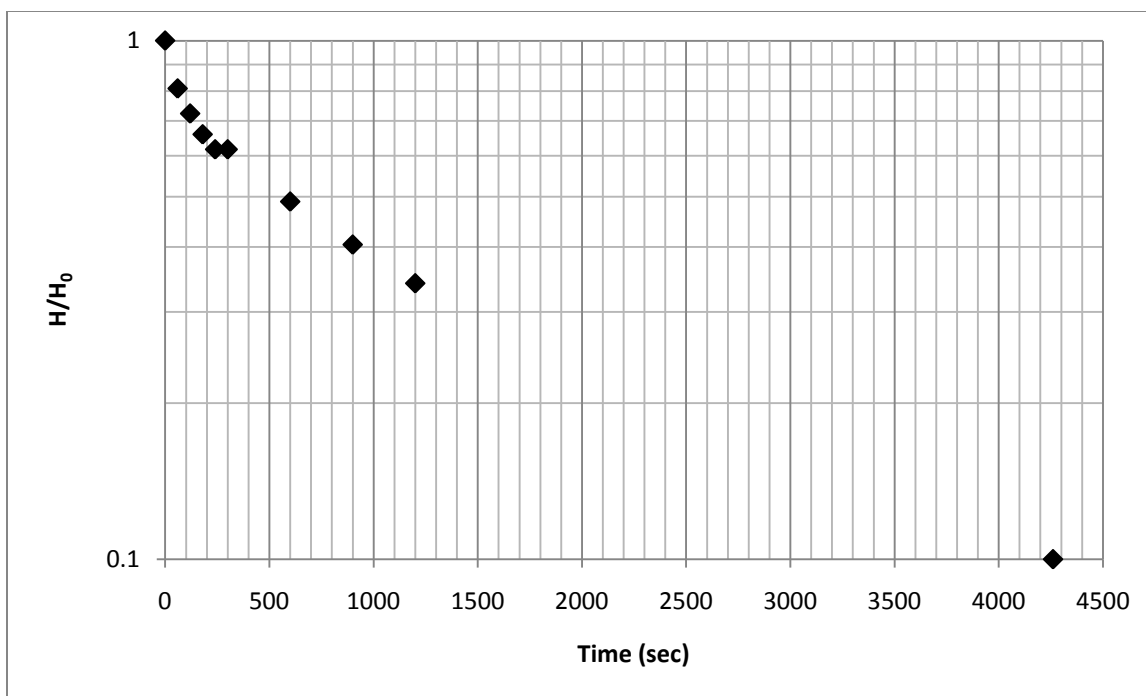


Appendix Figure 28. Hvorslev slug test for Deep Creek 375 m.

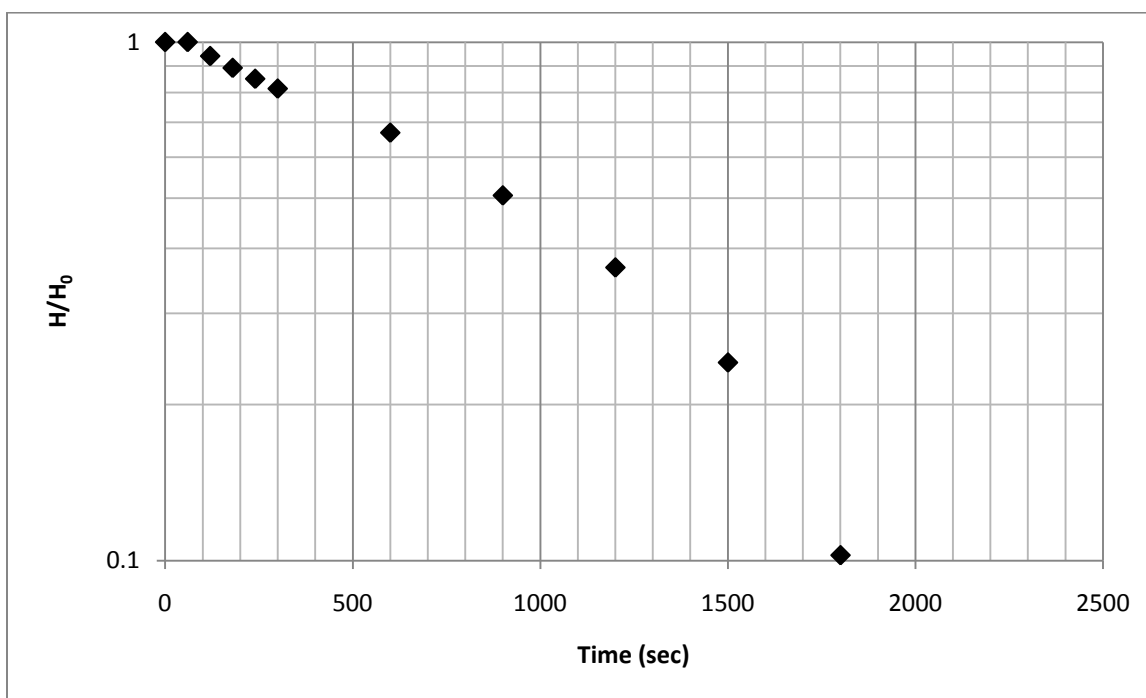


Appendix Figure 29. Hvorslev slug test for Cabin Creek 200 m.

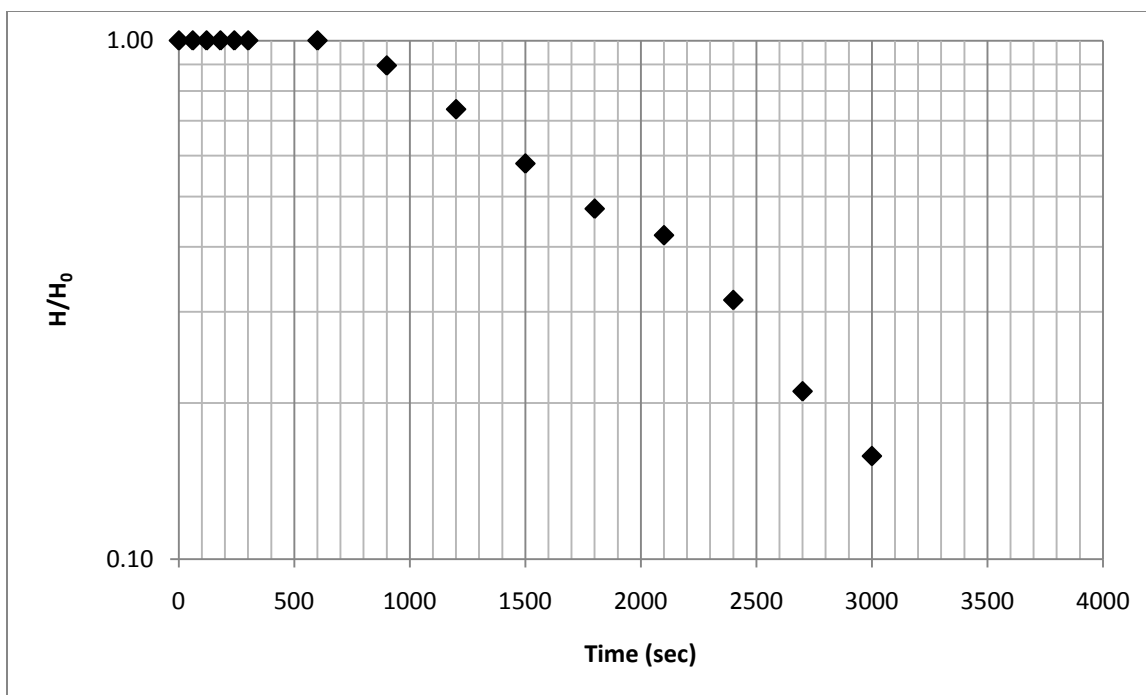




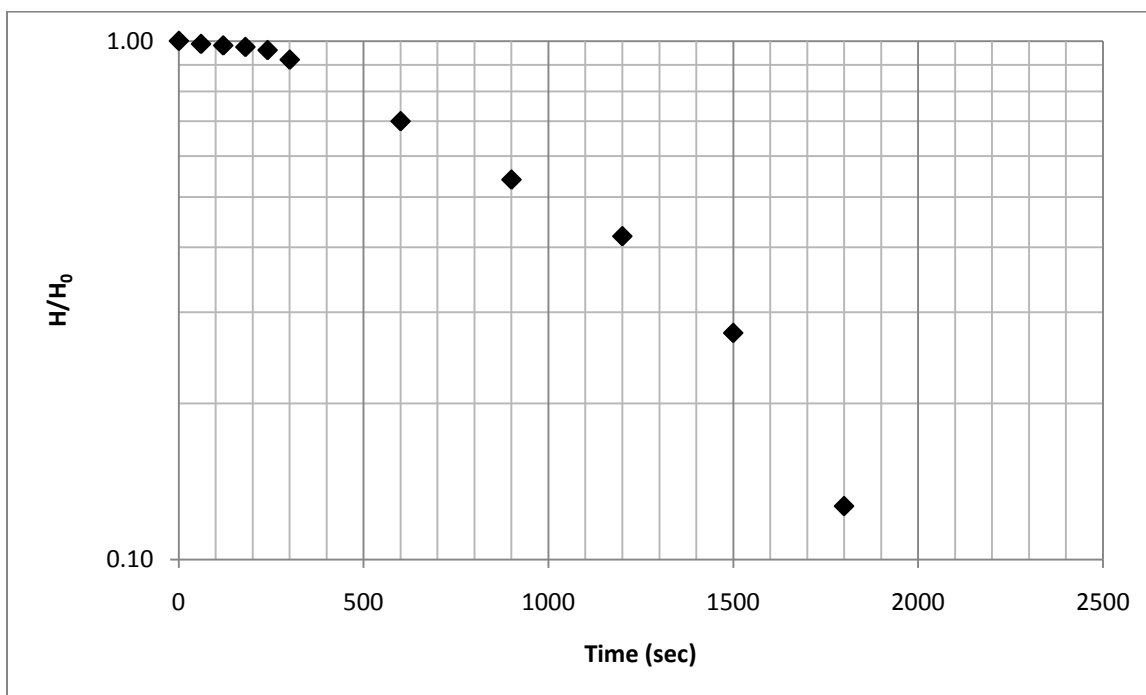
Appendix Figure 30. Hvorslev slug test for Cabin Creek 275 m.



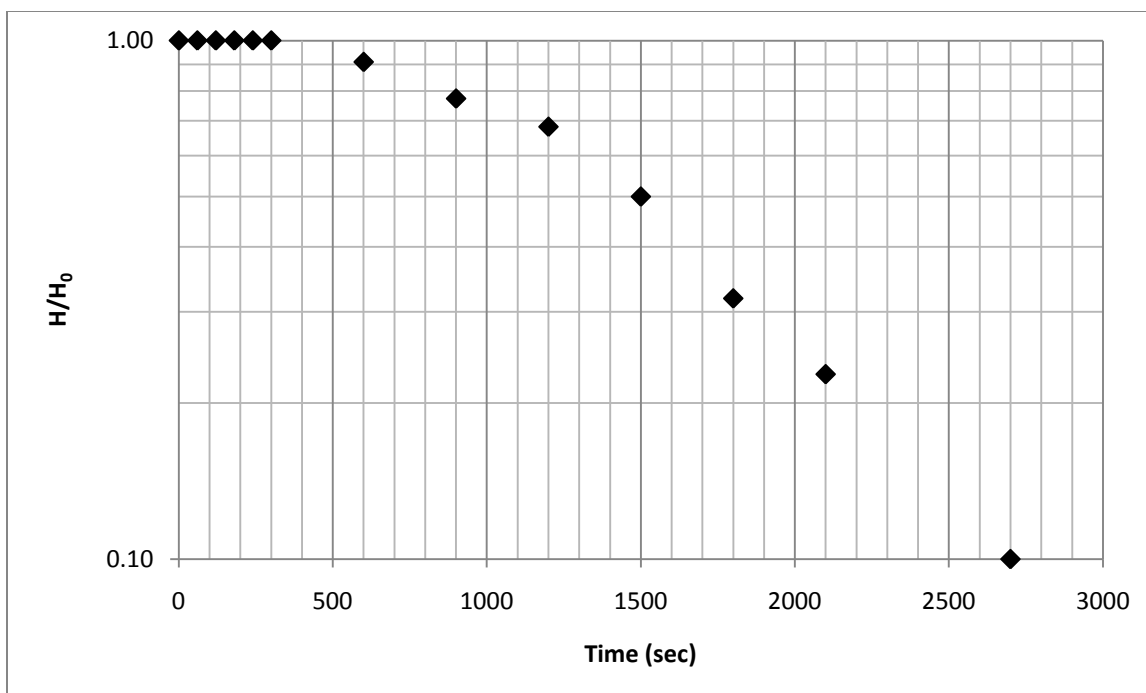
Appendix Figure 31. Hvorslev slug test for Cabin Creek 300 m.



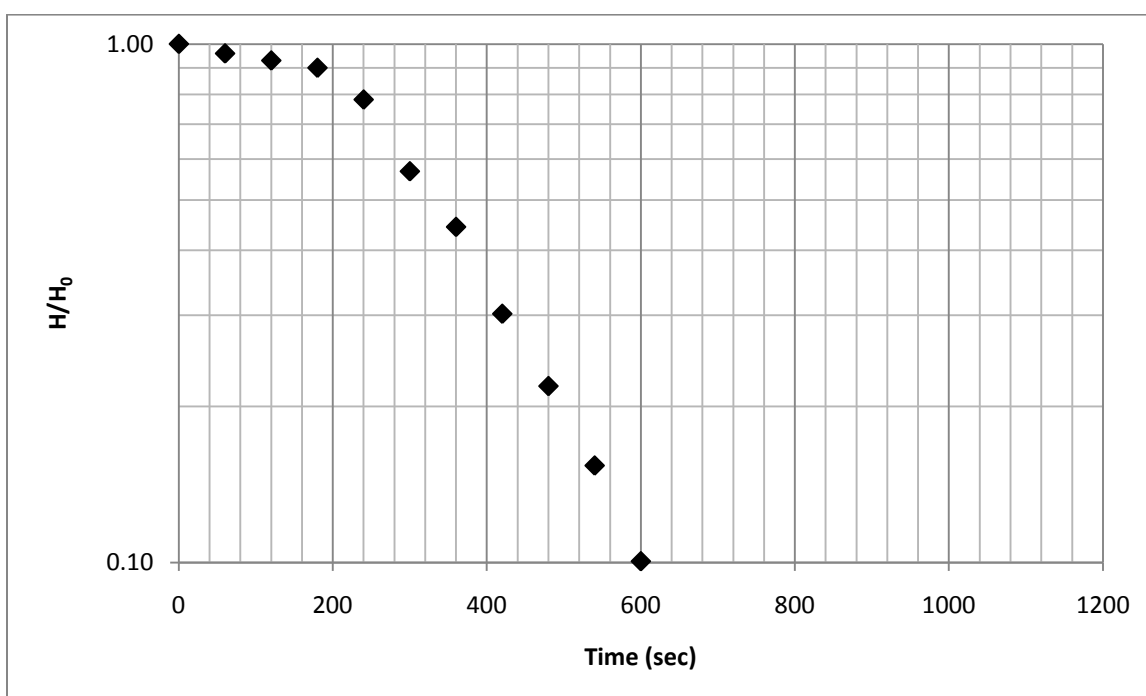
Appendix Figure 32. Hvorslev slug test for Creek 90 25 m.



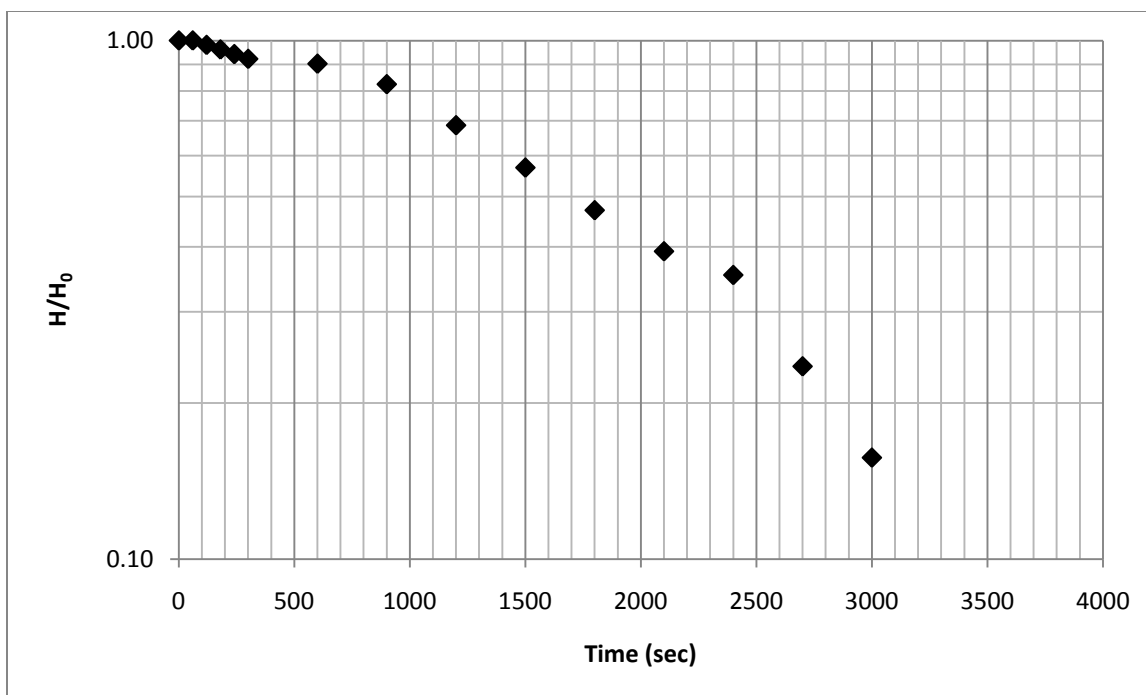
Appendix Figure 33. Hvorslev slug test for Creek 90 100 m.



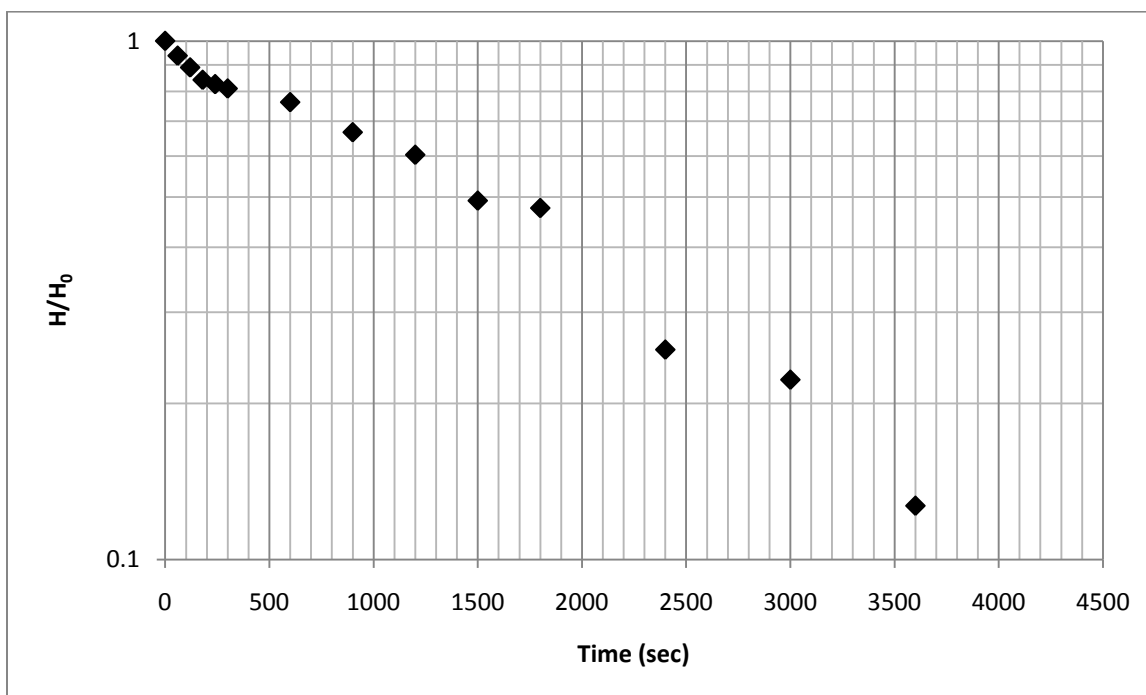
Appendix Figure 34. Hvorslev slug test for Creek 90 125 m.



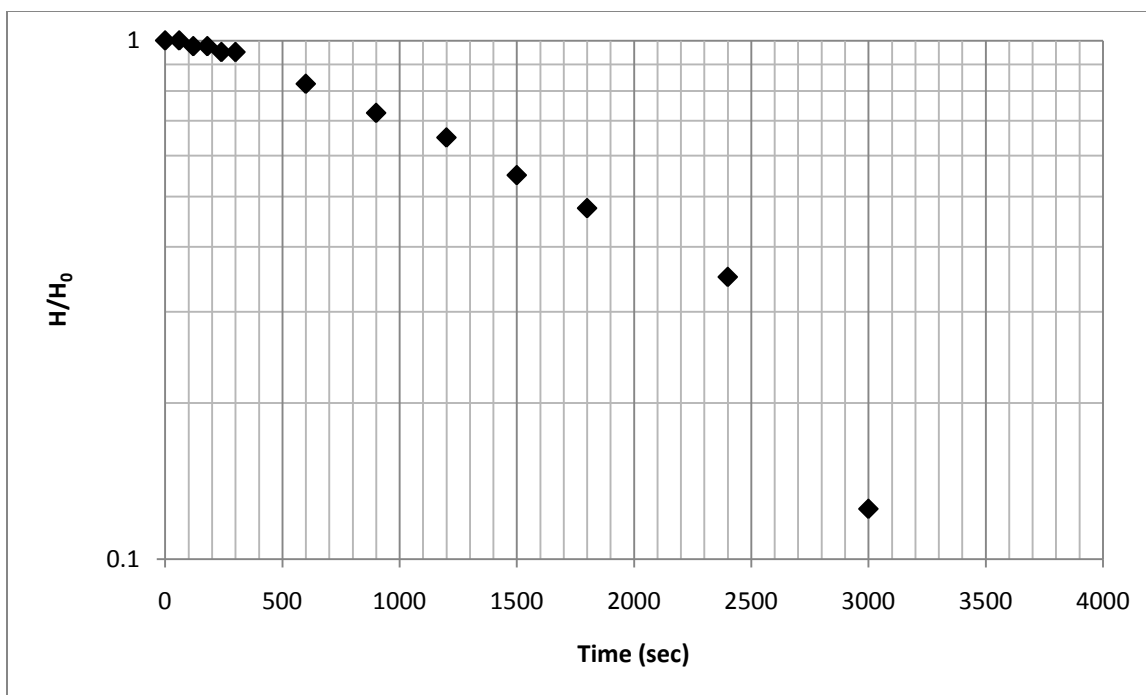
Appendix Figure 35. Hvorslev slug test for Creek 90 150 m.



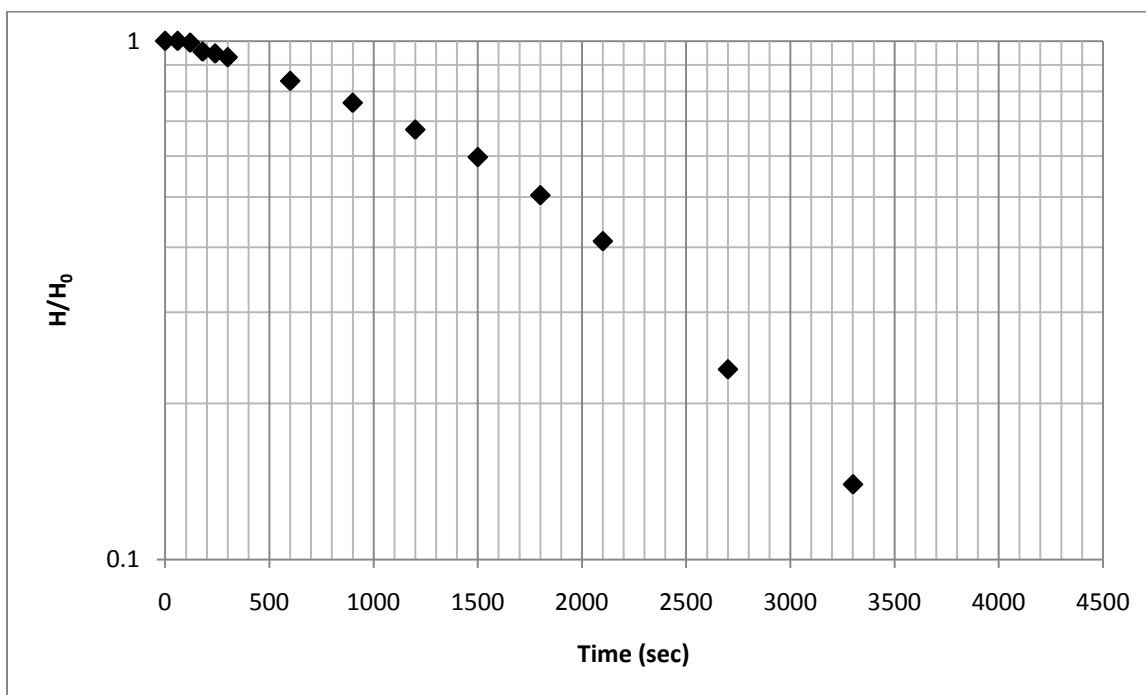
Appendix Figure 36. Hvorslev slug test for Creek 90 175 m.



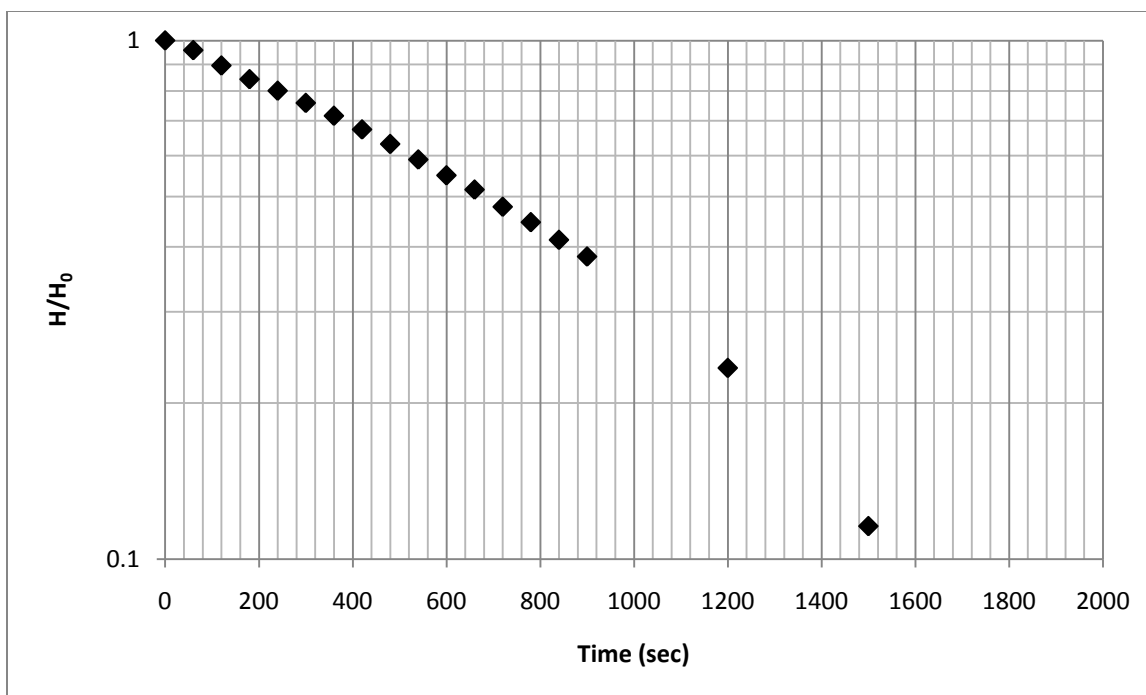
Appendix Figure 37. Hvorslev slug test for Creek 90 225 m.



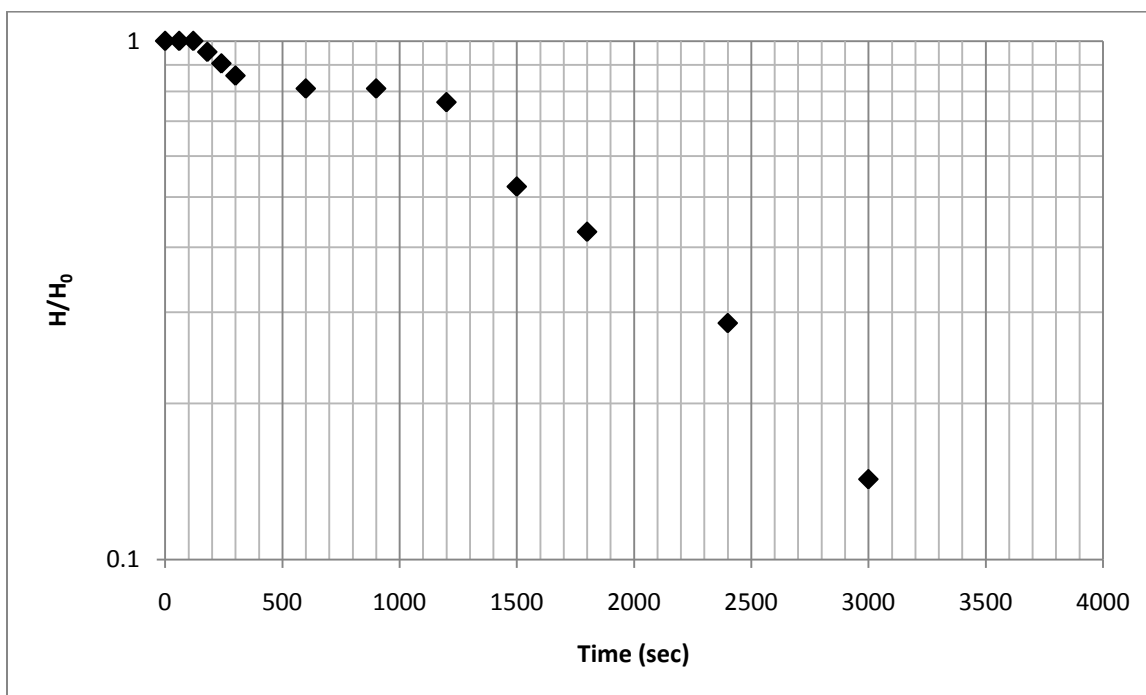
Appendix Figure 38. Hvorslev slug test for Creek 90 250 m.



Appendix Figure 39. Hvorslev slug test for Creek 90 300 m.



Appendix Figure 40. Hvorslev slug test for Creek 90 325 m.



Appendix Figure 41. Hvorslev slug test for Creek 90 350 m.

## *References*

- Alexander, R.B., Boyer, E.W., Smith, R.A., Schwarz, G.E., and Moore, R.B., 2007, The role of headwater streams in downstream water quality1: JAWRA Journal of the American Water Resources Association, v. 43, p. 41-59.
- Baxter, C., Hauer, F.R., and Woessner, W.W., 2003, Measuring groundwater–stream water exchange: new techniques for installing minipiezometers and estimating hydraulic conductivity: Transactions of the American Fisheries Society, v. 132, p. 493-502.
- Biksey, T.M., and Gross, E.D., 2001, The hyporheic zone: Linking groundwater and surface water— Understanding the paradigm: Remediation Journal, v. 12, p. 55-62.
- Boulton, A.J., 2000, River ecosystem health down under: assessing ecological condition in riverine groundwater zones in Australia: Ecosystem Health, v. 6, p. 108-118.
- Boulton, A.J., Findlay, S., Marmonier, P., Stanley, E.H., and Valett, H.M., 1998, The functional significance of the hyporheic zone in streams and rivers: Annual Review of Ecology and Systematics, v. 29, p. 59-81.
- Brierley, G.J., and Hickin, E.J., 1985, The downstream gradation of particle sizes in the Squamish River, British Columbia: Earth Surface Processes and Landforms, v. 10, p. 597-606.
- Brummer, C.J., and Montgomery, D.R., 2003, Downstream coarsening in headwater channels: Water Resources Research, v. 39, p. 1–14.
- Brunke, M., and Gonser, T., 1997, The ecological significance of exchange processes between rivers and groundwater: Freshwater biology, v. 37, p. 1-33.
- Carter, R.W., and Anderson, I.E., 1963, Accuracy of current meter measurements, Volume 89, p. 105–115.
- Cook, P.G., 2003, A guide to regional groundwater flow in fractured rock aquifers, CSIRO.
- Daniel, C.C., 1989, Statistical analysis relating well yield to construction practices and siting of wells in the Piedmont and Blue Ridge Provinces of North Carolina: U. S. Government Printing Office. Washington D. C., Geological Survey Water Supply Paper.
- Daniel, C.C., and Dahlen, P.R., 2002, Preliminary hydrogeologic assessment and study plan for a regional ground-water resource investigation of the Blue Ridge and Piedmont provinces of North Carolina, US Dept. of the Interior, US Geological Survey.
- Dansgaard, W., 1964, Stable isotopes in precipitation: Tellus, v. 16, p. 436-468.
- Day, T.J., 1976, On the precision of salt dilution gauging: Journal of Hydrology, v. 31, p. 293-306.

- Eaton, T.T., 2006, On the importance of geological heterogeneity for flow simulation: *Sedimentary Geology*, v. 184, p. 187-201.
- Efron, B., and Tibshirani, R., 1991, Statistical data analysis in the computer age: *Science*, v. 253, p. 390.
- Elmore, A.J., and Kaushal, S.S., 2008, Disappearing headwaters: patterns of stream burial due to urbanization: *Frontiers in Ecology and the Environment*, v. 6, p. 308-312.
- Fernald, A.G., Landers, D.H., and Wigington Jr, P.J., 2006, Water quality changes in hyporheic flow paths between a large gravel bed river and off-channel alcoves in Oregon, USA: *River Research and Applications*, v. 22, p. 1111-1124.
- Fetter, C.W., 1994, *Applied hydrogeology*, Macmillan College.
- Findlay, S., 1995, Importance of surface-subsurface exchange in stream ecosystems: the hyporheic zone: *Limnology and Oceanography*, v. 40, p. 159-164.
- Freeze, R.A., and Cherry, J.A., 1979, *Groundwater*.
- Frings, R.M., 2008, Downstream fining in large sand-bed rivers: *Earth-Science Reviews*, v. 87, p. 39-60.
- Gburek, W., and Folmar, G., 1999, Flow and chemical contributions to streamflow in an upland watershed: a baseflow survey: *Journal of Hydrology*, v. 217, p. 1-18.
- Gomez, B., Rosser, B.J., Peacock, D.H., Hicks, D.M., and Palmer, J.A., 2001, Downstream fining in a rapidly aggrading gravel bed river: *Water Resources Research*, v. 37, p. 1813-1823.
- Grimm, N.B., and Fisher, S.G., 1984, Exchange between interstitial and surface water: implications for stream metabolism and nutrient cycling: *Hydrobiologia*, v. 111, p. 219-228.
- Hamilton, P.A., and Helsel, D.R., 1995, Effects of Agriculture on Ground Water Quality in Five Regions of the United States: *Ground Water*, v. 33, p. 217-226.
- Harvey, J.W., and Bencala, K.E., 1993, The effect of streambed topography on surface-subsurface water exchange in mountain catchments: *Water Resources Research*, v. 29, p. 89-98.
- Hoey, T.B., and Bluck, B.J., 1999, Identifying the controls over downstream fining of river gravels: *Journal of Sedimentary Research*, v. 69, p. 40.
- Holcombe, R., 2003, *GEOrient* v. 9.1.
- Hsieh, P.A., 1998, Scale effects in fluid flow through fractured geologic media: Scale dependence and scale invariance in hydrology, p. 335-353.
- Kalbus, E., Reinstorf, F., and Schirmer, M., 2006, Measuring methods for groundwater? surface water interactions: a review: *Hydrology and Earth System Sciences*, v. 10, p. 873-887.



- Karr, J.R., and Dudley, D.R., 1981, Ecological perspective on water quality goals: Environmental management, v. 5, p. 55-68.
- Kennedy, C.D., Genereux, D.P., Mitasova, H., Corbett, D.R., and Leahy, S., 2008, Effect of sampling density and design on estimation of streambed attributes: Journal of Hydrology, v. 355, p. 164-180.
- Langland, M.J., Lietman, P.L., and Hoffman, S., 1995, Synthesis of nutrient and sediment data for watersheds within the Chesapeake Bay drainage basin: U. S. GEOLOGICAL SURVEY, EARTH SCIENCE INFORMATION CENTER, BOX 25286, MS 517, DENVER FEDERAL CENTER, DENVER CO 80225(USA).[nd].
- Lee, D.R., and Cherry, J.A., 1979, A field exercise on groundwater flow using seepage meters and mini-piezometers: Journal of Geological Education, v. 27, p. 6-10.
- Leopold, L.B., Wolman, M.G., and Miller, J.P., 1995, Fluvial processes in geomorphology, Dover Pubns.
- Likens, G., Bormann, F., Johnson, N., and Pierce, R., 1967, The calcium, magnesium, potassium, and sodium budgets for a small forested ecosystem: Ecology, v. 48, p. 772-785.
- Liu, Z.J., Weller, D.E., Correll, D.L., and Jordan, T.E., 2000, EFFECTS OF LAND COVER AND GEOLOGY ON STREAM CHEMISTRY IN WATERSHEDS OF CHESAPEAKE BAY1: JAWRA Journal of the American Water Resources Association, v. 36, p. 1349-1365.
- MacDonald, L.H., and Coe, D., 2007, Influence of headwater streams on downstream reaches in forested areas: Forest Science, v. 53, p. 148-168.
- Manga, M., and Kirchner, J.W., 2000, Stress partitioning in streams by large woody debris: Water Resources Research, v. 36, p. 2373-2379.
- Markewitz, D., Davidson, E.A., Figueiredo, R.O., Victoria, R.L., and Krusche, A.V., 2001, Control of cation concentrations in stream waters by surface soil processes in an Amazonian watershed: Nature, v. 410, p. 802-805.
- Marren, P.M., McCarthy, T.S., Tooth, S., Brandt, D., Stacey, G.G., Leong, A., and Spottiswoode, B., 2006, A comparison of mud-and sand-dominated meanders in a downstream coarsening reach of the mixed bedrock-alluvial Klip River, eastern Free State, South Africa: Sedimentary Geology, v. 190, p. 213-226.
- Meyer, J.L., Strayer, D.L., Wallace, J.B., Eggert, S.L., Helfman, G.S., and Leonard, N.E., 2007, The Contribution of Headwater Streams to Biodiversity in River Networks1: JAWRA Journal of the American Water Resources Association, v. 43, p. 86-103.
- Mohseni, O., and Stefan, H., 1999, Stream temperature/air temperature relationship: a physical interpretation: Journal of Hydrology, v. 218, p. 128-141.
- Moore, R., 2004, Introduction to salt dilution gauging for streamflow measurement: Part 1: Streamline Watershed Management Bulletin 7 (4): 20, v. 23.

- Moore, R.D.D., 1990, Construction of a Mariotte bottle for constant-rate tracer injection into small streams, p. 247-254.
- Oxtobee, J., and Novakowski, K., 2002, A field investigation of groundwater/surface water interaction in a fractured bedrock environment: *Journal of Hydrology*, v. 269, p. 169-193.
- Oxtobee, J., and Novakowski, K.S., 2003, Ground water/surface water interaction in a fractured rock aquifer: *Ground Water*, v. 41, p. 667-681.
- Peterson, B.J., Wollheim, W.M., Mulholland, P.J., Webster, J.R., Meyer, J.L., Tank, J.L., Martí, E., Bowden, W.B., Valett, H.M., and Hershey, A.E., 2001, Control of nitrogen export from watersheds by headwater streams: *Science*, v. 292, p. 86.
- Poole, G.C., and Berman, C.H., 2001, An Ecological Perspective on In-Stream Temperature: Natural Heat Dynamics and Mechanisms of Human-Caused Thermal Degradation: *Environmental management*, v. 27, p. 787-802.
- Rice, S., 1999, The nature and controls on downstream fining within sedimentary links: *Journal of Sedimentary Research*, v. 69, p. 32.
- Rice, S., and Church, M., 1996, Sampling surficial fluvial gravels; the precision of size distribution percentile sediments: *Journal of Sedimentary Research*, v. 66, p. 654.
- Scanlon, B.R., Healy, R.W., and Cook, P.G., 2002, Choosing appropriate techniques for quantifying groundwater recharge: *Hydrogeology Journal*, v. 10, p. 18-39.
- Schulze Makuch, D., Carlson, D.A., Cherkauer, D.S., and Malik, P., 1999, Scale dependency of hydraulic conductivity in heterogeneous media: *Ground Water*, v. 37, p. 904-919.
- Seal, R., and Paola, C., 1995, Observations of downstream fining on the North Fork Toutle River near Mount St. Helens, Washington: *Water Resources Research*, v. 31, p. 1409-1419.
- Sophocleous, M., 2002, Interactions between groundwater and surface water: the state of the science: *Hydrogeology Journal*, v. 10, p. 52-67.
- Sperry, J.M., and Peirce, J.J., 1995, A model for estimating the hydraulic conductivity of granular material based on grain shape, grain size, and porosity: *Ground Water*, v. 33, p. 892-898.
- Storey, R.G., Williams, D.D., and Fulthorpe, R.R., 2004, Nitrogen processing in the hyporheic zone of a pastoral stream: *Biogeochemistry*, v. 69, p. 285-313.
- Weller, D.E., Jordan, T.E., Correll, D.L., and Liu, Z.J., 2003, Effects of land-use change on nutrient discharges from the Patuxent River watershed: *Estuaries and Coasts*, v. 26, p. 244-266.
- West, J.B., Bowen, G.J., Cerling, T.E., and Ehleringer, J.R., 2006, Stable isotopes as one of nature's ecological recorders: *Trends in Ecology & Evolution*, v. 21, p. 408-414.

- White, D.S., 1993, Perspectives on defining and delineating hyporheic zones: *Journal of the North American Benthological Society*, v. 12, p. 61-69.
- White, D.S., Elzinga, C.H., and Hendricks, S.P., 1987, Temperature patterns within the hyporheic zone of a northern Michigan river: *Journal of the North American Benthological Society*, v. 6, p. 85-91.
- Wohl, E., and Jaeger, K., 2009, A conceptual model for the longitudinal distribution of wood in mountain streams: *Earth Surface Processes and Landforms*, v. 34, p. 329-344.
- Wolman, M.G., and Union, A.G., 1954, A method of sampling coarse river-bed material, *American Geophysical Union*.
- Wondzell, S.M., 2006, Effect of morphology and discharge on hyporheic exchange flows in two small streams in the Cascade Mountains of Oregon, USA: *Hydrological Processes*, v. 20, p. 267-287.
- Wondzell, S.M., and Swanson, F.J., 1999, Floods, channel change, and the hyporheic zone: *Water Resources Research*, v. 35, p. 555-567.
- Wroblicky, G.J., Campana, M.E., Valett, H.M., and Dahm, C.N., 1998, Seasonal variation in surface-subsurface water exchange and lateral hyporheic area of two stream-aquifer systems: *Water Resources Research*, v. 34, p. 317-328.